PERFORMANCE EVALUATION OF FLEXURAL AND SHEAR BEHAVIOURS OF LIGHTWEIGHT GEOPOLYMER CONCRETE

IFTEKHAIR IBNUL BASHAR

FACULTY OF ENGINEERING
UNIVERSITI MALAYA
KUALA LUMPUR

2022

PERFORMANCE EVALUATION OF FLEXURAL AND SHEAR BEHAVIOURS OF LIGHTWEIGHT GEOPOLYMER CONCRETE

IFTEKHAIR IBNUL BASHAR

THESIS SUBMITTED IN FULFILMENT OF THE REQUIREMENTS FOR THE DEGREE OF DOCTOR OF PHILOSOPHY

FACULTY OF ENGINEERING

UNIVERSITI MALAYA
KUALA LUMPUR

2022

UNIVERSITY OF MALAYA

ORIGINAL LITERARY WORK DECLARATION

Name of Candidate: **IFTEKHAIR IBNUL BASHAR**

Matric No: 17034346/2

Name of Degree: **DOCTOR OF PHILOSOPHY**

Title of Project Paper/Research Report/Dissertation/Thesis ("this Work"):

PERFORMANCE EVALUATION OF FLEXURAL AND SHEAR BEHAVIOURS OF LIGHTWEIGHT GEOPOLYMER CONCRETE USING PARTIAL INTERACTION THEORY

Field of Study:

STRUCTURAL ENGINEERING AND MATERIALS (CIVIL ENGINEERING)

I do solemnly and sincerely declare that:

(1) I am the sole author/writer of this Work;
(2) This Work is original;
(3) Any use of any work in which copyright exists was done by way of fair dealing and for permitted purposes and any excerpt or extract from, or reference to or reproduction of any copyright work has been disclosed expressly and sufficiently and the title of the Work and its authorship have been acknowledged in this Work;
(4) I do not have any actual knowledge nor do I ought reasonably to know that the making of this work constitutes an infringement of any copyright work;
(5) I hereby assign all and every rights in the copyright to this Work to the University of Malaya ("UM"), who henceforth shall be owner of the copyright in this Work and that any reproduction or use in any form or by any means whatsoever is prohibited without the written consent of UM having been first had and obtained;
(6) I am fully aware that if in the course of making this Work I have infringed any copyright whether intentionally or otherwise, I may be subject to legal action or any other action as may be determined by UM.

Candidate's Signature Date: Monday 3 October 2022

Subscribed and solemnly declared before,

Witness's Signature Date:

Name:

Designation:

PERFORMANCE EVALUATION OF FLEXURAL AND SHEAR BEHAVIOURS OF LIGHTWEIGHT GEOPOLYMER CONCRETE USING PARTIAL INTERACTION THEORY

ABSTRACT

Enunciation of the embryonic materials from industrial by-products is vital to address the ever-depleting virgin construction materials. The Fly ash (FA), palm oil clinker (POC), and manufactured sand (M-sand) are three industrial by-products from the coal operated power plants, palm oil industries, and quarry industries. These industrial by-products are available in abundance in Southeast Asia. Their regular generation as by-product from the high demandable main products - electricity, palm oil, and granite, are unavoidable and certain. So, these industrial by-products can ensure sustainability of production and supply on demand. FA is a well-known pozzolan. The chemical properties of FA collected from a type of coal operated power plant, are about consistent, and the particles are round and fine. These two specialities of FA have made it preferable more than other industrial pozzolanic by-product powders such as palm oil fuel ash, and rice husk ash. POC is lightweight, porous, and pozzolan; hence it is considered as a potential lightweight aggregate that could be used in geopolymer concrete. A concrete made of FA, POC, and M-sand is environment friendly; and implementation of that concrete in real construction will benefit to environment, and economical growth. It is imperative to exemplify the mechanical behaviour, material interaction properties (bond resistance, shear stress), and structural behaviour of a new material before using it in the structural application. This research project presented the failure mechanism of POC-based GC (P-GC) and granite-based GC (G-GC) under compression, bond properties, and structural behaviour through flexural, and shear test of reinforced concrete beams. The compression toughness and energy absorption at elastic and plastic states due to the influence of POC at micro-level

crack propagation were investigated. The pull-out load and slip response of a rebar embedded in P-GC and G-GC, was shown the role of aggregate in influencing the bond-slip responses. Further, Flexural and shear behaviour of reinforced concrete beams made of P-GC and G-GC were investigated and the experimental results were compared with the analysed results using partial interaction concept. The moment-curvatures of P-GC and G-GC beams were calculated from the compression load-deformation and rebar pull-out-slip results to comprehend the feasibility of P-GC in structural application. The results show that the ultimate moment of resistances of both beams were comparable for the concretes of similar grade. The elastic limit of P-GC was lower than G-GC, hence, and the first crack initiated in P-GC earlier compared to G-GC. The midspan-deflections varied due to the difference of stiffnesses of P-GC and G-GC. The outcome of the whole project is beneficial for the engineers to adopt POC as sustainable construction material.

Keywords: Palm oil clinker, lightweight geopolymer concrete, Compression toughness, Pull-out-slip, Partial interaction

PENILAIAN PRESTASI TINGKAH LAKU FLEKSURAL DAN RICIH KONKRIT GEOPOLIMER RINGAN MENGGUNAKAN TEORI INTERAKSI SEPARA

ABSTRAK

Penyingkiran bahan embrio daripada produk sampingan industri adalah penting untuk menangani bahan binaan dara yang semakin berkurangan. Fly ash (FA), klinker minyak sawit (POC), dan pasir buatan (M-sand) adalah tiga produk sampingan industri daripada loji kuasa kendalian arang batu, industri minyak sawit dan industri kuari. Produk sampingan perindustrian ini boleh didapati dengan banyaknya di Asia Tenggara. Penjanaan biasa mereka sebagai produk sampingan daripada produk utama yang memerlukan permintaan tinggi - elektrik, minyak sawit dan granit, tidak dapat dielakkan dan pasti. Jadi, produk sampingan perindustrian ini boleh memastikan kemampanan pengeluaran dan bekalan atas permintaan. FA ialah pozzolan yang terkenal. Sifat kimia FA yang dikumpul daripada sejenis loji kuasa kendalian arang batu, adalah kira-kira konsisten, dan zarahnya bulat dan halus. Kedua-dua keistimewaan FA ini telah menjadikannya lebih disukai daripada serbuk produk sampingan pozzolanik industri lain seperti abu bahan api minyak sawit, dan abu sekam padi. POC adalah ringan, berliang dan pozzolan; maka ia dianggap sebagai agregat ringan berpotensi yang boleh digunakan dalam konkrit geopolimer. Konkrit yang diperbuat daripada FA, POC, dan M-pasir adalah mesra alam; dan pelaksanaan konkrit itu dalam pembinaan sebenar akan memberi manfaat kepada alam sekitar, dan pertumbuhan ekonomi. Adalah penting untuk memberi contoh kelakuan mekanikal, sifat interaksi bahan (rintangan ikatan, tegasan ricih) dan kelakuan struktur bahan baharu sebelum menggunakannya dalam aplikasi struktur. Projek penyelidikan ini membentangkan mekanisme kegagalan GC (P-GC) berasaskan POC dan GC (G-GC) berasaskan granit di bawah mampatan, sifat ikatan, dan kelakuan struktur melalui ujian lentur dan ricih rasuk konkrit bertetulang. Keliatan mampatan dan

penyerapan tenaga pada keadaan elastik dan plastik disebabkan oleh pengaruh POC pada perambatan retak peringkat mikro telah disiasat. Beban tarik keluar dan tindak balas gelinciran rebar yang tertanam dalam P-GC dan G-GC, telah ditunjukkan peranan agregat dalam mempengaruhi tindak balas gelinciran ikatan. Selanjutnya, kelakuan lentur dan ricih rasuk konkrit bertetulang yang diperbuat daripada P-GC dan G-GC telah disiasat dan keputusan eksperimen dibandingkan dengan keputusan yang dianalisis menggunakan konsep interaksi separa. Lengkungan momen rasuk P-GC dan G-GC dikira daripada hasil ubah bentuk beban mampatan dan gelincir tarik keluar rebar untuk memahami kebolehlaksanaan P-GC dalam aplikasi struktur. Keputusan menunjukkan bahawa momen muktamad rintangan kedua-dua rasuk adalah setanding untuk konkrit gred yang sama. Had keanjalan P-GC adalah lebih rendah daripada G-GC, oleh itu, dan retakan pertama dimulakan dalam P-GC lebih awal berbanding dengan G-GC. Pesongan midspan berbeza-beza disebabkan oleh perbezaan kekakuan P-GC dan G-GC. Hasil daripada keseluruhan projek ini memberi manfaat kepada jurutera untuk mengguna pakai POC sebagai bahan binaan yang mampan.

Kata kunci: Klinker minyak sawit, konkrit geopolimer ringan, Keliatan mampatan, Gelincir tarik keluar, Interaksi separa

ACKNOWLEDGEMENTS

All praises are to the Almighty, Allah (subhanahu wata'la) who has created the opportunities for me, and who has given me the abilities to conduct my Ph.D. research.

Alhamdulillah. I am grateful to Allah swt for giving me the patience in this long journey of my Ph.D life.

I am glad that my parents always inspired me to complete my PhD works. I am pleased on my wife, and children for their understanding and supports. I wish Allah swt bestows them the best in this world and hereafter.

I thank my colleagues, and lab assistants for their assistance, and supports, whenever I needed.

I would like to acknowledge my supervisors Professor Dr U. Johnson Alengaram, and Professor Ir Dr Mohd Zamin Jumaat that their guidance is the most important achievement in my research life; I will try to keep remember whatever I have learnt from their guidance.

I acknowledge Dr Johnson strongly for his kind endeavour and encouragements to accomplish my Ph.D. research, and thesis. I thank Dr Johnson for his patience, and for being always hopeful, and confident about my strength, and ability. I wish the best for him.

I acknowledge Universiti Malaya for sponsoring a postgraduate research grant for my Ph.D. research work (PG006-2015B) and for recognising me as "Bright Spark" under HIR project (UM.C/625/1/HIR/MOHE/ENG/02).

TABLE OF CONTENTS

LIST OF FIGURES

LIST OF TABLES

CHAPTER 1: INTRODUCTION

1.1 Background

The construction of new structures and redevelopment demolishing existing structures are the cutting-edge demands due to increasing necessity of buildings and infrastructures. The construction materials generally comprise concrete, steel, timber, and mud; but concrete is the most consumed material, because of the ease of availability of its constituents, simple production technique, convenience to achieve any shape, and ease to adopt new techniques to alter its property to improve the energy efficiency.

The demand of concrete has been increasing continuously. Its production growth in 2050 is estimated to reach four times more than the demand in 1990 which is as at least 2 billion tons/ year (Crow, 2008). In recent time, where due to the global epidemic (COVID-19), when most of the business sectors are struggling to hold economical fall, the construction industries require continuing the development as normal as it is on demand. In the first nine months of COVID-19 in 2020, the value of construction was increased about 4% in the United States, compared to the same period in 2019 (U.S. Geological Survey, 2021). Despite of slowing down the construction, even residential construction did not reduce demand in this challenging period. Moreover, numerous construction industries announced to launch new product lines, zero-carbon research initiatives, and innovative plans to reuse and renew energies.

The major ingredients in concrete are cement (a binding material), and aggregates (coarse and fine aggregates). The usage of these conventional materials (cement, sand, crushed granite/ stone) has global concerns for possessing adverse impact to environment. The production of cement attributes to CO_2 emission about 8% of total global emission which was about 1.6 $GtCO_{2eq}$ in 2018 (Lamb et al., 2021) and conventional aggregates (e.g.,

mining sand, river sand, crushed stones) are directly involved in the depletion of natural resources.

As an example, the scenario of cement required for construction in United States (US) can be discussed. US produced 87 million tons of Portland cement in 2020 (U.S. Geological Survey, 2021). One ton cement production emits about a ton of CO_2 in the air. With this approximation, it estimates that US alone produced about 87 million tons of CO_2 in 2021. The necessity of cement has been increased, that's why it has been required to upgrade most of the cement plants of 94 numbers in 34 States, and 2 numbers in Puerto Rico. The consumer of these productions are generally ready-mixed concrete producers (70% to 75%), concrete product manufacturers (10%), contractors (8 to 10%), and other type of customers (5 to 12%). The percentage as shown in the bracket is based on the U.S Geological Survey (2021) report for year 2020 in US.

The growth of cement production is not only limited to US, but also, it is overwhelming in the whole world. An analysis of this tremendous growth of cement production has been shown in Figure 1.1, and 1.2. The average yearly worldwide cement production between years 1994 and 2002 was 1,556,811 thousand metric tons. The production rate has started increasing with a high rate from 2002. After twelve years, globally cement was produced 4,180,000 thousand metric tons in 2014 which is 2.5 times higher than cement production in 2002. These increases of cement production are attributed mainly to China and marginally to India. Countries other than China and India including United States, Puerto Rico, Brazil, Egypt, France, Germany, Indonesia, Iran, Italy, Japan, Republic of Korea, Mexico, Pakistan, Russia, Saudi Arabia, Spain, Taiwan, Thailand, Turkey, and Vietnam, have been producing a large amount of cement yearly, but the production rate has not increased much compared to China. The worldwide average cement production between years 1994 and 2011, is 404,532 thousand metric tons; afterward, the production increased up to 890,000 thousand metric ton in 2020. The average rate of increment of

production of all countries except China and India is estimated as 53,940 thousand metric tons per year, which is significantly less than the cement production rate of China between years 2002 and 2014 (144,167 thousand metric tons per year).

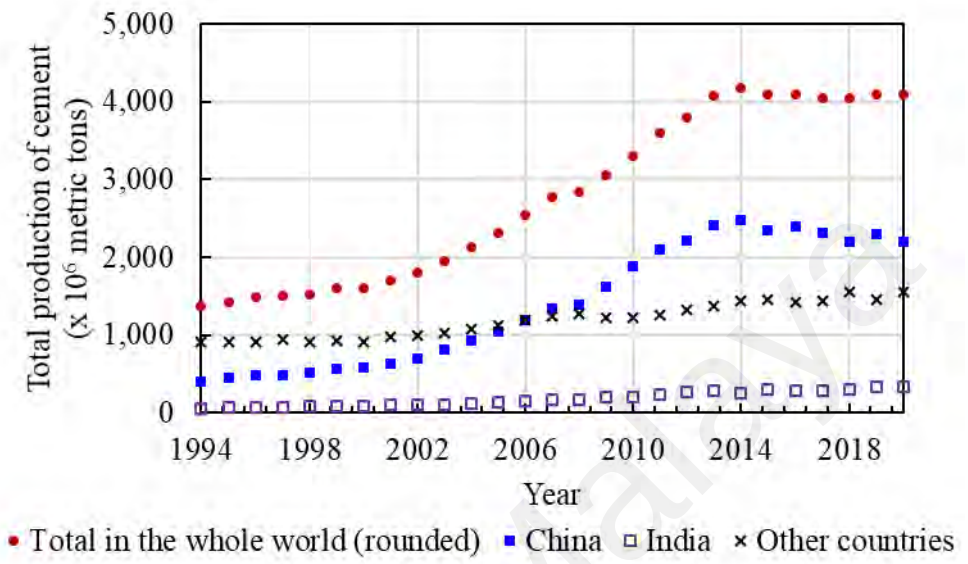

Figure 1.1: Production of cement from 1994 to 2020

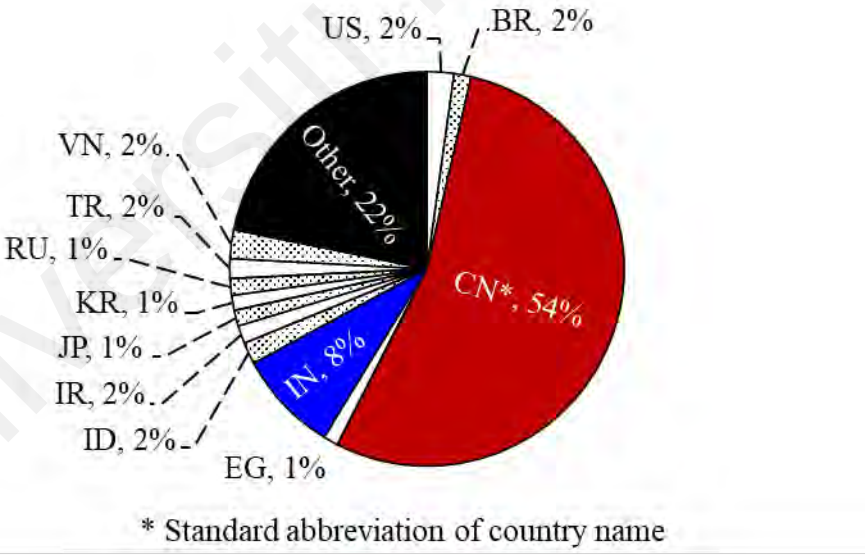

Figure 1.2: Cement production (%) in different countries in 2020

The rate of cement production has been increased at a high degree from 2002 to 2014 which is attributed to the high production of cement in China. In recent years (from 2010 to 2020), the rate of production of cement in India has increased, but the increment rate is very low compared to China. The cumulative rate of cement production from other

leading countries including United States, Puerto Rico, Brazil, Egypt, France, Germany, Indonesia, Iran, Italy, Japan, Republic of Korea, Mexico, Pakistan, Russia, Saudi Arabia, Spain, Taiwan, Thailand, Turkey, and Vietnam is not significantly changed from 1994 to 2020.

These continuous adversities to greenhouse and ecosystem raise the concern of endangering the future state of our green world. Thus, researchers (Mehta, 2005; Ochsendorf, 2005; Suhendro, 2014) suggested several steps to delay the risks of environmental damages, such as (a) reduction of fuel consumption improving efficiency in production process, (b) discovery of alternatives of cement and granites from industrial wastes (Ochsendorf, 2005; Suhendro, 2014).

The awareness of the adverse environmental impact for the concrete production using the conventional ingredients (cement, granite), thus paved away several opportunities, also challenges to the engineers, and researchers to exhume alternative way of concrete production that may have least ecological and environmental impact (Ibrahim & Razak, 2016). The simplest way to alter the method of concrete production is to introduce eco-friendly materials in concrete. As utilising an alternative source of natural ingredients in concrete production, does not reduce the problem of depletion of natural resources, researchers are interested on industrial wastes and by-products as these materials are currently burden for the environment because of their enormous regular generation from the operational activities in the industries. Generally, these products are just dump on earth which causes environmental pollution (Muthusamy et al., 2019). This is a burden for industrialists as well because these unprofitable dumping on their own land, reduces operational area; therefore, this is an indirect interest to the industrialists to have a solution of the industrial wastes.

United Nations General Assembly (2015) has suggested sustainability development goals. The utilisation of industrial wastes supports several goals such as affordable and clean energy, responsible consumption and production, climate action. So, finding an appropriate technique to utilize the wastes will not only benefit to the environment, but also, it will benefit to the economy making those wastes to wealth, and creating job scopes for the skilled and technical people.

Massive research has been advocated in the last six decades (Sandanayake et al., 2020) on various industrial wastes and by-products to use as substitutes of conventional constituents of concrete (Hamada et al., 2020a, b). However, any materials cannot be used as construction material just conducting tests on some properties. It requires thorough investigation on environmental impact in long run, strengths in various types of service conditions, durability, as well as sustainability of the waste product. So, before getting approval from the regulatory department, it requires stringent evaluation of the waste/ by-products. Hence, there are many wastes/ by-products those have been researching in laboratory, yet not implement to real construction (Hamada et al., 2020c). Without having authority approval as appropriate construction material, those products will not get a marketplace.

South-East Asian region generates abundant wastes/ by-products those are identified as potential and sustainable substitutes of concrete constituents. The industries involve producing those wastes are iron and steel industries (Kim et al., 2021), power plants (Ragipani et al., 2021), incinerated plants (Alderete et al., 2021), rice mills (Tayeh et al., 2021), and palm oil mills (Halim et al., 2021).

As the second largest producer of palm oil in the world after Indonesia, Malaysia produces millions of tonnes of palm oil wastes (Wardhani et al., 2021); some of those materials such as oil palm shell (Hamada et al., 2020), palm oil clinker (Muthusamy et al., 2021),

palm oil fuel ash (Hamada et al., 2020), etc. had been investigated as useful construction materials.

In addition to the sustainability advantage, there is a huge stake for marketability of such materials as the potential is fully exploited; thus, the economic impact due to the incorporation of these palm oil industrial by-products and wates is yet to be uncovered; the expansion of palm oil cultivation due to an increased demand for cooking oil and biodiesel would further increase the production of these waste materials. In the early 20th century, palm cultivation was reported as 400ha (Loh, 2017) which had reached about 4.5 million hectares (Sulaiman et al., 2011). Approximately 17.7 million tons of palm oil was extracted in Malaysia in 2008 (Chiew et al., 2011) that generated millions of tons of agricultural and industrial wastes in the form of oil palm shell (OPS), empty fruit brunches, palm oil trunk, palm oil fuel ash (POFA), and palm oil clinker (POC).

Alengaram et al. (2016) proved that oil palm shell can be used as blast resistant concrete by testing oil palm shell slabs under blast loading. Palm oil clinker powder, and palm oil fuel ash showed their potential as replacement for ordinary Portland cement and fly ash in the development of sustainable concrete, both in normal and geopolymer concretes. These materials have an added value due to sustainability issues, in addition to acceptable physical and chemical properties as filler and pozzolanic materials (Al-Mulali et al., 2015).

Both POFA and POC are pozzolanic materials (Karim et al., 2016) and these were utilised as a replacement of cementitious material and lightweight aggregate, respectively (Bashar et al., 2016; Kabir et al., 2017; Sharmin et al., 2017). The effect of utilizing POC as coarse aggregate was reported as a cause of producing higher creep and drying shrinkage in prestressed concrete and reduced UPV value for high porosity and irregular shape (Omar & Mohamed, 2002). However, the concrete mix design can be optimised by filling pores

by filler and pozzolanic materials (Abutaha et al., 2017) or increasing paste volume that is generally required for lightweight concrete design (Mo et al., 2017). Further utilization of POC in the structural concrete and the investigation of POC as a lightweight aggregate in the lightweight concrete would enable further research and meaningful use of it as lightweight aggregate (LWA) as known, the use of conventional crushed granite or other virgin materials is not environmentally friendly due to CO_2 emission owing to quarrying, transportation, crushing etc. of virgin aggregates; on the contrary, POC due to its lightweight could be easily crushed and transported, thus resulting in the lower energy consumption. The other advantage of POC include the lower thermal conductivity due to porous nature and lowering the construction and product costs (Almutairi et al., 2021; Shahid et al., 2016; Tayeh et al. 2021).

Research works have been carried out using POC as the replacement of coarse, and fine aggregates to address the sustainability and its environmental impact and characterization (Kanadasan et al., 2016); further work on the method of developing POC high-strength concrete was carried out by Abutaha et al. (2018); the utilisation of POC powder as a cement replacement in the development of self-compacting concrete (Kanadasan et al., 2016) was also explored. The microstructural investigation for pozzolanic reactivity of POC powder as a cement replacement (Karim et al., 2017) and the size effect of POC as coarse aggregate (Alhasanat et al., 2016) were investigated. The mechanical properties, compressive, flexure, & splitting tensile strengths, and modulus of elasticity along with shear properties of POC cement concrete were investigated (Lee, 2019; Malkawi et al., 2020). The structural behaviour with respect to the flexural and shear behaviours of POC-CC beam and wall/ panel was another feather on POC based concrete (Huda, 2017; Joohari et al., 2016; Mohammed et al., 2011).

Though a significant amount of research has been conducted on the investigation of properties of POC based concrete material, very limited research can be found at the

structural level. Another important aspect is the binding material in concrete. Substituting granite by POC does not omit CO_2 emission for using cement as binding material in concrete. Thus, it is important to find alternatives of all ingredients to minimize the negative impact to environment due to concrete production.

A novel technology, as termed as "Geopolymer" by Professor Joseph Davidovits (2008), may be beneficial in reducing CO_2. Geopolymer can be an ideal alternative of OPC based cementitious binding material in concrete. Geopolymer paste is a binding material. The reaction process of geopolymer is different from cement hydration process. It requires pozzolans to be activated using alkaline solution. The product that is produced after polymeric reaction, is known as zeolite. In cement hydration process, Calcium Silicate Hydrate (C-S-H) is produced that provides strength in concrete. Besides the production of C-S-H, hydration reaction produces $Ca(OH)_2$. $Ca(OH)_2$ has adverse effect in cement based concrete. In the other hand, in geopolymer reaction process, no $Ca(OH)_2$ is produced; but if any $Ca(OH)_2$ is available as chemical compound in the ingredients, it reacts and produce a strong bond with zeolite polymer chain. Therefore, in terms of strength and durability aspect geopolymer is considered better choice than cement-based concrete.

Fly ash (FA) is well known pozzolan and industrial by-products that can be utilised to produce geopolymer. So, a geopolymer concrete made of POC substituting granite and FA, substituting cement, could be a environmental friendly concrete. By nature, POC is lightweight. So, utilising POC in geopolymer concrete has another benefit to produce lightweight concrete. In past, researchers have been focused replacing either aggregate or binding material in concrete to produce eco-friendly concrete. Limited work can be found on POC-based lightweight geopolymer concrete.

Sharmin et al. (2015) investigated a comparison between oil palm shell (OPS), and POC-based geopolymer concrete. Sharmin et al. (2015) used geopolymer matrix and OPS-POC blends in various proportions to investigate engineering properties of concrete. The sand was replaced by POC-sand in this research. No research on POC-based geopolymer concrete at structural level can be found.

Omar & Mohamed (2002), and Mohammed et al. (2013, 2014) studied POC-cement based concrete in structural level. Flexural and shear response of reinforced concrete beam were investigated in this research. However, the structural performance in respect of aggregate-matrix bonding and failure mechanism were not investigated in those research works. The geopolymer matrix and POC composite are required to investigate separately as brittleness of paste has significant role in the structural behaviour, and design in its plastic stage.

Geopolymer paste is more brittle than cement-based paste material (Pan et al, 2011). Also, POC as being a pozzolanic harden material, its surface reacts with the geopolymer matrix; thus, the developed bond forms the POC and geopolymer matrix blend a homogeneous harden product (Bashar et al, 2021). So, the aggregate-matrix bond in cement-based concrete and geopolymer concrete should be different; and any experimental result involving POC in cement matrix should not be expected similar kind of behaviour for POC involving in geopolymer matrix.

1.2 Research gap and questions

Based on the above discussion, a significant gap has been found on POC-based geopolymer concrete (P-GC) that should be required to address before implementing P-GC as construction material for structural use in the construction industry. It is important to understand for engineers, the elastic and plastic stage of concrete, and during both stages, how the concrete material behaves. Also, it is important to know the role of the

aggregates, and mortar, while the concrete is under compression, tension, and shear. For reinforcement concrete, there is another material property – concrete and rebar bond properties, the global bond behaviour depends on individual material properties. When all the material properties are known, the structural behaviour under basic actions such as bending, and shear can be investigated using material properties. After a thorough review (Chapter 2), it is found that, POC is a sustainable industrial by-product, and the production can mitigate a large demand of granite in concrete production. Also, no previous research works have addressed the failure mechanism of POC-based concrete under compression, role of POC in geopolymer matrix to withstand pull-out bond-shear stresses, shear properties of P-GC, and especially, no research has been conducted on geopolymer concrete made of POC as coarse aggregate. However, this information/ knowledge is a common question to the engineers, and regulatory authority while approving a material for construction purpose.

1.3 Aim and objectives

The aim of this research project was to identify alternative source of concrete constituents, develop an appropriate structural grade concrete, and investigate thoroughly the structural performance.

The aim has been accomplished by fulfilling following objectives:

(1) To identify an alternative concrete constituents from industrial by-products. To comply this objective, all types of constituents: cement, fine aggregate, and coarse aggregate were required to alter by appropriate industrial by-products. Material availability, and compressive strength test were the basis of comparison and selection process.

(2) To investigate the failure mechanism of a developed lightweight concrete and to address the role of lightweight aggregate and mortar in failure mechanism.

(3) To investigate bond-shear properties between developed concrete and rebar

(4) To investigate the behaviour of concrete in structural scale, and to analyse the results in relation to the material properties.

For this purpose, beams made of the developed concrete were examined under bending actions for flexural failure, and shear failure.

The title of this project thus briefly explains the theme of this research project: flexural and shear performance of lightweight geopolymer concrete using partial interaction theory. Partial interaction theory has been used to analyse experimental responses and failure mechanism in relation to the role of concrete constituents.

1.4 Thesis outline

The thesis is outlined according to the flow of the research project. The first phase of this research was spent to identify appropriate industrial wastes for concrete constituents. Based on the preliminary research review, industrial by-products were chosen for investigation. As this project was based on Malaysia, the sustainable by-products were found from Malaysian industries. However, the project outcome may be beneficial to other end of the world, as the failure mechanism has been discussed in relation to the partial interaction among the raw materials. The contents of each chapter have been discussed below:

Chapter 1: The research gap is addressed and the aim as well as objectives are explained in this chapter; how the outcome of this research will benefit to engineering society has been stated.

Chapter 2: Sustainability of utilising industrial by-product (finally selected POC) as substitution of granite is studied in this chapter. The relevant research to date status of POC-based concrete is reviewed after its sustainability analysis.

Chapter 3: The physical and chemical properties of the constituents used in the whole project are reported in this chapter.

Chapter 4: An alternative of conventional mining sand is chosen from the quarry industry. Manufactured sand which is the processed product of by-product quarry dust. Quarry dust generates in quarry industry during crushing stones/ granites to smaller sizes. Quarry dust has irregular shape. That's why, this irregular shaped quarry dust is rotated in a chamber in high speed. Due to the centrifugal force, particles of quarry dust rub each-other, thus the irregular shape is modified to rounded shape. Then the particles of quarry dust form a shape closed to the mining sand. During the stage of this research, M-sand and quarry dust were used for filling lands/ cavity, and manufacturing cement bricks. It was not used in concrete production. So, the efficiency of M-sand has be explored in Chapter 3. Various types of geopolymer mortars were produces to investigate their compressive strength. The results were compared with the geopolymer mortar made of mining sand. Based on the research outcome of this investigation, M-sand was chosen as fine aggregate in the final mix design. The binding material was used Palm oil fuel ash with other pozzolanic materials. However, these binding by-products were changed in the final mix design.

Chapter 5: Oil palm shell (OPS) is one of the industrial by-products from the palm oil industry. Because of its spongy physical properties, it improves ductility of concrete which was proven in previous research work. Being encouraged from that research work, OPS was chosen in the beginning of this research as a constituent in geopolymer concrete,

and its fracture behaviour was examined. The research finding of that investigation is written in this chapter. Though OPS showed an excellent result, it was not selected finally for the main geopolymer lightweight concrete that was used for investigation at structural level. OPS is a natural organic material. Its surface consists of natural fibre. From the durability concern, OPS is expected to be corroded in highly alkaline activated geopolymer concrete. In short period (within 28-day), when the fracture was investigated, it didn't show any adversity; but there is a possibility of corrosion and weakening the aggregate concrete bonding and interlocking system in geopolymer concrete. That's' why, another alternative from palm oil industry which is an incinerated product of OPS and palm fibre, i.e., palm oil clinker (POC). Like chapter 3, the binder was used as Palm oil fuel ash blended with other industrial by-product pozzolans.

Chapter 6: The compressive ductility and compression toughness of POC-based geopolymer concrete were investigated in this chapter. The role of POC, in compression failure mechanism is explained in this chapter. An analytical analysis was conducted assuming a reinforced beam (made of POC-based geopolymer concrete) in under bending. An over reinforced beam was analysed until it fails at concrete compression zone. Thus, from compression stress-strain response, the moment-curvature of assumed beam is reported in this Chapter.

Chapter 7: The bond shear stress and slip responses of POC-based geopolymer lightweight concrete and rebar are investigated in this chapter. The role of POC as aggregate in geopolymer concrete is discussed. The interfacial bond shear properties can be extracted using analytical approach as suggested in Model code 2010. A slight variation of interfacial properties has been proposed at frictional stage of debonding in this chapter.

Chapter 8: The efficiency of POC-based lightweight geopolymer concrete is reported in this chapter based on the investigation of its application to structural level. Beams with various reinforcement ratio were prepared, and the flexural performance were investigated. In addition to this flexural analysis, beams were investigated for shear resistance as well. For this purpose, POC sizes were adopted in three types of variation with same proportions of constituents.

1.5 Novelty of this research project

This research project was designed to develop a lightweight geopolymer concrete from industrial by-products, to assess the suitability for utilisation in structural application, and to analyse the structural behaviour using the basic mechanical and partial interaction properties of concrete. So, the overall novelty of the whole project can be conferred to the recipe of POC-based structural grade lightweight geopolymer concrete which has satisfactorily showed comparable outcome of mechanical properties, and structural performance (flexural and shear response of reinforced beam) when compared with normal weight geopolymer concrete of similar strength. However, each research objectives claim specific novelties from the experimental outcome.

The specific novelties of individual objectives are summarised below:

(1) Chapter 4 (published in a journal of conference proceeding) reports one of the research outcomes that was directly related to the first objective of this project. The feasibility of M-sand as a substitute of mining sand was investigated in this research assessing its physical properties and compressive strength of mortar made of POFA-FA based geopolymer paste. Though the candidate in another publication (Bashar et al., 2014) proofed the potentiality

of M-sand as complete substitution of mining sand, this experiment was different from Bashar et al. (2014). The effect of molarity of alkaline dosages was investigated in Bashar et al. (2014). But this research shows the role of M-sand replacing in various proportions with mining sand from zero to 100% level where geopolymer paste made of POFA-FA blends were consistent in all recipes. So, the novelty of this work is that the comparable benefit of M-sand was clarified through this research experiments.

(2) Chapter 5 (published in an international high ranked journal) has less relation with the overall outcome of this research. But this research work has novelty. Oil palm shell (OPS) was used as complete substitute of granite in OPS-based geopolymer concrete in this research. OPS is an organic material (agricultural waste) which is bio-degradable, so it may have adversity in strength reduction in long run due to surface corrosion with the alkaline consisted in geopolymer matrix. OPS was used in this research for investigating the ductility of lightweight geopolymer concrete made of OPS as aggregate. The candidate was influenced to conduct this research by previous research on OPS-based concrete where cement was used as binding material. The excellent ductility profile of OPS-cement based concrete was reported in that previous research. But when a research on OPS-based geopolymer brick in another project of the candidate's group in the University of Malaya was conducted, the degradation of the strength and peeling off OPS from external surface after a long period was noticed. This was the ice break to rethink about OPS as substitute of granite in a concrete that requires high dosage of corrosive chemical for hardening. Therefore, POC was used in the final mix design as granite-substitute.

Though OPS was not used in the final mix design, which was used for investigation at structural level, this research has novelty. The fracture toughness of OPS-based concrete/ geopolymer concrete were not reported before this research. The findings of this research promote OPS as suitable lightweight aggregate for structural grade concrete for blast/ impact resistant structure. As OPS is bio-degradable, it may need treatment before using it in concrete for longevity of structural member.

(3) Chapter 6 (published in an international high ranked journal) reports the research on compression toughness of POC-based geopolymer concrete. This research is significant, as it explains the role of POC in geopolymer matrix when the concrete is under compression. Earlier researchers mostly investigated the compressive strength; but this research explored first time the damage mechanism of POC-based geopolymer concrete (P-GC) under compression stress.

(4) Chapter 7 shows the bond-shear resistance of POC-based geopolymer concrete. Research on pull-out experiment of lightweight aggregate (other than POC) concrete/ geopolymer concrete is available. But the role of the aggregate, and the actual bond shear interfacial properties were not investigated. This research has shown the role of POC as lightweight aggregate in bond resistance. The method of Model code 2010 has been implemented to extract more accurate interfacial bond-shear properties. Previous research on bond-shear properties of lightweight concrete/ geopolymer concrete, average bond shear was estimated by simply dividing the embedded surface area of the rebar. But in this research localised (interfacial) bond-shear properties have been extracted which is more accurate than average bond stress. Model code 2010 suggested a consistent

linear frictional property (after complete debonding). But this research identified that POC has a role in the debonding process, as POC (those located near the rib of rebar) crushes during debonding process. So, the frictional resistance degrades gradually. So, another novelty of this research is to adopt frictional branch linearly descended which Model code 2010 suggested consistent.

(5) Chapter 8 is the final stage of this research where structural performance (flexural, and shear) of POC-based reinforced concrete beam has been shown and analysed using the analytical concept of partial interaction involving the material properties (compression stress-strain, and bond-shear properties). The moments and curvatures of beams under bending stress have been analysed using the partial interaction concept which corresponded the experimental load-deflection result. This research claims its pioneered as POC-based geopolymer concrete reinforced beam was not examined by earlier research and no lightweight aggregate geopolymer concrete beam was investigated with the interaction properties.

CHAPTER 2: SUSTAINABILITY AND RESEARCH STATUS – REVIEW ON POC-BASED CONCRETE/ GEOPOLYNER CONCRETE

2.1 Introduction

The palm oil clinker (POC) and POC-based concrete/ geopolymer concrete are focused in this review. The candidate reviewed other research articles on lightweight concrete and their engineering application. However, research relevant to POC, and POC-based concrete/ geopolymer concrete have been discussed in this chapter; because the major portion of this thesis has covered POC-based lightweight geopolymer concrete. Chapter 4, and 5 are the preliminary findings before finalising P-GC to be investigated for structural performance. So, the review related to M-sand, and OPS have been discussed in respective chapters; Chapter 4, and 5.

Before advancing toward detail investigation of past research and their finding on POC-based concrete/ geopolymer concrete; it is important to understand if research on this topic will sustain for long period or not. Because of this, sustainable production of POC is the prime requirement. Therefore, the review on sustainability of POC generation is discussed before research findings on POC-based concrete below.

2.2 Sustainability of palm oil waste generation

The concept of sustainability is a term that relates to the interests concerning environment, society, and economy (Vallance et al., 2011). The technological, as well as non-technological solutions are questionable by this concept. The United Nations has seventeen sustainability goals for transforming present world through a sustainable development. Among those seventeen, affordable and clean energy, industry, innovation and infrastructure, sustainable cities, and communities, responsible consumption and production, climate action are closely related to sustainability of technological solutions. Thus manufacturing concrete material using industrial wastes and by-products have been

achieved a rising attention to researchers, engineers, governmental bodies, and industrialists.

Among the industries (especially, iron industry, rice mill, coal generated power plants), palm oil industries are potential to find alternative solution of conventional aggregate; because it generates, palm oil clinker, which is lightweight, pozzolan, and strong enough to accommodate in concrete as substitute of granite; and palm oil production is rising gradually globally; in other word, production of palm industrial by-products are growing rapidly, which ensures its sustainability.

Figure 2.1 has been produced a geographical locations and production of palm oil in 2018. The data has been extracted from the online statistics published by Food and Agricultural Organization of United Nations (FAOSTAT). It shows that palm oil has consumer in about one-third of the countries in the world.

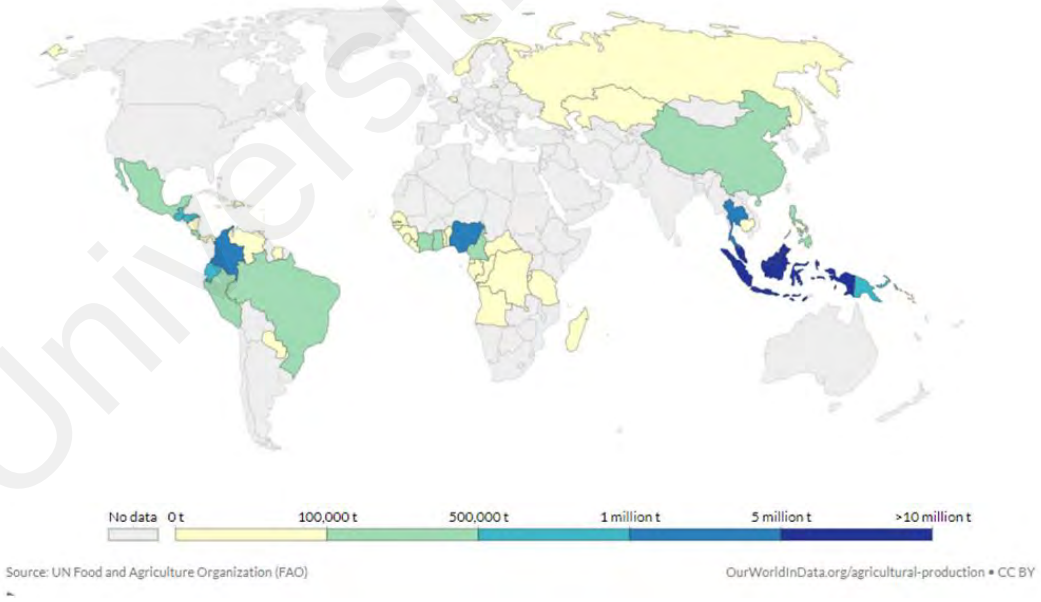

Figure 2.1: Worldwide production (tonnes) of palm oil in 2018 (Food and Agricultural Organization of the United Nations, n.d.)

The gradual ascending of palm oil demand can be seen from the global palm oil production from 1961 to 2021. Figure 2.2, and 2.3 is analysed based on the available data

in FAOSTAT. Figure 2.2 shows that palm oil demand has been yielding upward since its production initiated at industrial level in 1961. The rate of increment of global demand is increasing rapidly as well. The rate of increment was calculated as 148,000 MT/year between 1961 and 1977, which yielded upward 6 times after 1977. In recent years this rate of increment has been reached to 3017,000 MT/ year globally (Figure 2.3).

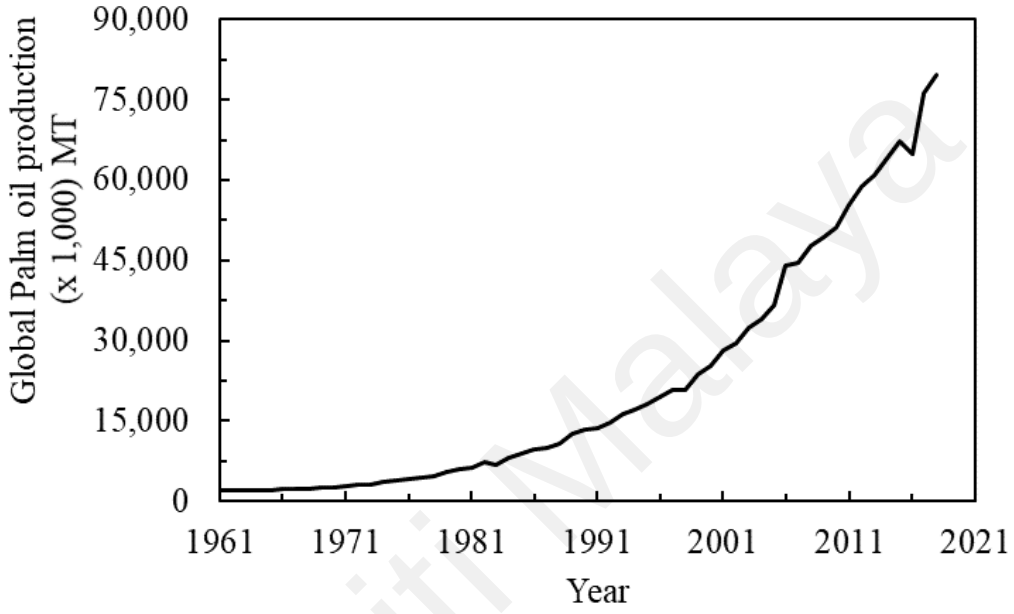

Figure 2.2: Global palm oil production (x 1,000 Metric tonnes)

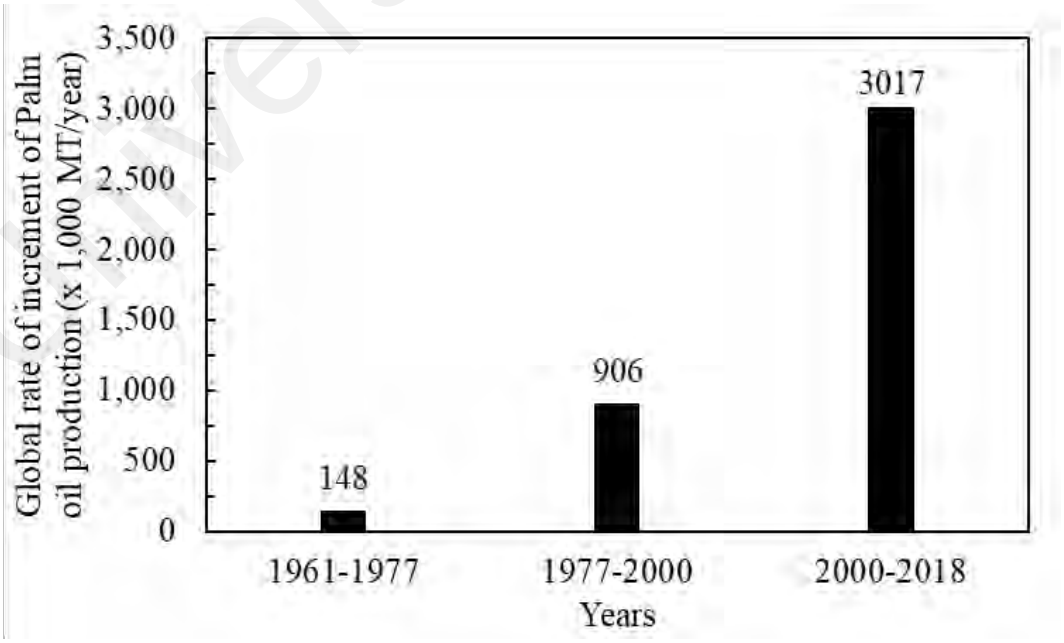

Figure 2.3: Global rate of increment of palm oil production since 1961 till 2018

Currently, palm oil is produced about 80,000,000 Metric ton/ year globally. Malaysia is the second largest producer of palm oil cultivation after Indonesia. Malaysia produced 19,919,331, and 19,516,141 tons of crude palm oil, alone, in 2017, and 2018, respectively (Malaysian Palm Oil Board, 2016, 2018). Huge wastes were generated during this large amount of production of palm oil. Palm oil is extracted from palm oil fruit bunch. About 21% of a palm oil fruit bunch is palm oil, and the remaining 79% is organic waste; thus the estimated wastes only from palm oil industries in Malaysia is about 90 million tons/year (Malaysian Palm Oil Board, 2018).

Sinoh et al. (2021) studied production of wastes from a palm oil mill in Malaysia. About 5tons of palm oil fruit was processed in a single batch for extracting palm oil. During the extraction process, following organic wastes were separated: crude palm oil, oil palm kernel, empty fruit bunch, palm mesocarp fibre, and oil palm shell at the amount of 1ton, 0.41ton, 1.17ton, 0.09ton, and 0.2ton respectively. Based on the proportions of waste generation from palm oil fruit bunch as reported by Sinoh et al., (2021), global total residue from palm oil industry can be analysed with the Figures 2.2, and 2.3 (Figure 2.4, 2.5). Figure 2.5 shows that the global rate of increment of boiler waste generation in 2018 was 1,627,000 Metric Ton.

Large amount of this boiler wastes can be utilised in concrete production as they are pozzolanic material. The main palm oil wastes those can be utilised in concrete production are oil palm shell, palm oil clinker, and palm oil fuel ash (Bashar et al., 2021). In this project as POC is the concern, review on research on POC-based concrete is discussed below.

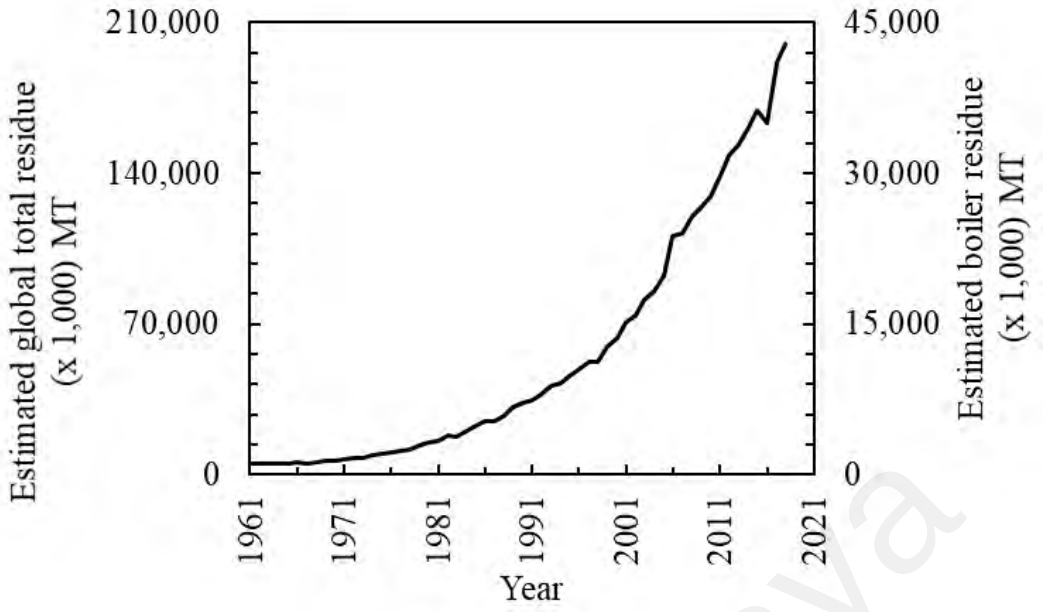

Figure 2.4: Estimated global total residue from palm oil industry

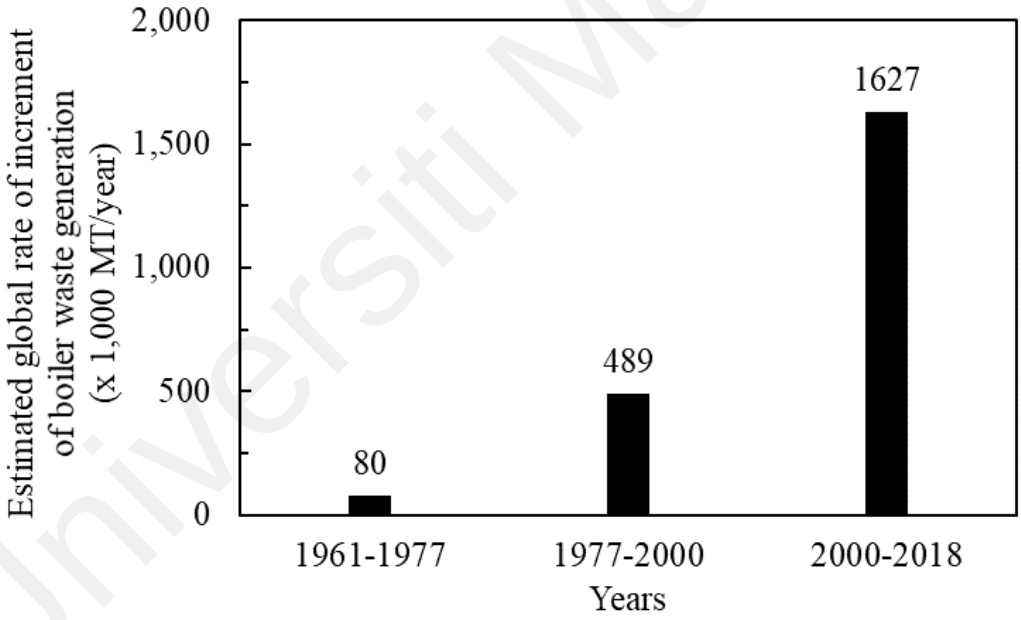

Figure 2.5: Estimated global rate of increment of waste generation from palm oil boiler

2.3 Research status of Palm oil clinker as concrete constituents

This section shows the gradual increase of interests on POC as lightweight aggregate among the research fellows. Zakaria (1986) might be the pioneer to develop a lightweight concrete using POC as aggregate. The short-term mechanical properties were investigated comparing the results with those of normal weight concrete. The research outcome

suggested to use POC up to 20% as aggregate in cement-based concrete. But a question was raised by the researcher, whether the presence of sulphate in POC would be aversive in cement hydration process.

Researchers attempted to reduce the adverse effect of porous nature of POC adopting various techniques. Abutaha et al. (2016) used Department of Environment, UK's method of concrete mix design to design 40 grade concrete, where granite was substituted by POC partially, and fully. The workability, and compressive strength could be achieved comparatively of same as those of normal weight conventional concrete made of granite as aggregate. After finding the potentiality of POC as lightweight aggregate in concrete POC powder was introduced to fill the external pores of POC prior to casting. The adopted method improved the compressive strength of concrete because of the filling pores and better compaction.

Due to porous physical characteristics of POC, it causes the concrete less workable. Kanadasan & Razak (2014) thus, attempted to improve compressive strength and workability using particle packing principle. Feen et al. (2017) investigated a comparable study between 100% granite and 100% POC based self-consolidated concretes' fresh and harden properties. By using low dosage of superplasticiser, the internal friction of POC porous surface was minimised and flowability was increased. The flowability of POC self-consolidated concrete was found more than granite based self-consolidated concrete due to the aggregate particle weight. As Kim et al. (2010) commented that the flowability of normal weight aggregate self-consolidated concrete is less than lightweight aggregate self-consolidated concrete due to the constraint of the heavier matrix and greater collision between aggregates in the mixture.

The suitability of POC as lightweight aggregate is reported by many researchers based on the physical properties of POC. Ahmad & Noor (2007) examined the specific gravity,

water absorption, moisture content, aggregate impact value, bulk density, crushing aggregate value. Various mix proportions were adopted to investigate the compressive strength of lightweight POC-based concrete. Structural grade lightweight concrete was able to produce using POC as aggregate. However, as POC is a porous material, it may consist of higher amount of moisture that influence the strength development in concrete. Thus, Ahmad & Noor (2007) suggested its higher moisture to be taken seriously while designing water quantity in the mix proportion.

Ahmmad et al. (2017) investigated the effect of binding material in compressive, flexural, splitting strength and modulus of elasticity of POC based light weight concrete. POC was used as complete substitute of conventional lightweight coarse aggregate. The binder properties were varied replacing cement with POC powder (POCP). Though 100% POC was used as coarse aggregate, the influence of POC powder as substitute of cement in strength development as pozzolanic material was the focus of investigation and its influence in workability and strength development were addressed. However, the influence of POC aggregate in the fracture mechanism was not investigated in this research.

Like other lightweight concrete, POC-based concrete requires higher amount of paste compared to normal weight concrete. Higher amount of paste has adverse effect in crack initiation at early stage due to drying shrinkage. Ahmad et (2008) reported a higher drying shrinkage in concrete where POC was used as fine and coarse aggregate. The lower elastic property of POC attributes to higher drying shrinkage (Neville & Brooks, 2010).

The chloride penetration through concrete may seriously affect the overall ductility of reinforced concrete in long run due to corrosion on rebar surface that raises a question of existence of required level of strength. Mohammed et. (2011) found that POC-based cement concrete had higher amount of penetration of chloride ion due to porosity in POC

aggregate. However, this penetration of chloride ion depends on the compactness of the concrete. In self-consolidated concrete, or in concrete with good workability, the external pores of POC is covered by matrix, that increases the compactness of the concrete. Kanadasan & Razak (2014) developed self-compacting concrete mix design where POC was used as lightweight aggregate. The particle packing concept was adopted to develop the mix proportions. The evaluation of fresh and harden properties of POC-based self-consolidated concrete suggested the suitability of POC as aggregate in structural grade concrete.

As POC is produced burning at high temperature (> 250°C), it may have less adversity in strength reduction while it is incorporated in concrete and that concrete experiences high temperature. Jumaat et al. (2015) investigated the temperature resistance of POC-based concrete. The weight loss, surface cracking, change of colours and the residual compressive strength were the evaluation criteria in this research. The experimental results were compared with the results of a lightweight concrete made of another palm oil industrial and agricultural waste, oil palm shell (OPS) as aggregate. The weight loss of POC-based concrete was insignificant, the number of cracks due to high temperature was reduced while volume of POC was increased, i.e., when the volume of paste was reduced. The shrinkage of POC-based concrete was not significantly differed from the shrinkage of conventional concrete; but this finding was contradictory with the findings reported by Ahmad et (2008). The difference in paste volume might be caused in variation of shrinkage response.

Omar & Mohamed (2002), and Mohammed et al. (2014) studied the flexural strength of POC-cement-based reinforced concrete beam. Less than 0.5% (Omar & Mohamed, 2002), and 0.35 to 2.23% (Mohammed et al., 2014) reinforcement ratios were used in beam manufacturing. A typical flexural failure was observed. The use POC thus assumed that it had no detrimental effect on flexural strength of reinforced beam. Mohammed et

al. (2014) found the ductility of POC-based beam less than the expected. The deflection was reported 10 to 45% less than the deflection suggested in British standard (1997) (This code has been withdrawn and replaced by Euro code 2 in recent years; but the old version cannot be completely ignored.). A contradictory to commentary can be found in Omar & Mohamed (2002)'s investigation. The mix proportion of concrete constituents may play significant role. Higher amount of paste volume in concrete, comparatively, reduces the ductility of concrete. In lightweight aggregate, generally requires high amount of paste; But if the paste volume is optimised, it may help to reduce the brittleness of concrete due to high volume of paste.

Mohammed et al. (2013) studied the shear behaviour of reinforced concrete beams made of POC as aggregate. Various strengths of POC-based concrete were used. The tension reinforcement ratio, shear span to effective depth ratio, were varied. The shear cracking response was comparatively similar to that of normal weight concrete made of granite as aggregate. The variation of shear span to effective depth ratio did not provide any significant variation in responses of concretes made of POC or granite as aggregate. The variation of tension ratio, and compressive strengths of POC-based concrete had significant influence in shear strength of the beam. Mohammed et al. (2013) compared the experimental results with the prediction formulae suggested by British standard (1997), ACI committee 318, and Eurocode 2. The shear capacity of POC-based on concrete while checked using these building standards, was found overestimated. Therefore, additional safety precautions to be taken were suggested to avoid shear failure of POC-based concrete. This overestimation was meaningful for POC-based concrete. Because POC is porous in nature, and the shear properties vary significantly, when concrete contains large and unpredictable number of pores.

The above literature review addresses research on cement based lightweight concrete where POC was used as lightweight aggregate. The following review have been addressed research on POC-based lightweight geopolymer concrete.

Like Jumaat et al. (2015), Sharmin et al. (2015) investigated a comparison between OPS and POC-based geopolymer concrete. The difference between this two research is that, Sharmin et al. (2015) used geopolymer matrix, and OPS-POC blends in various proportion to investigate engineering properties of concrete, whereas Jumaat et al. (2015), used cement-based matrix, and OPS and POC were not blended. Overall Sharmin et al. (2015) used POC sand as fine aggregate in geopolymer matrix. 50 to 75% of mining sand was replaced by POC sand. The modulus of elasticity and splitting tensile strength was reduced with increment of substitution of mining sand by POC sand. The modulus of elasticity of geopolymer concrete made of 50% substituted POC sand was noticeably less (only 5 GPa) than geopolymer concrete made of mining sand without any substitution. The reasons of reduction of modulus of elasticity and tensile strength of concrete were attributed to OPS for its spongy physical property (Alengaram et al., 2011), and POC for its porous physical nature. Multiple number of micro-cracks were generated while the tension stress was executed, these micro-cracks were appeared for low stiffness of POC (Shannag, 2011).

Above the major and significantly related research on POC-based concrete has been discussed. More research works on development of various mix proportion, and their mechanical properties are available; none of the research addressed the flexural and shear behaviour of geopolymer lightweight concrete where POC had been used as 100% lightweight aggregate. Moreover, the effect of variations of POC sizes in shear resistance of geopolymer beam had not been addressed in earlier research. The role of POC in flexural and shear response of beam is important to know before applying POC-based geopolymer concrete in structural application. Therefore, this research has been focused

to evaluate the flexure and shear responses and the role of POC as lightweight aggregate has been discussed in relation to the discussion of Chapter 5, 6, and 7. The outcome of the finding in this research will be useful for structural engineers and authority to recognise the value of POC as aggregate in geopolymer concrete.

CHAPTER 3: CONSTITUENTS OF GEOPOLYMER CONCRETE

3.1 Overview

The constituents used in the final recipe for the core experiments consisted of fly ash (FA) as binding material, liquid sodium silicate and 14*M* NaOH solution as alkaline reagent for activating pozzolans, manufactured sand (M-sand) as fine aggregate, and granite & palm oil clinker (POC) as coarse aggregate. Other than these ingredients, there were additional raw materials those were used in geopolymer recipes for thorough examination on suitable constituents for this project. Those involved palm oil fuel ash (POFA) & metakaolin (MK) as binding material, and oil palm shell (OPS) as coarse aggregate. POFA was eliminated in the final mix design due to its significant inconsistency of physical and chemical properties. MK was required to mix with POFA at a certain proportion to overcome the limitation of alumina in POFA which was required to achieve desired amount of compressive strength of geopolymer concrete. FA consisted of enough alumina, so, MK was not blended with FA in the final recipe. OPS as agro-industrial waste was intended initially to use as lightweight aggregate. as it improves ductility of concrete (Alengaram et al., 2008, 2016). However, OPS was replaced by POC in final recipe due to two reasons: POC is more sustainable than OPS, and due to being natural, OPS is degraded in corrosive environment. Geopolymer concrete requires alkaline reagents for activating pozzolans. So, OPS has less potentiality than POC as the degradation at the interface between OPS and geopolymer matrix may reduce strength significantly after a long period. Therefore, OPS was replaced by POC which itself is a pozzolan and it is possible for POC-based geopolymer concrete to enhance interfacial bond-strength over time. Though, POFA, MK, and OPS are not used in the final recipe, these industrial by-products, and agricultural wastes, have promising properties to benefit a concrete product. Hence, this chapter includes discussion of all raw materials used in the whole project and the research outcome of POFA-MK-OPS-based lightweight

geopolymer concrete. At the end of this chapter, the limitation of using OPS as a constituent in geopolymer concrete for a permanent structure is explained.

3.2 Binding materials

Palm oil fuel ash (POFA), metakaolin (MK), and fly ash (FA) were used in this project as binding material before finalising the recipe for core experiments (Chapter 4 to 7). However, only FA was used as the main precursor in the final recipe of geopolymer concrete.

POFA is produced as industrial product in palm oil mill. Palm oil is one of the main national income sources in Malaysia and Indonesia. The continuous cultivation of palm tree and the regular extraction of palm oil from palm fruit generates abundant agricultural wastes such as empty fruit bunch, palm fibre (PF), oil palm shell (OPS), and oil palm kernel shell. Palm industries use a proportion of PF-OPS blend in burner to produce temperature up to 250^0C for producing light amount of energy, or up to 800^0C for producing electricity. The fine end-by-product in the boiler is POFA. For this project, POFA was collected from Jugra palm oil mill, Malaysia. The raw POFA was sieved through 300μm size sieve, then dried in an oven, and grounded 30,000 times in a grinding machine.

Metakaolin ($Al_2Si_2O_7$) is a pozzolan which is produced from calcined clay and lime blend through calcination at 500^0C or more (up to 800^0C). Due to presence of high calcium, MK helps to achieve early age strength, and produces Calcium Silicate Hydrate (C-S-H) reacting with $Ca(OH)_2$, thus improves strength over time. MK was collected from Malaysian local supplier for this project.

FA is a pozzolanic by-product of electricity generation power plants. It is produced burning coals at high temperature. The fine particles of FA are driven out of coal-fired boilers with flue gases (Taylor, 1997). Millions of tons of FA are generated each year

from coal-fired power station and petrochemical industries (Scheetz & Earle, 1998) which is the fifth largest industrial by-product in the world (Mukherjee et al., 2008). However, due to having fine particles, it should not be disposed on ground to prevent environmental pollution and it is required to utilise properly to get benefit from its chemical compositions. FA was collected from Lafarge Malaysia (Malayan Cement). No treatment was required for using FA in concrete. But the collected FA was stored in an airtight container before using in concrete.

The chemical composition of POFA, MK, and FA used in this research is shown in Table 3.1. POFA and FA contained total amount of SiO_2, Al_2O_3, and Fe_2O_3 76.14%, and 87.15%, respectively, for which, both pozzolans are classified as F. ASTM International (2012) classifies any pozzolan containing these three oxide compounds 70% or more as Class F.

Table 3.1: Chemical composition of POFA, MK, and FA (weight %)

	CaO	SiO_2	Al_2O_3	MgO	Na_2O	SO_3	K_2O	Fe_2O_3	LOI
POFA	5.57	67.72	3.71	4.04	0.6	1.07	7.67	4.71	6.20
MK	0.04	52.68	42.42	0.12	0.07	0.05	0.34	2.02	1.40
FA	5.31	54.72	27.20	1.10	0.43	1.01	1.00	5.15	6.80

The particle size distributions of POFA, MK, and FA are shown in Figure 3.1, and 3.2. The percent of POFA, MK, and FA passing through 45μm sieve were recorded as 95%, 80%, and 70%, respectively. MK, and FA are finer and more uniformly graded than POFA.

3.3 Fine aggregate

One of the prime motivations in this research is to utilise industrial wastes as concrete constituents. Therefore, manufactured sand (M-sand) which is a treated end-product of industrial by-product, quarry dust. Quarry dust is produced during crushing stones in granite industry.

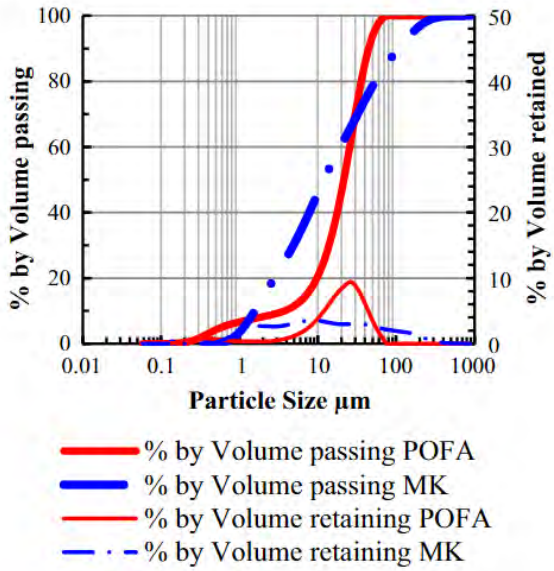

Figure 3.1: Particle size distribution of POFA, and MK

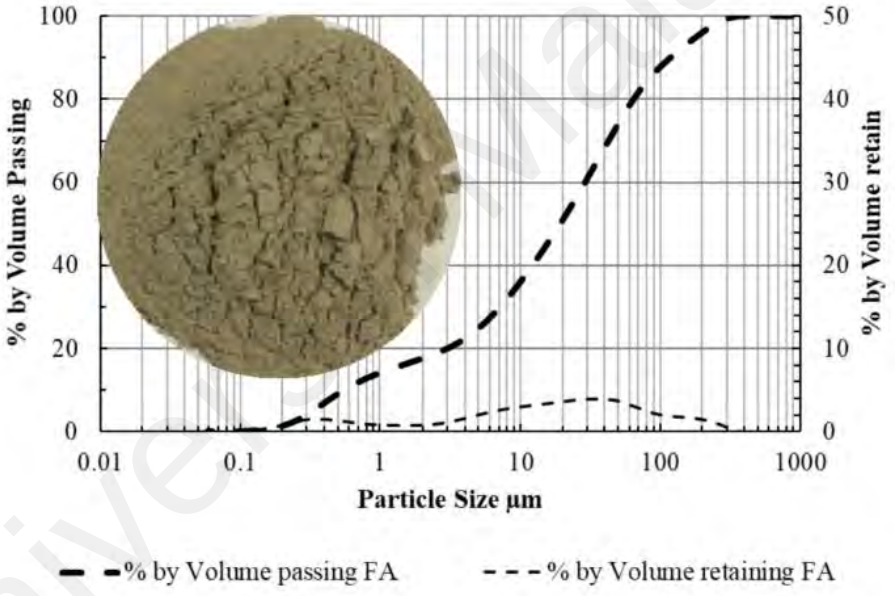

Figure 3.2: Particle size distribution of FA

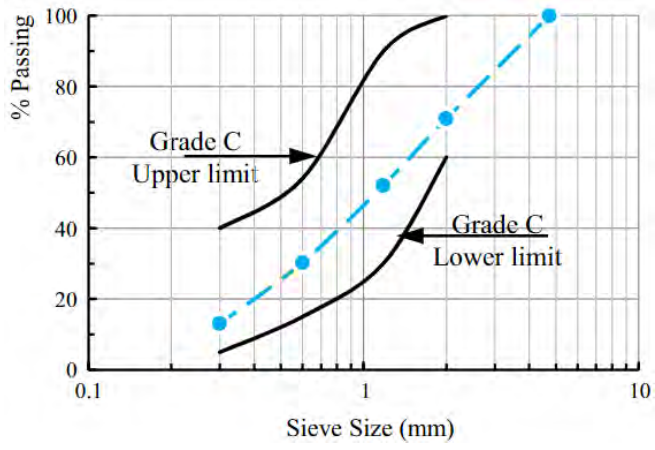

Figure 3.3: Particle size distribution of M-sand

The flaky-elongated shape and sharpen corners of quarry dust are removed using centrifugal forces, that gives a smoothen and round shape of each particle. This end-product is known as M-sand. Previous study (Bashar et al., 2014, 2016b) proves that M-sand provides similar efficiency as mining or river sand shows as fine aggregate in concrete. The particle size distribution of M-sand is shown in Figure 3.3. The fineness modulus is 2.66 and the distribution of particle sizes falls within upper and lower limits of Grade C sand as classified by British Standards Institution (2012).

3.4 Coarse aggregates

Locally available industrial wastes were prioritised to utilise as an alternative of conventional coarse aggregate (granite). The utilisation of feasible substitutes can reduce depletion of natural resources, also, increases their value. Malaysia, Indonesia, Philippine, and other several countries produce abundant oil palm shell (OPS) and palm oil clinker (POC) as agricultural waste and by-products from palm oil industries. Palm industries are main source of economic development in many countries in South-East Asia. Hence, the generation of OPS and POC is a continuous process, it ensures the sustainability. Thus, these two wastes/ by-products got attention of many researchers to utilise as concrete constituents.

OPS is the external shell of palm seed which is required to crush for extracting palm oil from seed. This shell is hard, & ductile, and the inner & outer surfaces of OPS (Figure 3.4) have rows of natural fibres those are beneficial to having concrete-fibre interfacial lock. Its ductile property helps to improve ductility of concrete (Alengaram et al., 2008, 2016). The mechanical properties of OPS-based cement concrete in normal condition (Mannan & Ganapathy, 2002), and at heated condition (Yew et al., 2014) were reported comparable to those properties of granite-based cement concrete.

There was no significant research carried out on OPS-based geopolymer concrete until this PhD candidate has published as part of this research project (Bashar et al., 2016a).

Outer surface Inner surface

Figure 3.4: Oil palm shell (OPS)

The physical properties of coarse aggregates used in this PhD project is shown in Table 3.2. OPS is lightweight aggregate due to its natural organic formation. The specific gravity of OPS is half of granite. It has high rate of water absorption which is about 24 times more than that of granite. As it's ductility is higher than granite, it has less aggregate impact value. At a constant rate of impact load on OPS in closed-side steel mould, OPS shrinks producing less amount of broken particle, whereas granites are broken into small particles due to brittle characteristics. OPS was soaked in water for 24h in water before being used in casting. The surface of OPS was dried before casting to control water quantity in geopolymer concrete.

Table 3.2: Physical properties of coarse aggregates

	Fineness modulus	Specific gravity	Water absorption (24h)	Aggregate impact value
Granite	7.43	2.67	<1	11.9
Crushed OPS	6.25	1.32	24.74	3.93
POC	2.62	1.70	3.30	56.4

The palm oil clinker (POC) was adopted as substitute of granite (coarse aggregate) in the final mix design of geopolymer lightweight concrete instead of OPS. POC is produced in palm oil mill as by-product from burner.

Figure 3.5: Palm oil clinker aggregate (POC)

3.5 Activation of pozzolans

The pozzolans (POFA, FA, GGBS) require alkaline reagent for activation and further geopolymerization for binding the concrete constituents (Van Jaarsveld et al., 1997). The alkaline activator was produced using 14*M* sodium hydroxide (NaOH) and liquid sodium silicate (Na_2SiO_3) of molar ratio (SiO_2:Na_2O) of 2.5. NaOH and Na_2SiO_3 were mixed at a weight proportion 1:2.5 at least 24 h before casting. The geopolymerization is a complex process and the mechanism yet clearly understood. However, Xu and Van Deventer (1999) presented a mechanism that consists of dissolution, transportation, or orientation, and a reprecipitation (polycondensation) steps.

The aluminosilicate pozzolans are the source of $n(Si_2O_5, Al_2O_2)$. In presence of alkaline activator ($2n SiO_2 + 4n H_2O$ + NaOH), pozzolans are activated, dissolved, and produce a geopolymer unit of -Si-O-Al-O-Si-. The geopolymerization continues until Na^+, and geopolymer unit reach to a balanced state. The end product is alike zeolites such as analcite ($NaAlSi_2O_6.H_2O$), Chabazite ($(Ca,K_2,Na_2,Mg)Al_2Si_4O_{12}.6H_2O$), Clinoptilolite

($(Na,K,Ca)_{2\text{-}3}Al_3(Al,Si)_2Si_{13}O_{36}.12H_2O$), Heulandite ($(Ca,Na)_{2\text{-}3}Al_3(Al,Si)_2Si_{13}O_{36}.12H_2O$), natrolite ($Na_2Al_2Si_3O_{10}.2H_2O$), Phillipsite ($(Ca,Na_2,K_2)_3Al_6Si_{10}O_{32}.12H_2O$), and Stilbite ($NaCa_4(Si_{27}Al_9)O_{72}.28(H_2O)$).

$$n(Si_2O_5, Al_2O_2) + 2nSiO_2 + 4nH_2O + NaOH \rightarrow Na^+ + n(OH)_3\text{-Si-O-Al}^-(OH)_2\text{-O-Si-}(OH)_3$$

3.6 Selection of constituents for final mix design

3.6.1 Only fly ash as binding material instead of POFA, and MK blend

The purpose of utilising Palm oil fuel ash (POFA), and Metakaolin (MK) blend in the preliminary research (Chapter 4, and 5) was to investigate the potentiality of utilising POFA as binding material in geopolymer concrete. The candidate has published these research findings: POFA blended with MK (Bashar et al., 2016a), and GGBS-FA (Bashar et al., 2016b), has shown promising results. However, for this research, investigation on lightweight aggregate from palm oil industry was the prime concern, it was required to finalise a binding material, the properties of which is more consistent. The fineness and chemical composition of fly ash was found most consistent among other industrial pozzolans. It has been given permission by the authorities in many countries to utilise as substitute of cement. Whereas, POFA has limitation in consistency in physical and chemical properties. The fineness of POFA is possible to control by sieving to required fine size; but it contains a high percentage of unburnt organic powder. Therefore, the loss on ignition (LOI) of POFA varies from low to high range. In this research (Chapter 4, and 5), the LOI of POFA is comparable with that of FA. However, this is not guaranteed that POFA from the next batch of boiler contains similar amount of LOI. Because, in palm oil industry, the boiler temperature and burning period may vary depending on the energy required for the mill.

The micrographs of FA and POFA show that the fine particles of FA is smooth and round (Figure 3.6), and POFA has micro-pores in fine irregular particle. Because of being highly

porous, POFA requires more liquid to achieve desired amount of workability in geopolymer concrete. To compensate the workability, high amount of alkaline activator (liquid) is required to add, as additional water reduces geopolymer reaction as well as concrete strength. Also, POFA-based geopolymer requires more paste volume to achieve required workability than FA-based geopolymer concrete.

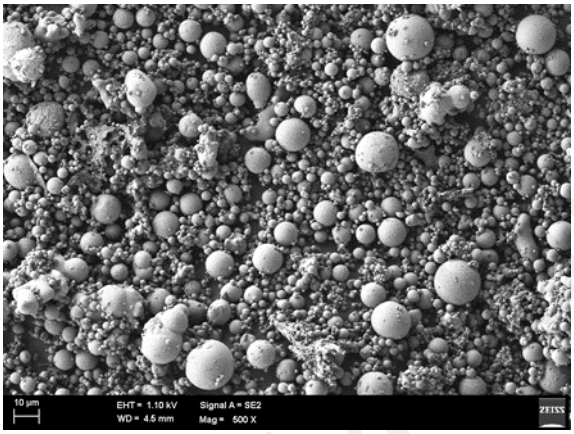

(a)

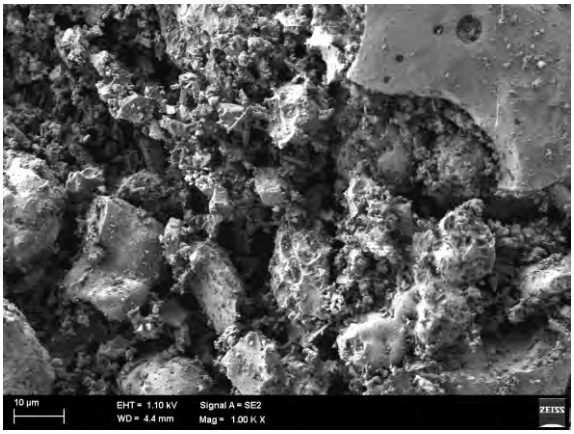

(b)

Figure 3.6: Micrograph of (a) Fly ash and (b) Palm oil fuel ash

The chemical properties of POFA (Table 3.1) shows that it has only 3.71 % Al_2O_3 which is very low amount required for Zeolite production in geopolymer reaction process. To overcome this limitation, POFA has been blended with GGBS and FA (Chapter 4), and only with MK (Chapter 5) as GGBS, FA, and MK contain alumina.

Therefore, FA was selected as the binding pozzolan in the final mix design which is used to investigate the potentiality of lightweight aggregates from palm oil mill for structural application (Chapter 6, 7, 8, and 9).

3.6.2 M-sand as fine aggregate instead of mining sand

M-sand has been selected as fine aggregate in the final mix design of this research. The physical properties of M-sand are comparable with the conventional mining sand. The compressive strength of mortar consisted of M-sand has achieved similar strength as mortar made of mining sand (Chapter 4, candidate published – Bashar et al., 2016b). However, utilisation of M-sand reduces depletion of natural sand, and burden of high-volume quarry dust production as waste in quarry industries. Thus, utilisation of M-sand replacing conventional mining sand in concrete provides benefit to environment.

3.6.3 POC as lightweight aggregate instead of OPS in geopolymer concrete

OPS and POC, both as agricultural waste and industrial by-product, are required to utilise appropriately for environmental benefit. Their potentiality as lightweight aggregates in concrete have been reported by many researchers (Alengaram et al., 2008; Bashar et al., 2016a, 2022; Islam et al., 2017; Mannan & Ganapathy, 2002; Mo et al., 2017). However, geopolymer concrete requires alkaline environment to activate pozzolans; so, the aggregates those are used in geopolymer concrete should be such physical condition that they should not be affected in corrosive environment. As OPS is an organic and bio-degradable material, it has high possibility for corrosion. Because of this reason, it was required to rethink about the lightweight aggregate among the palm oil industrial wastes and by-product. The candidate has conducted research on OPS as lightweight aggregate in geopolymer concrete and investigated its fracture properties. This research was a preliminary plan to utilise OPS as coarse aggregate in geopolymer concrete; but later, OPS was replaced by POC due to its durability concern.

CHAPTER 4: DEVELOPMENT OF SUSTAINABLE GEOPOLYMER MORTAR USING INDUSTRIAL WASTE MATERIALS

4.1 Introduction

Millions of tons of industrial wastes are being generated every year and these wastes cause environmental issue due to shortage of storage facility and safe disposal; this subsequently leads to land and water pollution in the vicinity of factories. The quarry industry produces millions of tons of wastes in the form of quarry dust (QD). About 25% of QD is produced from the production of crushed granite stones for coarse aggregate by stone crusher (Appukutty & Murugesan, 2009). These wastes are dumped in the factory yards and hence reuse of QD might help in reducing the overuse of mining and quarrying. It is to be noted that QD has flaky and sharp edges and hence the removal of these edges would result in more rounded shape particles that could be used as fine aggregates as a replacement for conventional sand. The product of QD after the removal of flaky and sharp edges is known as manufactured sand (M-sand) and the use of this kind of sustainable material could lead to prevention of environmental catastrophe.

Besides the depletion of natural resources, another environmental problem is the greenhouse gas emission. One of the main reasons for the greenhouse gas is the emission of carbon dioxide (CO_2) from the production of ordinary Portland cement (OPC). The development of cement less concrete had been a challenge to the researchers. Davidovits (2008) was one of the pioneers to introduce the term “geopolymer”. Hardjito and Rangan (2005) produced cementless geopolymer concrete using fly ash-a pozzolanic industrial by-product. Rukzon and Chindaprasirt (2009) reported that palm oil fuel ash (POFA), fly ash (FA), blast furnace slag (BFS) and rise husk ash (RHA) have a potentiality to be pozzolanic material. Kupaei et al. (2013) and Liu et al. (2014a) also reported the suitability of POFA and FA to develop lightweight geopolymer concrete. The microstructural and thermal characteristics of POFA/FA based geopolymer mortar was

investigated by Ranjbar et al. (2014) and Liu et al. (2014b). It is known that 85% of world's palm oil is being produced in Indonesia and Malaysia (Nagiah & Azmi, 2013). The abundant production of POFA and FA has increased the potential of these materials to be used as sustainable green materials in the development of geopolymer concrete.

The main objective of this research is to investigate the development of the compressive strength of geopolymer mortar using five locally available waste materials such as FA, POFA, BFS as binders and M-sand, QD as fine aggregates. The effect of M-sand and QD as fine aggregates using POFA and FA as binders was investigated at the outset. An appropriate fine aggregate was used in the next stage of this research to investigate the role of oxide composition of POFA, FA and BFS in geopolymer mortar.

4.2 Experimental programme

4.2.1 Properties of POFA, FA, and BFS

The X-ray fluorescence (XRF) result in Table 4.1 shows that both POFA and FA contain more than 70% of SiO_2, Al_2O_3 & Fe_2O_3 and hence both pozzolans could be categorised as class F according to ASTM International (2012). BFS contained high percent of CaO (45.83%). The fineness of POFA, FA and BFS (above 66% of particles finer than 45 μm) satisfied the standards for natural pozzolans in concrete as recommended in ASTM C618-12. About 90% particles of POFA and FA were found below 38.27 and 101.74 μm, respectively. Figure 4.1 shows all the five local materials used in this investigation.

Table 4.1: Chemical composition of POFA, FA and BFS

	Chemical composition (% by weight)													
	CaO	SiO_2	Al_2O_3	MgO	Na_2O	SO_3	P_2O_5	K_2O	TiO_2	MnO	Fe_2O_3	Cl	CuO	LOI
POFA	4.34	63.41	5.55	3.74	0.16	0.91	3.78	6.33	0.33	0.17	4.19	0.02	0.45	6.54
FA	5.31	54.72	27.28	1.10	0.43	1.01	1.12	1.00	1.82	0.10	5.15	0.36	0.01	0.01
BFS	45.83	32.52	13.71	3.27	0.25	1.80	0.04	0.48	0.73	0.35	0.76	0.08	0.02	-

LOI = loss on ignition

	Physical properties		
	POFA	FA	BFS
Colour	Black	Grey	Off-white
Specific gravity	2.2	2.4	2.9

4.2.2 Properties of N-sand, M-sand, and QD

The major characteristics such as shape, grading and maximum size of N-sand, M-sand and QD are those that affect the fresh and hardened concrete properties. One of the distinct physical properties of QD is its angular shape and this affects the workability of concrete. However, using vertical shaft impact (VSI) technology, the angular shape could be minimized, and the resulting product is christened as M-sand (Figure 4.1(d)). The specific gravity and water absorption of N-sand, M-sand and QD were found in the ranges of 2.61 – 2.79 and 0.81 – 0.92, respectively. The fineness moduli of N-sand, M-sand and QD were found as 2.88, 2.66 and 2.67, respectively.

Figure 4.1: (a) FA; (b) BFS; (c) POFA; (d) M-sand; (e) QD

4.2.3 Mix design, specimen preparation and testing

Different proportions of N-sand, M-sand and QD were varied at the initial stage of this research while keeping the binder/aggregate ratio, water/ binder ratio, activator and curing condition constant. Six mix proportions were used in the second stage varying the binders BFS, POFA and FA in different proportions to investigate the role of oxide compounds in the geopolymer mortar. The details mix proportions are shown in Table 4.2. The activator, sodium hydroxide (NaOH) solution and liquid sodium silicate (Na_2SiO_3) were mixed 24 hours before being used in the mix. The binders were thoroughly mixed in dry condition with fine aggregates at a speed of 140 r/min and the

alkaline activator was then added. The water was gradually added into the mixture and mortar was cast in the 50- mm cube mould and vibrated. The mortars along with moulds were cured in curing chamber at 65°C for 24 hours; then the mortar specimens were removed from moulds and kept in a room temperature and relative humidity of 28°C and 79%, respectively. The compressive strength test was carried out at the ages of 3-, 7-, 14- and 28-day in accordance with ASTM International (2020).

Table 4.2: Mix proportion (kg/m^3)

Investigation: effect of N-sand, M-sand, and QD			
ID	N-sand	M-sand	QD
N100	1029	-	-
M100	-	1029	-
Q100	-	-	1029
NMQ1	514	257	257
NMQ2	257	514	257
NMQ3	257	257	514

Investigation: effect of BFS, POFA, and FA					
ID	BFS	POFA	FA	SiO_2/Al_2O_3	CaO/Al_2O_3
M1	460	-	-	2.37	3.30
M2	-	460	-	11.43	0.78
M3	-	-	460	2.01	0.19
M4	230	230	-	4.98	2.60
M5	-	230	230	3.60	0.29
M6	230	-	230	2.13	1.25

Binder : fine aggregate = 1 : 1.15
POFA : FA = 1 : 1
Water / binder = 0.2
Molarity of NaOH = 14*M*

Binder : M-sand = 1 : 4
Water / binder = 0.4
Molarity of NaOH = 12*M*

Alkaline activator / binder = 0.4; Modulus of Na_2SiO_3 = SiO_2 / Na_2O = 2.5; NaOH solution / liquid Na_2SiO_3 = 2.5.

4.3 Results and discussion

4.3.1 Effect of N-sand, M-Sand and QD on the development of compressive strength

The development of compressive strengths of geopolymer mortar using different proportion of N-sand, M-sand and QD were investigated at the ages of 3-, 7-, 14-, and 28-day (Figure 4.2). The results show that the 28-day compressive strengths for the mixes varied between 21 and 28 N/mm^2. About 76% of the 28-day compressive strength was achieved at the age of 3-day. The pattern of early age strength development supported the findings as reported by previous researchers (Davidovits, 2008; Lloyd & Rangan, 2009). The variation of compressive strength may be because of shape, texture and particle size distribution (Quiroga & Fowler, 2004) of N-sand, M-sand and QD since all other ingredients and conditions remain consistent. Mixes M100 and Q100 showed comparable strength development with N100. The mix, N100 contained rounder and smoother

particle than M100 and Q100 (Quiroga & Fowler, 2004). Hudson (1999) reported that rough aggregates had a propensity for increasing water demand for a given workability. Thus, for a given water content, N100 was more workable than mixes M100 and Q100 (Quiroga & Fowler, 2004) due to smoother surface compared to M-sand and QD. The comparison between the mixes with N100 and M100 showed comparable strengths; however, a slight reduction of strength in M100 could have been due to higher water absorption. The angularity of QD had a positive effect on the compressive strength (Quiroga & Fowler, 2004; Kaplan, 1959) and enhanced the bond between the matrix and the aggregates due to its surface texture (Galloway, 1994).

An insignificant strength reduction was noticed among the mixes due to the increment of either N-sand or QD (Figure 4.2). The voids created due to the combination of semi-rounded, rounded and rough shape could have influenced the strength reduction. Dumitru et al. (1999) also reported the slight reduction of compressive strength in normal weight concrete due to M100 and Q100. Since M100 and Q100 developed comparable strength, both could be considered as viable sustainable replacement for conventional N-sand.

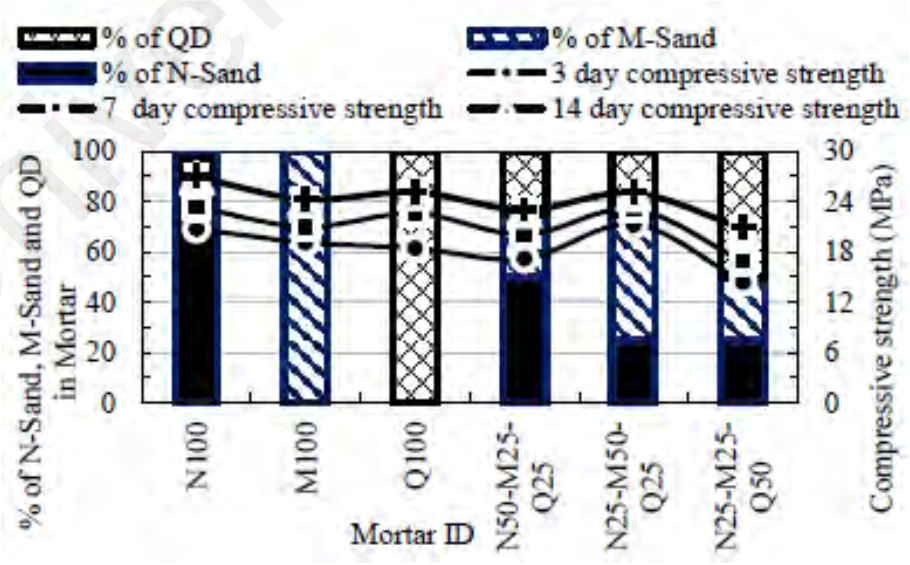

Figure 4.2: Compressive strengths for different mix proportions of N-sand, M-sand and QD.

4.3.2 Role of oxide composition on the development of compressive strength

The development of compressive strengths of mixes M2 (POFA-100%) and M3 (FA-100%) is shown in Figure 4.3. The mix-M3 produced about 50% lower compressive strength than M2 and this could be attributed to reactivity of POFA. Somna et al. (2011) reported that the finer particle and curing in high temperature increased the reactivity in the geopolymerization process. The mix-M4 gained about 5 times higher compressive strength than M5 due to the high volume of BFS.

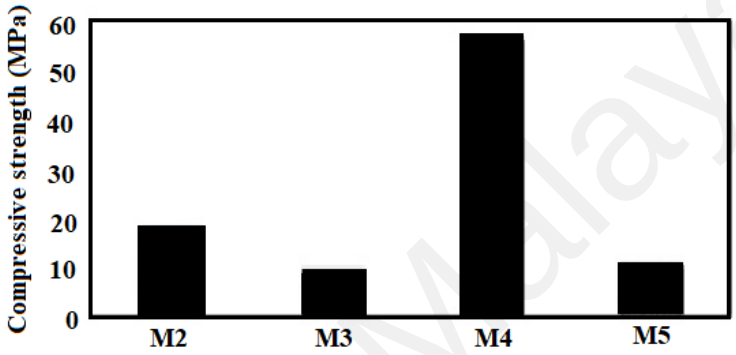

Figure 4.3: Effect of POFA on the compressive strength of mortar

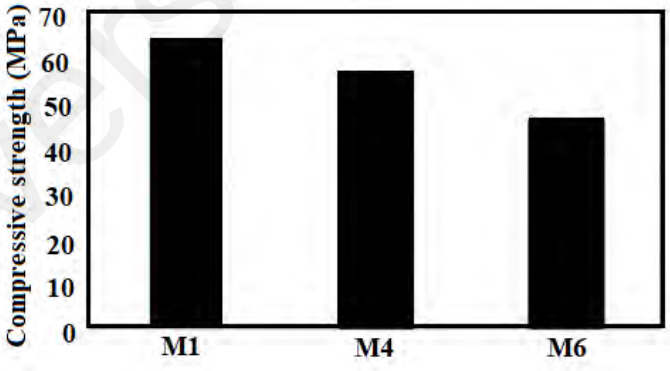

Figure 4.4: Effect of BFS on the compressive strength of mortar

The significant effect of BFS is also noticeable in Figure 4.4. The mix-M1 (BFS-100%) achieved higher compressive strength than the mixes M4 and M6. The effect of the replacement of 50% of BFS by either POFA or FA could be compared with the result achieved by mixes M4 and M6, respectively. Thus, the mix-M4 gained more compressive strength than M6 that could be attributed to the reactivity in geopolymer matrix between

POFA and BFS than BFS and FA. The variation of strength might also be induced by the ratios of SiO_2/Al_2O_3 and CaO/Al_2O_3. The ratios of SiO_2/Al_2O_3 and CaO/Al_2O_3 in the mixes M1 and M3 were 2.37, 3.34 and 2.01, 0.19, respectively. The lowest compressive strength of M3 that contained 100% FA might be attributed to the lowest SiO_2/Al_2O_3 and CaO/Al_2O_3 ratios of 2.01and 0.19, respectively as shown in Table 4.2.

4.4 Summary

The use of M-sand is recommended as a potential replacement for conventional N-sand in concrete as it produced comparable strength in the geopolymer mortar. The shape and water demand of fine aggregates in mortar affected the strength development of POFA-FA based geopolymer mortar. The high ratio of SiO_2/Al_2O_3 and CaO/Al_2O_3 attributed to the development of high compressive strength of geopolymer mortar. The fineness of pozzolans could also influence the development of compressive strength. The geopolymer mortar of binary mix of equal weight proportion of POFA and BFS as binding materials and M-sand as fine aggregate produced a 28-day compressive strength of about 56 MPa. Based on this investigation, POFA could be considered as an ideal pozzolan in the development of geopolymer concrete.

CHAPTER 5: FRACTURE BEHAVIOUR OF OPS-BASED GEOPOLYMER CONCRETE

5.1 Introduction

Geopolymer concrete (GC) could be an alternative of ordinary Portland cement concrete (OPC) (Davidovits, 2008). The greenhouse effect by the emission of CO_2 from the calcination during cement production can be relegated through the application of geopolymer technology in the construction industry. The production of one tonne of cement directly generates 0.55 tonnes of chemical CO_2 and requires the combustion of carbon fuel to yield an additional 0.4 tonnes of CO_2. Conversely, there is no CO_2 production in the geopolymerisation process. The polymeric reaction between silica and alumina exploits in geopolymer using alkaline activators. The alkalinity of the activator can be low to mild or high. The main contents in geopolymerisation process are the silicon and the aluminium. The binder can be produced by a polymeric synthesis of the alkali-activated material from either geological origin or any by-products consisting of silica and alumina as known as pozzolanic material. Hence, the application of geopolymer technology could also be advantageous in term of making use of waste by-product materials from industry.

Palm oil fuel ash (POFA) is one of the largest industrial pozzolanic by-products in the South-East Asia. The abundance and availability of POFA created an ideal platform for the researchers to work on this pozzolanic material as source material in the development of cleaner and sustainable material like GC. Research works on POFA-based geopolymer concrete are limited and the incorporation of metakaolin (MK) along with POFA is another avenue for research towards utilisation of local waste materials in the development of GC.

Besides the environmental pollution due to the production of cement, the consumption of large quantity of natural sand and coarse aggregates (47 billion tonnes/year, Steinberger et al., 2010) has led to a decrease in ground water levels and natural disaster in many countries. In order to ensure sustainable development, researchers, from all around the world have focused their research on applying waste materials to replace the conventional materials (Rukzon & Chindaprasirt, 2009; Safiuddin et al., 2011a; 2011b; Alengaram et al., 2013). Recently, one industrial by-product from the quarry industry as known as manufactured sand (M-sand) and another agro-waste material named oil palm shell (OPS) have drawn the attention of many researchers in the production of lightweight concrete and as full replacement of mining sand (Bashar et al., 2014; Mo et al., 2014; Liu et al., 2014).

Raman et al. (2011), Balamurugan and Perumal (2013), and Ji et al. (2013) reported the potentiality of using quarry fines as a replacement of river/mining sand. The quarry industries produce millions of tons of wastes in the form of quarry dust (QD). These wastes are dumped in the factory yards and hence reuse of QD might help in reducing the overuse of mining and quarrying. The sophisticated technology known as Vertical Shaft Impact Crusher System allows QD to be centrifuged to remove flaky and sharp edges. The end product is commonly known as manufactured sand (M-Sand) and it is popular in some of the developing countries (Westerholm et al., 2008).

Apart from the initiative to utilise M-sand to wholly replace conventional sand, OPS has been used to replace conventional crushed granite aggregate. Researchers (Yap et al., 2014; Liu et al., 2014; Kupaei et al., 2013) explored the suitability of OPS as lightweight aggregate and found that structural grade lightweight concrete could be produced using OPS as coarse aggregate (Mo et al., 2015). During the last three decades, many research works have been carried out using OPS in OPC concrete as lightweight aggregate to replace conventional crushed granite aggregate (Mo et al., 2014; Liu et al., 2014;

Alengaram et al., 2011; 2013; Okpala et al., 1990; Abdullah, 1996); Yap et al. (2014) reported the possibility of significant cost saving due to density reduction as the OPS concrete has about 17–25% lesser density compared to conventional normal weight concrete.

In this research work, high volume of POFA combined with M-sand and OPS as fine and coarse aggregates, respectively were used in the development of a cleaner GC. Like OPC, GC was found good in compressive resistance and weak in tensile properties. Its weakness in tensile resistance could be overcome by using the steel fibres (Guo et al., 2014; Kidalova et al; 2012). The concrete with high compressive strength shows brittleness characteristics due to the low tensile strength which affects a weak bond in the transition zone of the cement matrix (Oehlers et al., 2011; Visintin et al., 2012a). The bond weakness due to low tensile strength of concrete could be mitigated by adding steel fibres in concrete and the use of single type of fibres could improve the tensile property of concrete (Visintin et al. 2012b; 2012c; 2013). Knight et al. (2013) reported the contribution of fibres in the enhancement of strength and toughness retention. The usage of steel fibres in concrete also enhances the toughness as well as impact resistance of concretes (Rashiddadash et al., 2014). Regardless the improvement of tensile properties of concrete using steel fibres, a weak transition zone between steel fibres and paste was observed by the researchers (Zhang et al., 2014a; Oehlers et al., 2013) and this weak bonding was caused due to a lot of porosity in the transition zone. By using appropriate material, the porosity could be reduced as well as consolidate the transition zone (Zhang et al., 2014b; Oehlers et al., 2012a; 2012b). Madhkhan et al. (2012) suggested the usage of pozzolanic material to reduce the porosity in concrete.

The mechanical properties of GC using conventional crushed granite aggregate were reported (Sarker, 2011; Rajerajeswari et al., 2013; Posi et al., 2013). However, the use of POFA and MK as binders and OPS and M-sand as coarse and fine aggregates in GC is

entirely a new area of research, The use of high volume of POFA of 90% and MK as source materials in GC would enable researchers to entirely utilise POFA as sole binder in the development of GC in future; further, the utilisation of M-sand and OPS as fine and coarse aggregates would pave way for the development of lightweight concrete as OPS is considered as lightweight aggregate (Alengaram et al., 2010; 2011; 2013; Bashar et al., 2014). On the other hand, the higher aggregate impact resistance of OPS would enable to test the ability of OPS to resist other engineering properties such as fracture. In addition, to overcome the brittle behaviour of GC, the effects of steel fibres with two different aspect ratios have been investigated and reported through this research work. Ten concrete mixes were prepared and tested for mechanical properties and fracture behaviour of the hardened OPS geopolymer concrete (OPSGC) and the experimental results were compared with normal weight geopolymer concrete (NWGC). The fracture behaviours investigated through four-point bending test include fracture strength, fracture toughness and peak deflection.

The novelty of this research work lies in the development of geopolymer lightweight concrete using high volume POFA, with low content of MK; the addition of two local waste materials-M-sand and OPS as fine and coarse aggregates is another aspect of novelty. This is the first time the effect of M-sand and OPS in GC was investigated. The enhancement of ductile properties of GC by replacing crushed granite aggregates by OPS and by the addition of steel fibres with two aspect ratios and different volume fractions is another innovative aspect of this research work.

5.2 Experimental programme

5.2.1 Materials

The test result based on X-ray fluorescence (XRF) analysis of both POFA, and MK is shown in Table 5.1 and it shows that both contained more than 70% of SiO_2, Al_2O_3 &

Fe_2O_3 and hence both could be categorised as Class F in accordance with ASTM International (2019).

Table 5.1: Chemical composition of POFA and MK (%)

	CaO	SiO_2	Al_2O_3	MgO	Na_2O	SO_3	K_2O	Fe_2O_3	LOI*
POFA	5.57	67.72	3.71	4.04	0.16	1.07	7.67	4.71	6.20
MK	0.04	52.68	42.42	0.12	0.07	0.05	0.34	2.02	1.40

* LOI – Loss on ignition

Figure 5.1 represents the particle size distribution of POFA and MK. The physical properties of POFA and MK are shown in Table 5.2, and it was found that MK was finer and more uniformly graded than POFA. The percent of POFA and MK passing through 45µm sieve were recorded as 95% and 80%, respectively (Figure 5.1) which complies with the recommendation by ASTM International (2019).

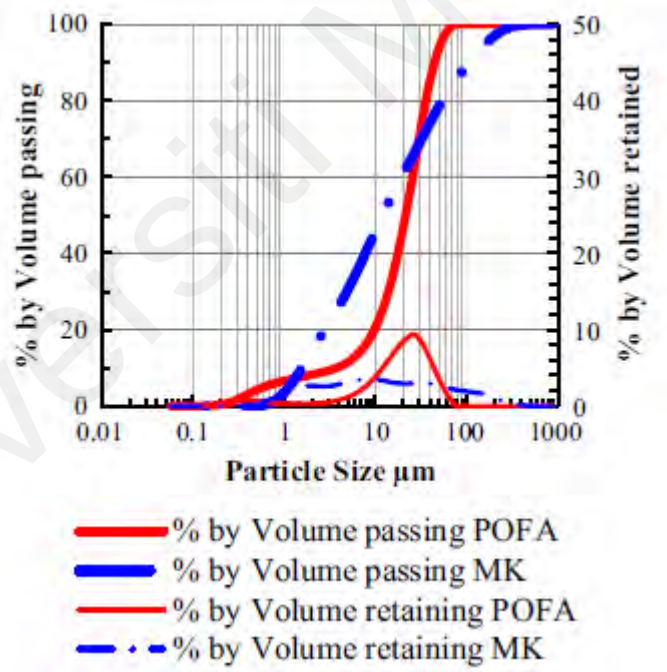

Figure 5.1: Particle size distribution of POFA and MK

Table 5.2: Physical properties of POFA and MK

	Colour	SG	SSA	$D_{[4,3]}$	$D_{[3,2]}$	$D_{[v,\ 0.1]}$	$D_{[v,\ 0.5]}$	$D_{[v,\ 0.9]}$
POFA	Black	2.2	1.72	20.06	3.49	3.23	18.46	38.27
MK	Off-white	2.5	4.33	10.95	1.39	0.48	4.26	32.67

SG = Specific gravity; SSA = Specific surface area, m^2/g; $D_{[4,3]}$ = volume moment mean, µm; $D_{[3,2]}$ = Surface area moment mean, µm; $D_{[v,\ 0.1]}$, $D_{[v,\ 0.5]}$, $D_{[v,\ 0.9]}$ = D10%, 50%, 90% of particle by volume below this size, respectively.

M-sand of Grade C (particle size grading) was used (Table 5.3). Lightweight crushed OPS were used as the whole replacement of conventional crushed granite aggregate. The fineness modulus, specific gravity, water absorption and aggregate impact value (AIV) of OPS and granite were determined based on ASTM International (2012a), ASTM International (2019a), and ASTM International (2020). The 24h water absorption of OPS was found 25% (Table 5.4); since the AIV of OPS were 3 times lower than that of granite, it has been proved that OPS has good impact resistance due to natural fibres. OPS were soaked in water for 24 h in water before being used for casting. Hooked-end type steel fibres of length 60 mm and 35 mm with aspect ratio 80 and 65, respectively were used. The steel fibres had a minimum tensile strength of 1100 MPa as specified by the manufacturer. Potable water was used for all concrete casting.

Table 5.3: Physical properties of M-sand

SG		Absorpt. (%)	FM	D_{10} (mm)	D_{30} (mm)	D_{60} (mm)	C_u	C_c
OD	SSD							
1.97	2.63	0.91	2.66	0.30	0.55	1.42	4.80	0.73

SG = Specific gravity; OD = Oven dry; SSD = Saturated surface dry; Absorpt. = Absorption; FM = Fineness modulus; $C_u = D_{60}/D_{10}$ = uniformity coefficient; $C_c = D_{30}^2/(D_{10} \times D_{60})$ = Coefficient of curvature

Table 5.4: Physical properties of coarse aggregate

	FM	SG	Absorpt. (%)	AIV (%)
Granite	7.43	2.67	< 1	11.9
Crushed OPS	6.25	1.32	24.74	3.93

FM = Fineness modulus; SG = Specific gravity; Absorpt. =Absorption; AIV = Aggregate impact value

5.2.2 Preparation of Alkaline solution and mix design

The alkaline activator using 14*M* sodium hydroxide (NaOH) and liquid sodium silicate (Na_2SiO_3, ratio of SiO_2/Na_2O = 2.5) was prepared at least 24 h before the casting. The sodium silicate liquid was mixed with 14*M* NaOH solution by weight proportion of 1:2.5.

Steel fibres of aspect ratio (AR) 65 and 80 were added with OPSGC in a rate of 0.25%, 0.50% and 0.75% and with NWGC in a rate of 0.50% as a control mix (Table 5.5).

5.2.3 Casting, specimen preparation, curing and testing of fresh and harden concrete

The binders were mixed with the aggregates and steel fibres in the drum mixture of capacity 0.2 m^3 (Figure 5.2). The alkaline activator was then added and mixed properly and then the additional water was added to the mixture. The fresh density of the concrete was then measured. The specimens were cured at 65°C temperature in curing chamber for 48h after 3h of casting and then kept in room temperature of 28°C and relative humidity of 79%. Three specimens were prepared for each test and the average values are reported. The dimensions of specimens and testing standards are shown in Table 5.6. The fracture testing arrangement is shown in Figure 5.3 while Figure 5.4 shows the test specimen with the groove.

Table 5.5: Mix design with variables of steel fibres proportion and aspect ratio

Designation	POFA	MK	M-sand	OPS	Granite	AR65/35	AR80/60	A/B	W/B
OPSGC	508	56	636	212	-	-	-	0.5	0.11
OPSGC65/0.25						19.75	-		
OPSGC80/0.25						-	19.75		
OPSGC65/0.5						39.50	-		
OPSGC80/0.5						-	39.50		
OPSGC65/0.75						59.25	-		
OPSGC80/0.75						-	59.25		
NWGC	510	57	380	-	753	-	-	0.4	0.2
NWGC65/0.5						39.50	-		
NWGC80/0.5						-	39.50		

Table 5.6: Specimens for testing of concrete

Test (age) - Standards	Specimens and dimensions (mm)
Compressive strength (3,7,14&28d)-BS EN12390-3:2019	Cubes: 100×100×100
Indirect tensile strength (28-day)-BS EN12390-6:2009	Cylinders: Ø100×200
Flexural strength (28-day)-BS EN12390-5:2009	Prisms: 100×100×500
Static modulus of elasticity (28-day)-ASTM C469-14	Cylinders: Ø 150×300
Fracture toughness (28-day)-ASTM C1609M-19	Prism: 100×100×500 with a 30mm groove

Figure 5.2: Casting of geopolymer fibre reinforced concrete

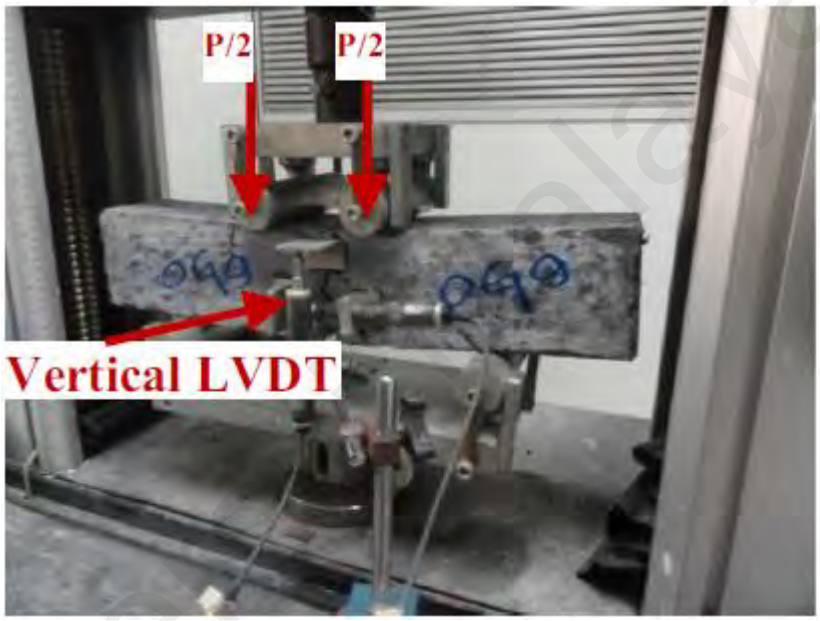

Figure 5.3: Fracture test according to ASTM C1609/C1609M-12

Figure 5.4: Specimens for fracture test

5.3 Results and discussion

5.3.1 Workability and density of concrete

The slump value is one of the important characteristics of the workability of fresh concrete. Though there is no code of practice available for workability tests for

geopolymer concrete (Islam et al., 2015), slump test was carried out to check the workability of the mixes. As expected, zero slump was obtained for the mixes; one of the reasons attributed to zero slump is the use of large quantity of POFA as binder; since POFA has high loss on ignition value it will absorb more water and hence could reduce the workability. Further high silica content in POFA makes the mix more viscous. Generally, geopolymer concretes with high binder content such as POFA or GGBFS result in low slump. Further, OPS is lightweight and hence zero slump was expected, nevertheless using appropriate vibration, the concrete was compacted and upon demoulding no honeycomb was found.

In normal Portland cement concrete the addition of water or superplasticiser enhances the workability of concrete. On the contrary, the usage of excessive water decreases the rate of geopolymerisation (Davidovits, 1991; 1994) as well as the strength of concrete. Therefore, minimum required water was used in consistent rate, and this attributed to zero slump.

The fresh densities of all mixes are shown in Table 5.7. The difference among the fresh densities of OPSGC with and without steel fibres is solely attributed to the proportion of additional steel fibres as all other material proportions were kept constant. As shown in Table 5.5, three mixes of NWGC-one without steel fibres and two mixes with steel fibres of AR65 and 80 of 0.5% (volume fraction) were used for comparison. As expected, higher specific gravity of crushed granite aggregate resulted in higher fresh density of NWGC compared to OPSGC. The fresh densities of all OPSGCs with steel fibres fulfilled the requirement for lightweight aggregate concrete as defined in BS EN 1992-1-1:2004 and the variation of the densities among the mixes was due to different proportions of steel fibres.

5.3.2 Compressive strength

The compressive strengths development at the ages of 3-, 7-, 14- and 28-day are shown in Table 7. The early strength development was found 82–97% and 85–98% of the 28-day compressive strength at the ages of 3- and 7-day, respectively for all geopolymer concrete with or without fibres and this could be attributed by geopolymerisation process during heat curing (Hardjito & Rangan, 2005). The 28-day compressive strength results show that OPSGC achieved 28-day compressive strength of 30 MPa and according to ACI 213R-14, this strength is within the range for structural grade concrete.

Table 5.7: Development of compressive strength

Designation	ρ (kg/m^3)		f_{cu} (MPa)				f_{cu}/ρ
	Fresh	28-day	3-day	7-day	14-day	28-day	
OPSGC	1,830	1,782	28.7	29.0	30.0	30.0	16.84
OPSGC65/0.25	1,845	1,816	28.3	30.6	29.4	31.4	17.26
OPSGC80/0.25	1,845	1,811	28.0	29.4	28.5	30.0	16.54
OPSGC65/0.5	1,880	1,819	26.8	29.0	30.2	30.9	16.99
OPSGC80/0.5	1,860	1,815	26.1	27.2	31.9	31.9	17.55
OPSGC65/0.75	1,890	1,814	30.5	30.9	26.8	31.3	17.25
OPSGC80/0.75	1,875	1,813	29.2	28.5	30.5	30.5	16.85
NWGC	2,045	2,020	26.4	27.0	27.6	27.6	13.67
NWGC65/0.5	2,084	2,022	27.9	28.2	29.1	29.2	14.42
NWGC80/0.5	2,084	2,023	30.3	30.5	31.1	31.7	15.65

ρ = density; f_{cu} = cube compressive strength

Despite the addition of steel fibres in the mixes, the increase in compressive strength was found minimum. In addition, the volume of steel fibres and the aspect ratio (AR) did not have any significant influence on the compressive strength as the 28-day compressive strengths of all these OPSGC mixes were found within 30–32 MPa (Table 5.7). Though research works (Gao et al., 1997; Neves & Almeida, 2005) showed that higher AR provided better performance, it was not evident in the mixes with AR80 and AR65. Mo et al. (2014) related the occurrence of micro-crack in the lightweight aggregate during loading as an explanation of how the steel fibres helped improving compressive strength.

It is known that lightweight aggregate has less aggregate crushing value than normal weight aggregate. Therefore, cracks occurred in the coarse aggregate before extending into the mortar (Mo et al., 2014).

Gao et al. (1997) reported that a sufficient bonding between steel fibres and binding material increased the compressive strength of lightweight concrete. However, insignificant improvement of compressive strength was noticed for OPSGC and NWGC with steel fibres in this research work. This could be due to the porosity in geopolymer concrete which was induced by the viscous geopolymer binding matrix.

OPSGC with steel fibres of AR65 (OPSGC-65) achieved slightly higher compressive strength than OPSGC 80 for the same volume of steel fibres in concrete. Steel fibres of AR 65 (SF(AR65)) had 3.33 times more surface area than same volume of SF(AR80). The large surface area of steel fibres might enhance the bond resistance and crack propagation due to stiffness of fibres (Neves & Almeida, 2005). However, a reverse result was noticed for NWGC; NWGC-80/0.50 achieved slightly higher compressive strength than NWGC-65/0.50. The mortar quantity to total surface area of steel fibres and aggregates might have a relation that altered the result. As seen in Table 5.5, the total amount of mortar ingredients (quantity of binder and fine aggregate) was 1.27 times less in NWGC than OPSGC.

Compressive strength and density are related to each other. Higher value of the ratio of compressive strength to density (f_{cu}/d) ratio was found for lightweight concrete compared to normal concrete. As seen from Table 5.7, OPSGC, OPSGC-80/0.25 and NWGC-65/0.50 achieved compressive strength of about 30 MPa, but the strength to density ratios of OPSGC were found higher than the NWGC due to high density of the latter.

5.3.3 Flexural strength

The steel fibres play an important role in the development of flexural strength and its significance in the development of flexural strength is more than that in the development of compressive strength. The experimental values of flexural strengths of OPSGC and NWGC with different volumes of steel fibres and AR65 and AR80 are shown in Table 5.8. The increment of flexural strength due to the addition of steel fibres was noticed in the range of 7–18% in OPSGC. The highest flexural strength of 5.14 MPa was achieved for OPSGC-80/0.75. The improvement of flexural strength due to the increase in steel fibres was noticed for both mixes with AR65 and AR80; further, this improvement was found higher in the case of AR80 compared to that of AR65.

Table 5.8: Flexural, indirect tensile strengths and modulus of elasticity

Designation	f_f (MPa)	f_t (MPa)	E (GPa)		f_f/f_t
			Exp.	Eq. (5.1)	
OPSGC	4.33	2.22	6.25	-	1.95
OPSGC65/0.25	4.69	2.81	6.56	-	1.67
OPSGC80/0.25	4.65	2.55	8.68	7.64	1.82
OPSGC65/0.5	4.72	2.88	8.69	-	1.64
OPSGC80/0.5	4.80	2.89	9.10	8.72	1.66
OPSGC65/0.75	4.86	2.93	8.72	-	1.66
OPSGC80/0.75	5.14	3.07	10.00	7.97	1.67
NWGC	3.41	2.31	22.35	-	1.48
NWGC65/0.5	3.61	2.62	22.70	-	1.38
NWGC80/0.5	3.67	2.60	23.21	-	1.41

f_f = flexural strength at 28-day age; f_t = indirect tensile strength at 28-day age; E = modulus of elasticity at 28-day age

OPSGC-65/0.25 achieved about 8% more flexural strength (4.69 MPa) compared to OPSGC (4.33 MPa); with further increase in the fibres volume (OPSGC-65/0.50 and OPSGC-65/0.75), the increment was found higher (9% and 12%). Thus, the volume of steel fibres added in the mixes had direct influence on the flexural strength (Figure 5.5). Higher volume of steel fibres achieved higher flexural strength. Gencel et al. (2011) studied the mechanical performance of fibre-reinforced self-compacting concrete with fly

ash and reported the significance of steel fibres in the improvement of flexural strength of concrete.

The influence of steel fibres in concrete and the volume of steel fibres could be understood from the mechanism of flexural strength behaviour of concrete prism under loading. The concrete prism specimens were subjected to bending during flexural strength test; the tensile and compressive strength in prism section depend on the position of the neutral axis (Criswell, 1986; Hoyle, 1984; Neville, 1995). Gencel (2011) reported that the compression phase of the prism was stressed about 11–17% of the compressive strength of the material at the failure loading. Therefore, compression zone had an insignificant role to failure. By contrast, tension zone played role in the development of flexural strength. Randomly distributed steel fibres controlled the tension zone by withstanding crack generation and thus enhanced the flexural strength (Atis & Karahan, 2009). High volume of steel fibres might withstand more crack generation in tension zone and thus enhanced the flexural strength of concrete.

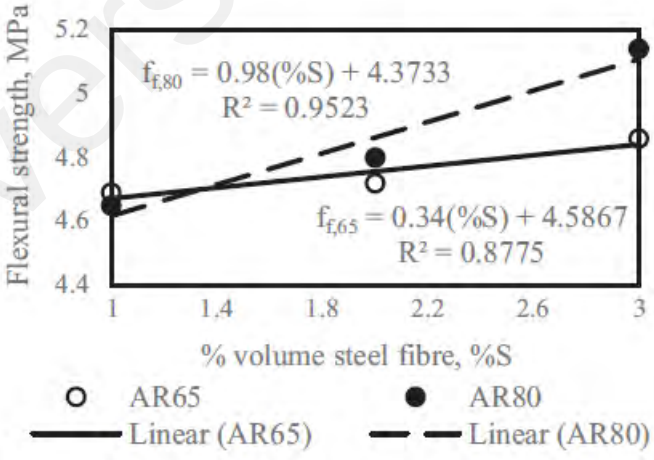

Figure 5.5: Development of flexural strength for different % volume of steel fibres

The aspect ratio (length/diameter) of steel fibres had direct influence on the development of flexural strength. The flexural strength enhancement of 8–12% and 7–18% was found for AR65 and AR80, respectively with 0.25%, 0.5% and 0.75% of steel fibres volume.

As seen from Figure 5., the mixes with AR80 showed higher gradient than the corresponding mixes with AR65. A comparison between mixes with same volume fraction, but different AR shows that mixes with higher AR produced higher flexural strength. Since AR is the ratio of length to diameter of the steel fibres, AR80 has more surface area than AR60 and this would influence stronger bond between the steel fibres and binding matrix by improving the stiffness to resist crack propagation. Other research works (Gao et al., 1997; Koksal et al., 2008) also support this finding and Köksal et al. (2008) investigated the effectiveness of higher AR and concluded that longer steel fibres had higher capability of delaying crack propagation in concrete.

NWGC produced the lowest flexural strength among all the mix proportions. On contrary, OPSGC performed better flexural strength. The improvement of flexural strength due to the OPS was reported by other research work (Yap et al., 2013). As seen in Table 5.8, NWGC and OPSGC achieved flexural strength of 12.35% and 14.43% of 28-day compressive strength. Alengaram (2010) reported these values for cement based normal weight and OPS concrete as 14% and 10%, respectively. According to Alengaram (2010), percent of flexural strength of 28-day compressive strength was more in normal weight concrete than OPS concrete. The slight reduction of flexural strength in OPS based concrete was due to lower strength and stiffness of OPS. However, as seen in current research work, the reverse result might be affected by the volume of M-sand content in OPSGC and NWGC. OPSGC which contained more volume of M-sand than as mixed in NWGC, might have better compact ability by the fine particles of M-sand and thus enhanced the percent of flexural strength of 28-day compressive strength. Alengaram (2008) also found that the increment of fine aggregate content enhanced the flexural performance of concrete.

Generally, the failure in tension occurs due to the breakdown of bond between the matrix and the surface of the aggregate or by fracture of the matrix itself and not by fracture of

the aggregate. Since there is less evidence on aggregate fracture compared to bond failure between binding matrix and aggregate (Figure 5.6), the bond failure governs the flexural strength.

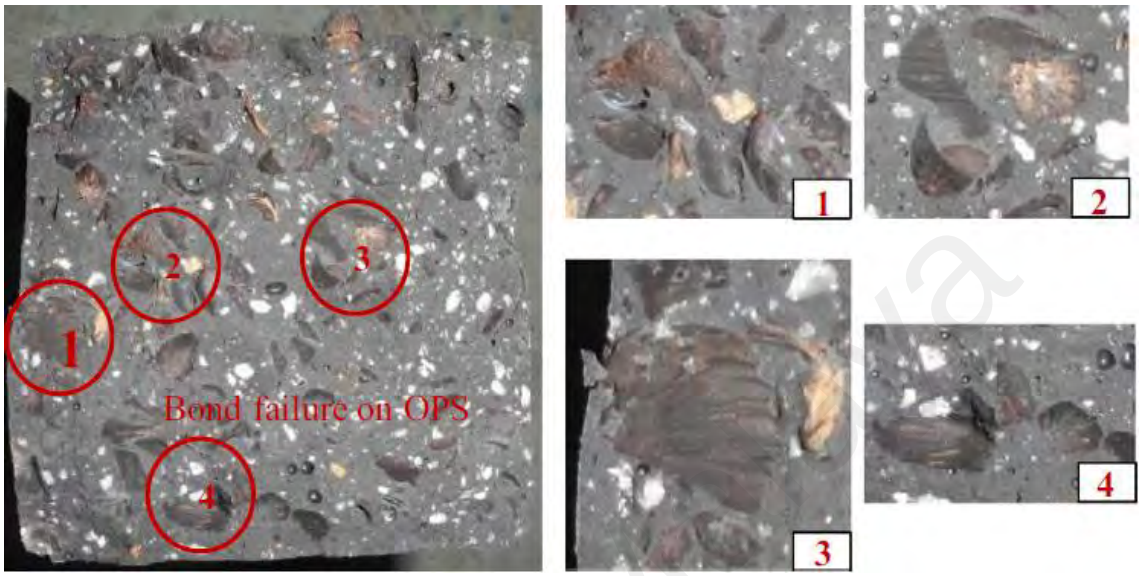

Figure 5.6: Bond failure between OPS surface and binding matrix

5.3.4 Indirect tensile strength

The splitting tensile test, which is known as the indirect tensile strength test, provides the maximum tensile load which may be induced on the concrete member before cracking. The results on the effects of volume and aspect ratio of steel fibres in the development of indirect tensile strength (ITS) are shown in Table 5.8.

The addition of steel fibres increased ITS of both OPSGC and NWGC and this was supported by previous research works (Wang & Wang, 2007; 2013). The increments of ITS of OPSGC due to the addition of 0.25, 0.50 and 0.75% of fibres were found as 27–32% and 15–38%, for mixes with AR of 65 and 80, respectively. The mix OPSGC-80 achieved higher ITS than OPSGC-65 for 0.5% and 0.75% steel fibres volume. The load that induced overstress in non-fibre reinforced concrete and led to develop crack and substantial failure in concrete, would withstand further crack propagation due to the

addition of steel fibres (Gencel et al., 2011). Wang and Wang (2013) reported the improvement of ITS up to 92.50% due to addition of fibres from 0% to 2% of volume.

The mechanism of crack propagation in fibre-reinforced concrete could be explained from Figure 5.7 (Mandell et al., 1985; Huang & Talreja, 2006). Once crack propagated in the matrix, the effective stiffness was reduced due to the fracture (Huang & Talreja, 2006). The tensile stress was then transferred through steel fibres. The steel fibres bridged micro cracks and prevented further propagation to macro cracks as well as expansion and thus substantially improved the ITS.

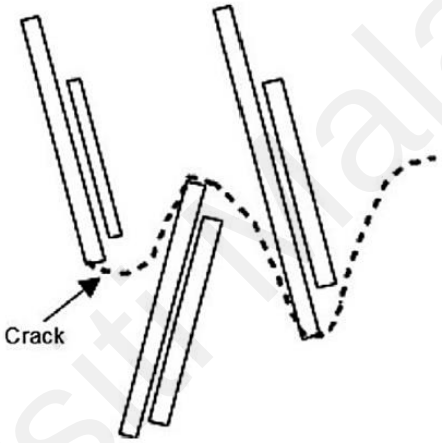

Figure 5.7: Fibre's avoidance mode of crack propagation; schematically reproduced from Mandell et al. (1985)

The ITS values of both mixes-NWGC-65/0.50 and NWGC-80/0.50 show an increase of about 13% compared to the corresponding control concrete-NWGC. The ratios between the 28-day ITS and compressive strength for OPSGC and NWGC were found as 7% and 8%, respectively. The highest ITS in OPSGC-80/0.75 could be attributed to both steel fibres and increase in volume of steel fibres. The ratio of flexural to splitting tensile strength was found about 1.67 for OPSGC-65 and OPSGC-80.

Figure 5.8 represents a relationship between ITS and percentage of steel fibres volume with AR of 65 and 80. The intersection between the slopes of AR65 and 80 as shown in

Figure 5.8 shows that the ITS of about 2.9 MPa could be achieved by the addition of about 0.55% steel fibres volume.

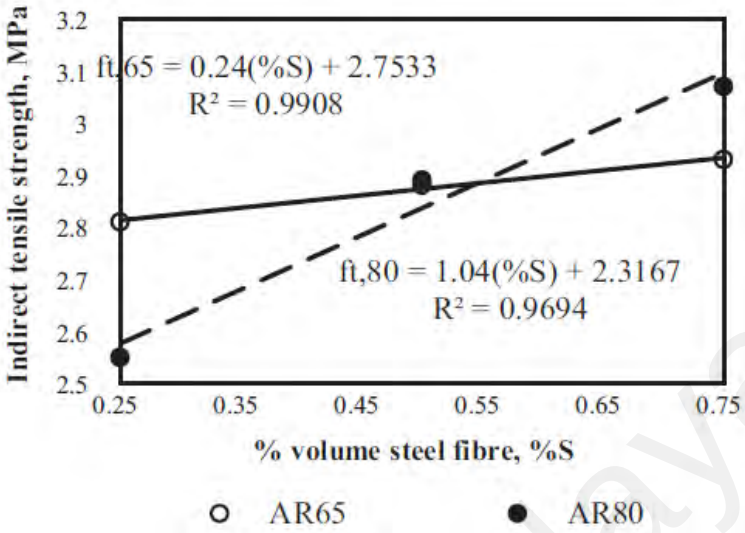

Figure 5.8: Development of indirect tensile strength for different % volume of steel fibres

5.3.5 Static modulus of elasticity

The Young's modulus of elasticity (MoE) is shown in Table 8 for the different volume of steel fibres addition in OPSGC and NWGC. The MoE of OPSGC was 3.5 times less than NWGC. The highest value of MoE in OPSGC was found for OPSGC-80/0.75 as 10 GPa. It is noted that flexural and indirect tensile strength also showed the highest result for OPSGC-80/0.75. The addition of steel fibres improved the MoE 4–60% and 1–4% of OPSGC and NWGC, respectively; higher volume of steel fibres in concrete resulted higher MoE. Kurugöl et al. (2008) reported similar outcome that addition of steel fibres increased the MoE.

A comparison of volume of steel fibres and MoE is shown in Figure 5.9. MoE increased with increment of % volume of steel fibres in both AR65 and 80. Mo et al. (2014) proposed following Eq. (5.1) to correlate the MoE with the compressive strength of fibre reinforced OPS based lightweight concrete containing steel fibres of AR80.

$$E = 6.31\sqrt{f_{cu}} - 26.9 \quad (5.1)$$

A comparison between the experimental result and the above equation is shown in Table 5.8. The deviation of the estimated result could be due to the usage of different proportion of OPS and binding material.

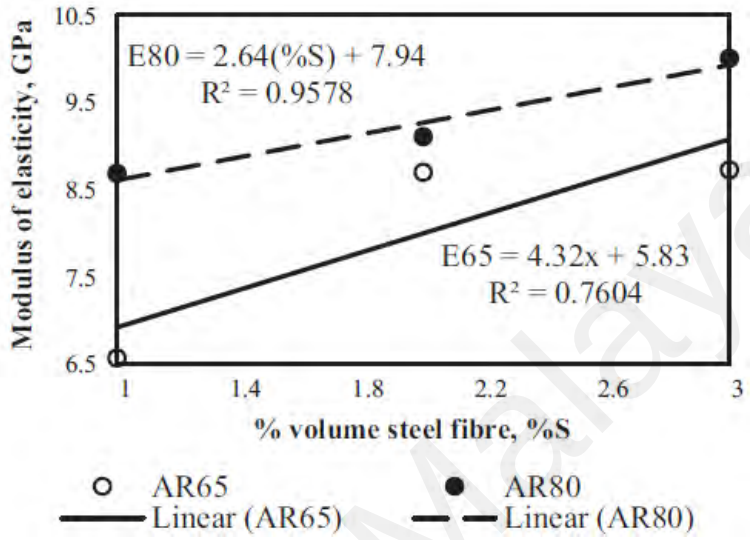

Figure 5.9: Development of MoE for different % volume of steel fibres

A typical stress–strain curve of concrete specimen is shown in Figure 5.10(a) and (b) shows the experimental stress–strain curves of six selected concrete specimens with and without fibre in lightweight and normal weight geopolymer concrete. Figure 5.10(a) defines the different stages of concrete before crushing under compression load. The elastic behaviour of concrete lasts up to about 40% of the ultimate load and then the plastic behaviour of concrete takes place. The non-linear plastic state is a function of the microcracks at paste-aggregate interface. The concrete reaches the ultimate stress through non-linear strain-hardening followed by strain softening once the micro-cracks in concrete accumulate in large amount.

In general, all specimens behaved elastically within the elastic limits as observed from Figure 5.10(b). Fibred and non-fibred OPSGC had higher strains compared to fibred and non-fibred NWGC at ultimate stress. Hence OPSGC with and without fibres produced

lower MoE than the corresponding NWGC. For Portland cement based normal weight concrete, the strain of 0.002 mm/mm corresponding to the ultimate stress is well established and the strain during crushing of concrete reaches between 0.0028 mm/mm and 0.0045 mm/mm. In this investigation, the strains at ultimate stress for both fibred and non-fibred OPSGC and NWGC were found about 0.006 mm/mm and 0.0035 mm/mm, respectively.

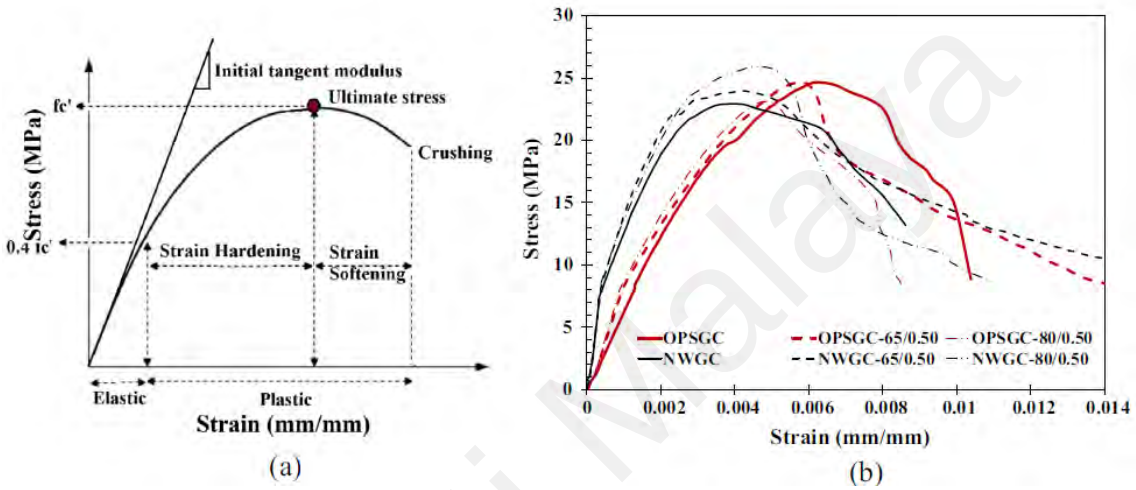

Figure 5.10: (a) Typical Stress–Strain curve of concrete in compression; (b) stress–strain curves from this experiment

The higher strain in OPSGC is attributed to the low stiffness of OPS aggregates and its ductile property. Islam et al. (2015) reported a strain of about 0.003 mm/mm at ultimate stress for POFA (40%)-GGBS (60%) based OPSGC. However, in this research, the POFA content is 90% with 10% MK and hence the high content of POFA could influence strain in the specimens Similar to Portland cement concrete, steel fibres enhanced the ductility of OPSGC and NWGC. The elastic limit of fibred and non-fibred OPSGC and NWGC was obtained at about 33% of the ultimate stress. After initial tangent modulus, the curves show yielding of concrete in non-linear manner and this could be defined as plastic state of concrete. During the plastic stage, the strain hardening, and strain softening took place and this was followed by the crushing of concrete. The aggregate and binder matrix have significance in the development of ductility. The higher ductility

characteristic of OPSGC is governed by OPS and high volume of POFA in binding matrix.

The effect of AR of steel fibres on ductility in both the OPSGC and NWGC is noticeable as shown in Figure 5.10(b). The mixes with fibres of AR65 showed higher ductility than the corresponding mixes with AR80. The low ductility of mixes with fibres of AR80 could be attributed to the number of fibres as the fibres with AR65 has higher number compared to AR80 for a given volume of fibres; thus, with lower number of fibres in the mixes with AR80, the distribution of fibres was not uniform throughout the cohesive geopolymer matrix.

5.3.6 Characteristics of fracture toughness

The steel fibres have significant effect on the fracture behaviour of concrete. The fracture failure is shown in Figure 5.11. Table 5.9 shows the characteristic properties of fracture toughness. These properties were derived from the load deflection curve and shown the performance of fibre-reinforced concrete. According to ASTM International (2019c), toughness properties are recommended to determine for two deflection limits as L/600 and L/150, whereas L is defined as beam span. The end point deflection which was calculated at L/150, was a constant value of 2.0 for all types of concrete material in this experiment (Table 5.9).

Figure 5.11: Fracture failure

The first peak load (P_1) is the load for the first point of zero slope in the load–deflection curve. The non-fibred OPSGC and NWGC achieved first peak load of 6.99 and 6.09 kN, respectively. The higher value of P1 signified the ductile property of OPSGC as well as hardened composite of OPS and geopolymer matrix. The value of P_1 varied from 6.39 to 11.16 kN and 6.13 to 7.05 kN with the addition of 0.25, 0.50 and 0.75% volume of $SF_{(AR65)}$ and $SF_{(AR80)}$, respectively.

Table 5.9: Fracture characteristics for different mix designs

	Fracture characteristics (Part 1)						
Designation	Δ (mm)	P_1 (kN)	δ_1 (mm)	f_1 (MPa)	P_p (kN)	δ_p (mm)	f_p (MPa)
OPSGC	-	6.99	1.14	2.61	6.99	1.14	2.61
OPSGC65/0.25	2.00	6.10	1.94	3.79	6.10	1.94	3.79
OPSGC80/0.25	2.00	6.13	1.51	3.75	6.13	1.51	3.75
OPSGC65/0.5	2.00	6.39	0.86	3.54	6.39	0.86	3.54
OPSGC80/0.5	2.00	6.25	0.26	3.34	6.25	0.26	3.34
OPSGC65/0.75	2.00	7.12	1.06	4.16	7.12	1.06	4.16
OPSGC80/0.75	2.00	7.05	1.03	3.84	7.05	1.09	3.84
NWGC	-	6.05	0.39	3.64	6.05	0.39	3.64
NWGC65/0.5	2.00	6.01	1.62	3.68	6.01	1.62	3.68
NWGC80/0.5	2.00	6.00	1.35	3.67	3.86	6.32	2.37

Δ = end point deflection; P_1 = first peak load; δ_1 = first peak deflection; f_1 = first peak strength; P_p = peak load; δ_p = deflection at peak load; f_p = strength at peak load

	Fracture characteristics (Part 2)						
Designation	P_{600}^D (kN)	P_{150}^D (kN)	f_{600}^D (MPa)	f_{150}^D (MPa)		T_{150}^D (J)	$R_{T,150}^D$
OPSGC	1.74	6.99	0.65	2.61		3.03	0.02
OPSGC65/0.25	0.09	3.83	0.06	2.38		3.41	0.03
OPSGC80/0.25	0.68	2.92	0.41	1.79		4.86	0.04
OPSGC65/0.5	3.92	0.36	2.17	0.20		4.22	0.03
OPSGC80/0.5	4.43	3.15	2.37	1.68		6.82	0.06
OPSGC65/0.75	5.07	4.63	2.97	2.71		6.37	0.04
OPSGC80/0.75	2.90	5.42	1.58	2.95		8.19	0.06
NWGC	0.04	0.18	0.02	0.11		0.94	0.01
NWGC65/0.5	2.54	2.35	1.56	1.44		3.01	0.03
NWGC80/0.5	1.31	3.24	0.80	1.99		4.40	0.04

P_{600}^D, P_{150}^D = residual load; f_{600}^D, f_{150}^D= residual strength; T_{150}^D=Toughness; $R_{T,150}^D$=equivalent flexural strength ratio

The highest value of P_1 (11.16 kN) was achieved for OPSGC-65/0.75 and an insignificant deviation of P_1 was noticed for $SF_{(AR80)}$. The first peak load is influenced by bond between steel fibres and mortar. The effect of steel fibres in OPSGC was found more significant than that in NWGC. NWGC-65/0.5 and NWGC-80/0.5 achieved P_1 as 5.85 and 3.22 kN, respectively. It should be noted that NWGC was designed as a control mix to compare with fibred and non-fibred OPSGC. It was noted that both OPSGC and NWGC showed enhanced P_1 due to the addition of SF. The first peak strength (f_1) was related directly to P_1 by arithmetical equation of P_1/cross-sectional area and thus f_1 gave an idea of ductility performance of concrete as shown in Table 5.9. The first-peak deflection (d_1) of a beam under flexure could be related to P_1 and ductile performance of concrete. The higher deflection to achieve the same value of P_1 connoted that concrete absorbed more energy to gain P_1; however, this information is not sufficient to decide about the ductility of a concrete. The ductility could be understood from the toughness of a concrete. ASTM C1609/C1609 M-12 calculates the toughness at the deflection of L/150. Both the OPSGC-80/0.25 and OPSGC-80/0.50 needed similar P_1 of value 6.13 kN to reach d_1 to 1.51 and 0.26 mm, respectively; however, OPSGC-80/0.50 absorbed more energy and gained 1.6 times higher toughness than OPSGC-80/0.25 due to the presence of higher volume of steel fibre. OPSGC-80/0.25 reached maximum d_1 of 1.51 mm at P_1 of 6.13 kN.

First peak deflection (FPD): The first peak deflection (FPD) is the measure of the deflection during the first peak load. Figure 5.12 shows a comparison of the first peak deflection of all the mix designs with and without steel fibres of AR65 and 80 in FOPSGC and NWGC. The FPD was measured about 34% higher for OPSGC than NWGC and this could be due to higher ductility of the former. It should be noted that OPSGC and NWGC have no steel fibre, therefore, no residual deflection could be found, and an immediate failure of the specimens was observed after the first peak load. An addition of 0.25% and

0.5% of steel fibres of AR65 has insignificant effect and reduces the FPD whereas, 0.75% of steel fibres of AR65 has slight improvement of FPD.

The highest FPD was observed for the addition of 0.25% of steel fibres with AR80 in OPSGC. The longer fibre size and an appropriate mix proportion of 0.25% of AR80 in OPSGC could be attributed to the enhanced performance of mix with AR80. The addition of steel fibres with NWGC improves FPD and AR80 has better role than AR65 in the FPD.

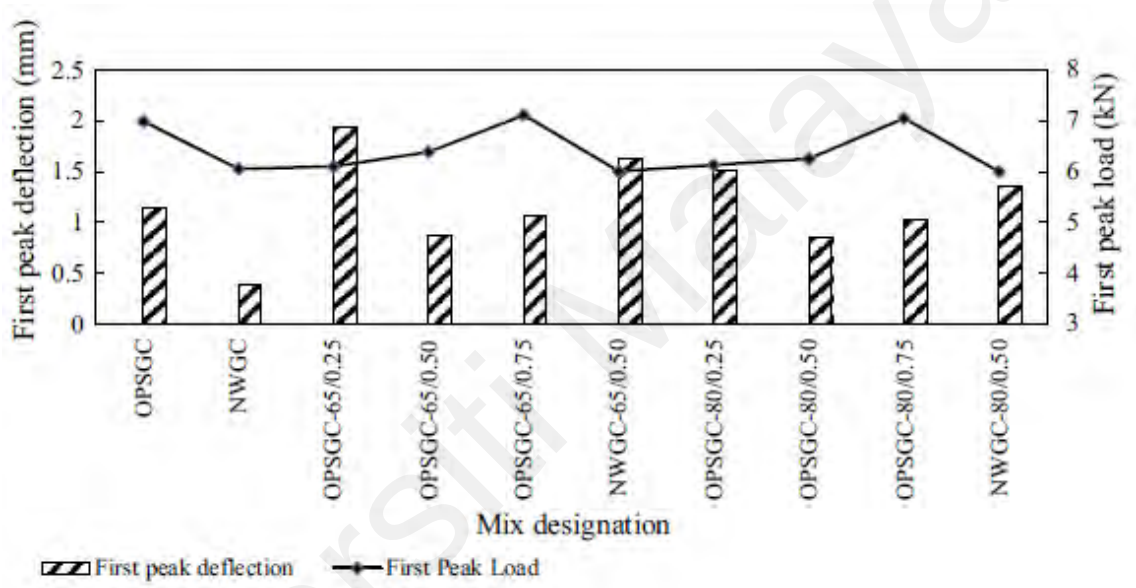

Figure 5.12: First peak deflection for all mix designs

5.3.7 Fracture strength

The first-peak strength (FPS) has the significance in characterisation of the fibre-reinforced concrete (ASTM International, 2019c). The behaviour of first peak load and the first peak strength of fibred and non-fibred OPSGC and NWGC are shown in Figure 5.13.

The FPS of non-fibred NWGC was 1.4 times higher than that of non-fibred OPSGC. A slightly different The FPS was improved on the addition of steel fibres in both OPSGC and NWGC. The addition of 0.75% steel fibres of AR65 shows the highest FPS. The OPSGC containing 0.75% volume of steel fibres with AR80 produced 41% lower

strength than the corresponding volume of fibres with AR65. The higher FPS of AR65 was found for 0.25% and 0.5% volume of steel fibres. This could be attributed by the total surface area of the steel fibres that has an important role in the development of bond strength. For a given volume of steel fibres, the number of fibres with AR65 is more than that of AR80 and hence in an identical % volume of fibres, AR65 consists of more surface area than AR80.

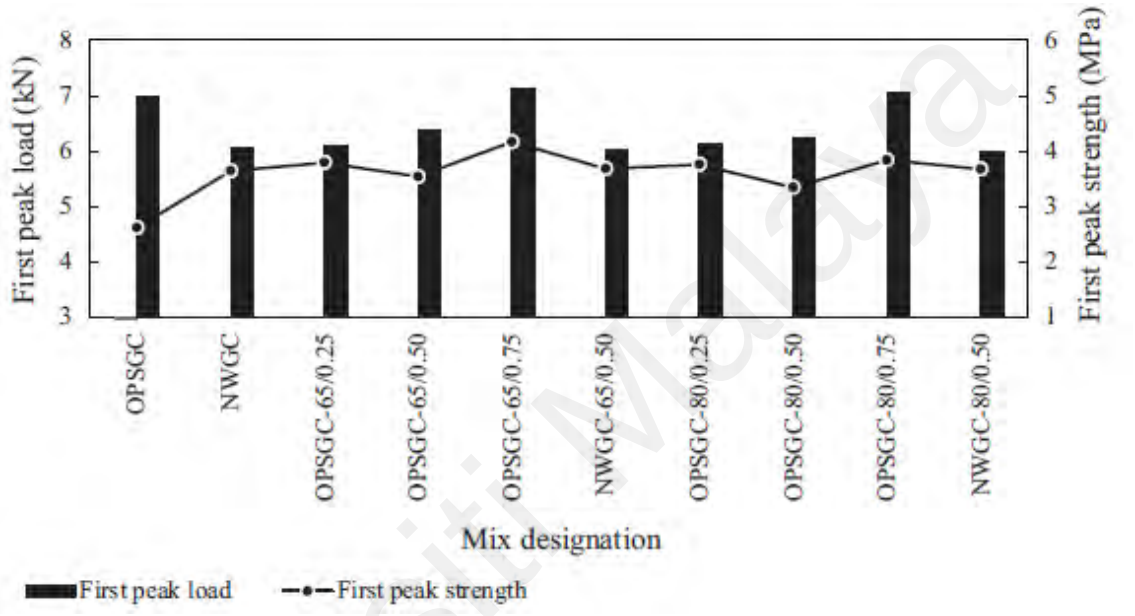

Figure 5.13: First peak load and strength

It is noticed that 0.75% of steel fibres gives the highest FPS among 0.25%, 0.5% and 0.75% of volume in both case of AR65 and AR80. A slight reduction of FPS was found for 0.50% volume of steel fibres.

The residual load (RL) and residual strength (RS) are two important characteristics of fracture behaviour and are determined generally for the limiting deflection of 1/600 and 1/150 of beam span. The RS at specified deflections characterises the residual capacity of the specimen after cracking. Figure 5.14 shows the RL and RS of all mix proportions of OPSGC and NWGC with/without fibres.

OPSGC, which contains OPS as aggregate and no fibre, achieved more RL and RS than the NWGC without fibre (NWGC). The RL (L/150) and RS (L/150) of OPSGC are relatively 62% and 75% higher than the RL (L/600) and RS (L/600); however, this variation was found lower in NWGC.

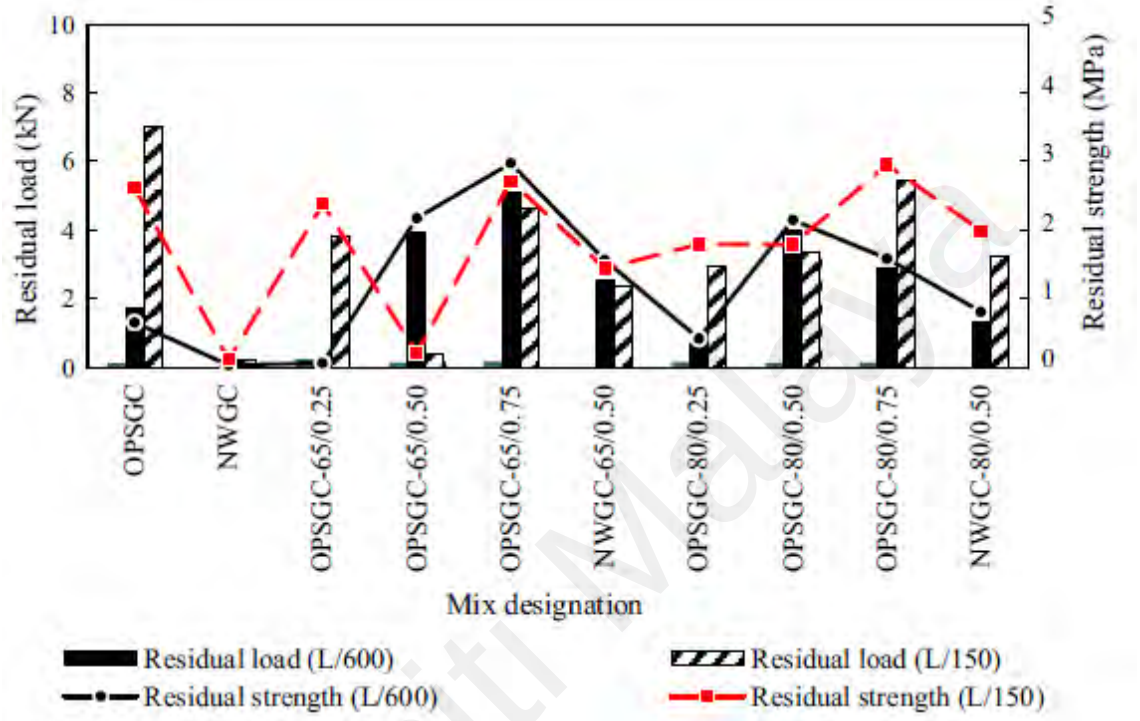

Figure 5.14: Residual load and strength

The addition of steel fibres influences the RL as explained below. The highest RL (L/150) and RS (L/150) were obtained for 0.75% volume of steel fibre of AR65. The OPSGC with steel fibre AR65 of 0.75% volume achieved about 74% higher RL (L/150) and RS (L/150) than that of OPSGC-80/0.75. Similar reduction in RL (L/150) and RS (L/150) was also found in OPSGC-80/0.25 and OPSGC-80/0.50.

The values of RL and RS in two-deflection limit of L/600 and L/150 indicate the progressive failure, which reflects the ductility of the concrete material.

5.3.8 Fracture toughness

The toughness and equivalent flexural strength ratio are shown in Figure 5.15. The toughness determines the capacity of energy absorption of the specimen and is expressed

in terms of Joules (J). The higher toughness indicates the better post-cracking response (Mo et al., 2014) and the better ductility performance of the fibre reinforced concrete.

The non-fibred OPSGC and NWGC achieved toughness as 3.03 and 0.94 J, respectively and it indicated the ductility of OPSGC compared to NWGC. Further, the toughness as well as the ductility increased by the addition of steel fibres. Similar findings were reported by Yap et al. (2014) and Mo et al. (2014). The stronger ductile property of OPS compared to crushed granite aggregate enabled OPSGC to produce up to 3.2 times higher toughness than NWGC. Mo et al. (2014) reported an increment in toughness of 6 to 17 times compared to the control concrete by increasing volume from 0.5% to 1%. Sahin and Köksal (2011) reported an increase in the fracture energy of 2.2–3.6 by adding $SF_{(AR80)}$ in grade 45 of normal weight concrete.

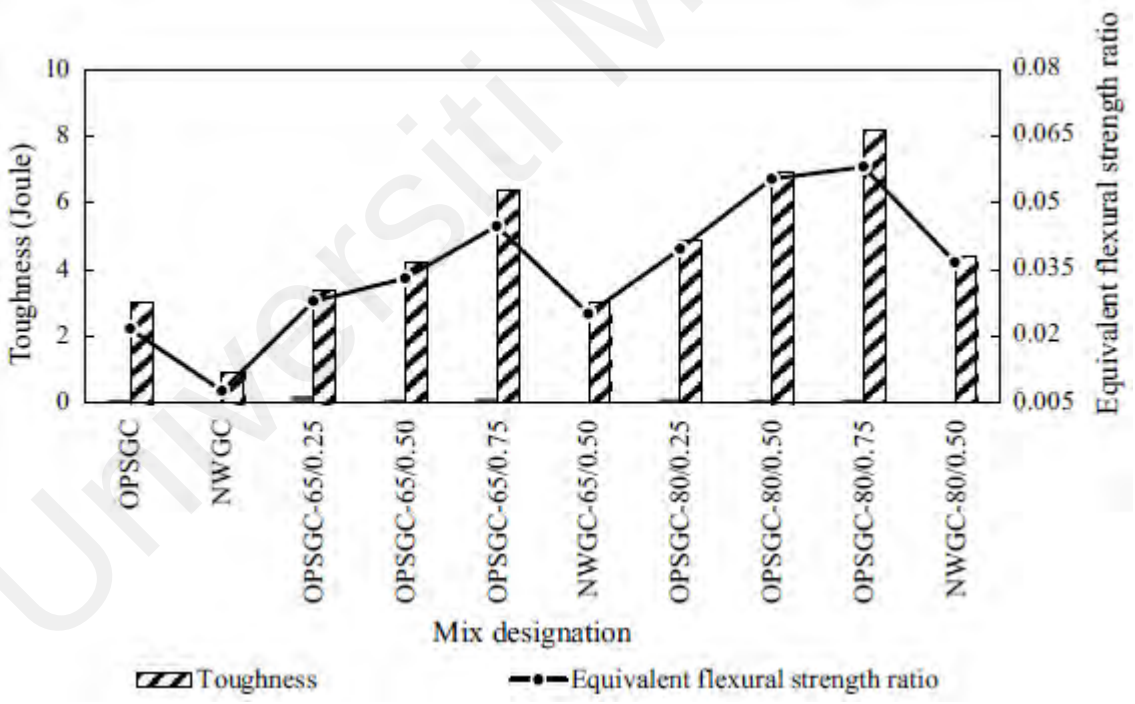

Figure 5.15: Toughness and equivalent flexural strength ratio

Results show that OPSGC-65/0.50 and -/0.75 achieved up to 2 times higher toughness compared to OPSGC-65/0.25. With higher aspect ratio, similar trend in the enhancement in the toughness was noticed in OPSGC-80/0.25. The increment of volume of steel fibre

enhanced the stiffness of concrete matrix which led to produce stronger bridge to withstand crack propagation in concrete. As seen from Figure 5.14, both the increase in the volume and aspect ratio enhanced the toughness of concrete.

ASTM International (2019c) relates the toughness and first peak load in the calculation of equivalent flexural strength ratio and the equation to calculate this ratio is given below:

Equivalent flexural strength ratio,

$$R^{D}_{T,150} = \frac{150.T^{D}_{150}}{f_1.b.d^2}.100\% \quad (5.2)$$

where, T^{D}_{150} – specimen toughness in Joules, f_1 – First-peak strength in MPa, b and d are breadth and width of the specimens in mm. The equivalent flexural strength ratio OPSGC-80/0.75 was the highest and as seen from Figure 5.15, it changes relatively with change in toughness.

5.4 Summary

The use of high volume POFA in the development of OPSGC was investigated, in addition, the effect of volume fraction and aspect ratio (AR) of steel fibre on the mechanical properties of OPSGC and fracture behaviour of fibre reinforced OPSGC and NWGC was also investigated and reported in this research. Based on the experimental investigation, the following conclusions are drawn:

1. The volume fraction and aspect ratio (AR) of steel fibre had little or no influence on the compressive strength of both OPSGC and NWGC.
2. The use of steel fibres with higher aspect ratio enhanced the flexural and splitting tensile strengths and this could be attributed to due to the capability of fibres with longer lengths in delaying crack propagation in concrete.

3. The bonding between steel fibre and binder influenced the development of flexural and splitting tensile strengths and this is in turn related to the surface area of the steel fibre.
4. It has been observed from the failure mode of OPSGC, bond failure of OPS along the convex surface governed the failure of flexural specimens; however, the flexural and splitting tensile strengths of OPSGC were found higher than that of the corresponding NWGC. This could be attributed to the effect of stronger bond on the concave face and along the rougher surfaces of the crushed OPS.
5. The mixes with fibres of AR65 showed higher ductility than the corresponding mixes with AR80, as the former had higher number of fibres compared to the latter for a given volume of fibres; the lower number of fibres in the AR80 mixes reduced the ductility.
6. Though the addition of fibres in OPSGC slightly influenced the modulus of elasticity of the concrete, it was significantly lower than the corresponding NWGC. On the other hand, lower modulus of elasticity had higher ductility characteristics.
7. The addition of high volume of steel fibre with low aspect ratio in OPSGC showed higher energy absorption.
8. The toughness and equivalent flexural strength ratio of OPSGC were found higher than the corresponding NWGC and this could be attributed to ductility of OPS.
9. The values of residual load and residual strength in two deflection limits of L/600 and L/150 indicated the progressive failure, which reflects the ductility of fibred OPSGC.
10. OPSGC produced higher residual load and strengths than the corresponding NWGC which signified the better ductile property of OPSGC.

CHAPTER 6: ENUNCIATION OF EMBRYONIC PALM OIL CLINKER BASED GEOPOLYMER CONCRETE AND ITS ENGINEERING PROPERTIES

6.1 Introduction

The depletion of natural resources due to high demand of ever-increasing construction materials and activities paved way for more opportunities and challenges to researchers and engineers to unearth alternate materials with the least ecological and environmental effect (Ibrahim & Razak, 2016). Over the last six decades (Sandanayak et al., 2020), industrial by-products and wastes have been advocated as an alternative to conventional construction materials (Hamada et al., 2020a; 2020b). However, due to the regulations and the stringent measures that are in place to get these materials acceptable as construction materials, some of these materials are at the research stage and have not gone beyond the laboratories to the real construction markets or projects (Hamada et al., 2020c). The challenges that are faced with these new industrial by-products and waste materials in the utilization as viable alternative materials is the legitimacy of the materials in the longevity of the concrete and products produced from these materials. The major advantage of these materials is in line with the sustainability concept; thus, a thorough understanding of the material properties as construction materials, and more importantly, the suitability of these materials as a viable and reliable alternative is imperative (Sandanayak et al., 2020).

Throughout the world, the plentiful availability of waste & industrial by-products and the issue of dumping these in open fields had been a perennial issue (Muthusamy et al., 2019). This has not only opened an opportunity for civil engineers to exploit these materials for their advantage but also to play a major role in the sustainability development goals (Affordable and clean energy, responsible consumption and production, climate action; United Nations General Assembly, 2015). In the South-East Asian region, the availability of such materials from the coal operated power plants (Ragipani et al., 2021), iron & steel

industries (Kim et al., 2021), rice mills (Tayeh et al., 2021a), palm oil industries (Halim et al., 2021), incinerated plants (Alderete et al., 2021), etc. paves way for a meaningful utilization of those materials. As the second largest producer of palm oil in the world after Indonesia, Malaysia produces millions of tonnes of palm oil wastes (Wardhani et al., 2021); some of those materials such as oil palm shell (Hamada et al., 2020c), palm oil clinker (Muthusamy et al., 2021), palm oil fuel ash (Hamada et al., 2020a; 2020b], etc. had been investigated as useful construction materials. Alengaram et al. (2016) proved that oil palm shells can be used as blast resistant concrete by testing oil palm shell slabs under blast loading. Palm oil clinker ash and palm oil fuel ash showed their potential as replacement for ordinary Portland cement and fly ash in the development of sustainable concrete, both in normal and geopolymer concretes. These materials have an added value due to sustainability issues, in addition to acceptable physical and chemical properties as filler and pozzolanic materials (Al-mulali et al., 2015). In addition to the sustainability advantage, there is a huge stake for marketability of such materials as the potential is fully exploited; thus, the economic impact due to the incorporation of these palm oil industrial by-products and wastes is yet to be uncovered; the expansion of palm oil cultivation due to an increased demand for cooking oil and biodiesel would further increase the production of these waste materials. In the early 20th century, palm cultivation was reported as 400 ha (Loh, 2017) which had reached about 4.5 million hectares (Sulaiman et al., 2011). Approximately 17.7 million tons of palm oil was extracted in Malaysia in 2008 (Chiew et al., 2011) that generated millions of tons of agricultural and industrial wastes in the form of oil palm shell (OPS), empty fruit bunches, palm oil trunk, palm oil fuel ash (POFA) and palm oil clinker (POC).

Both POFA and POC are pozzolanic materials (Karim et al., 2016) and these were utilised as a replacement of cementitious material and lightweight aggregate, respectively (Bashar et al., 2016; Kabir et al., 2017; Sharmin et al., 2017). The effect of utilizing POC as coarse

aggregate was reported due to higher creep and drying shrinkage in prestressed concrete and reduced UPV value for high porosity and irregular shape (Omar et al., 2002). However, the concrete mix design can be optimised by filling pores by filler and pozzolanic materials (Abutaha et al., 2017) or increasing paste volume that is generally required for lightweight concrete design (Mo et al., 2017). Further utilization of POC in the structural concrete and the investigation of POC as a lightweight aggregate in the lightweight concrete would enable further research and meaningful use of it as lightweight aggregate (LWA) as known, the use of conventional crushed granite or other virgin materials is not environmentally friendly due to CO_2 emission owing to quarrying, transportation, crushing etc. of virgin aggregates; on the contrary, the POC due to its lightweight could be easily crushed and transported, thus resulting in the lower energy consumption. The other advantage of POC include the lower thermal conductivity due to porous nature and lowering the construction and product costs (Almutairi et al. 2021, Shahid et al., 2016; Tayeh et al., 2021b).

Due to flaky irregular shapes of POC, it might be implicit as deleterious for ease bond failure (Kanadasan & Razak, 2015); some of the vital characteristics of POC based concrete are yet to be investigated. It is imperative to understand the stress–strain mechanism of POC based lightweight concrete. Depending on the volume of the paste that encapsulates the POC in the concrete, the compressive ductility behaviour could be varied, and it does not always get influenced by the aggregates only. The available research experiments addressed the strength characteristics of POC lightweight aggregate-based cement concrete; however, no detail research works were found in the literature that address the compressive ductility and failure behaviour of POC lightweight aggregate geopolymer concrete.

This research article is focused on the utilization of POC as coarse aggregate in fly ash-based geopolymer concrete. The compressive ductility behaviour of POC-based

lightweight geopolymer concrete and its failure mechanism were explored. The moment–curvature analysis of an idealised beam section was conducted for a comparative analysis of the flexural performance of POC based lightweight geopolymer concrete (P-GC) and granite based normal weight geopolymer concrete (G-GC). The deflection of P-GC beam was higher than that of G-GC though the compressive strength of both concretes were within a comparable range. The lower stiffness of P-GC at elastic range attributed to higher deflection. This research findings agree the suitability of using P-GC in structural application.

Research works have been carried out using POC as the replacement of coarse, and fine aggregates to address the sustainability and its environmental impact and characterisation (Kanadasan, 2016); further work on the method of developing POC high-strength concrete was carried out by Abutaha et al. (2018); the utilization of POC powder as a cement replacement in the development of self-compacting concrete (Kanadasan, 2016) was also explored. The microstructural investigation for pozzolanic reactivity of POC powder as a cement replacement (Karim et al., 2017) and the size effect of POC as coarse aggregate (Alhasanat et al., 2017) were investigated. The mechanical properties, compressive, flexure, & splitting tensile strengths, and modulus of elasticity along with shear properties of POC cement concrete (POC-CC) were investigated (Lee, 2018; Malkawi et al., 2020). The structural behaviour with respect to the flexural and shear behaviours of POC-CC beam and wall/ panel was another feather on POC based concrete (Huda, 2017; Joohari et al., 2018; Mohammed et al., 2011).

Despite lots of research on POC concrete (POCC), still there is a gap of investigation of compressive ductility property and its failure mechanism under compression. The compressive ductility is the measure of the ability of concrete that may undergo significant plastic deformation before failure. The knowledge of compressive ductility of POCC is vital to analyse the flexural strength of a POCC structural element at the plastic

limit. The significance on the understanding the inherent mechanics of the ductility of POCC and the need for further investigation as outlined by various research works is paramount (Ahmmad et al., 2014, 2016; Huda et al., 2015, 2016; Sharmin et al., 2015).

Ahmmad et al. (2014) reported that increase of POC as replacement for conventional sand in concrete caused a reduction in the modulus of elasticity and ultimate load capacity of concrete. The limit of the conventional sand replacement by POC sand was reported at 37.5%. Due to a high volume of the pores in POC particles, there is a necessity for more cement content compared to conventional mining or river sand; therefore, for mixes with an equivalent amount of cement in POC and conventional based sand concretes, different strength grade of concretes were produced. As stated, there is a need for a higher amount of cement paste is required to fill the pores in POC particle; this causes an increase of cement-paste requirement to achieve the same bonding strength between aggregates and the mortar. The improvement of the strength of POCC was found by using the pre-soaked POC in saturated -surface dry condition before casting POCC. Abutaha et al. (2018) also suggested that pre-treated POC by filling pores by cement or any pozzolanic powder during the casting process improves the strength of concrete. Generally, the modulus of elasticity of lightweight aggregate concrete is found lower than the normal weight concrete due to the lower stiffness of the LWA and it ranged from 5 to 28 GPa (Mehta & Monteiro, 2006). Sharmin et al. (2015) reported that there is a significant role of the binding matrix in the modulus of elasticity of concrete.

Based on the literature review POC as an ingredient in concrete plays an important role in compressive strength and elastic property. However, no in-depth research finding on crack propagation and its influence on the structural element were reported. These gaps are addressed in this research article so that the performance of POC based geopolymer

concrete in structural element can be analysed and mathematical models can be adopted for future design work.

This research article is focused on the utilization of POC as coarse aggregate in fly ash-based geopolymer concrete. The compressive ductility behaviour of POC-based lightweight geopolymer concrete and its failure mechanism were explored. The moment–curvature analysis of an idealised beam section was conducted for a comparative analysis of the flexural performance of POC based lightweight geopolymer concrete (P-GC) and granite based normal weight geopolymer concrete (G-GC). The deflection of P-GC beam was higher than that of G-GC though the compressive strength of both concretes were within a comparable range. The lower stiffness of P-GC at elastic range attributed to higher deflection. This research findings agree the suitability of using P-GC in structural application.

6.2 Experimental programme

6.2.1 Raw materials

Fly ash (FA) was used as the main precursor which was activated by 14 *M* sodium hydroxide (NaOH) along with the liquid sodium silicate (Na_2SiO_3). The liquid Na_2SiO_3 and 14 *M* NaOH solution weight proportion was 1:2.5. Manufactured sand (M-sand) was used as the fine aggregate. POC and crushed granite were used as coarse aggregates in the P-GC and G-GC, respectively. The physical and chemical properties of these raw materials have been discussed in Chapter 3.

6.2.2 Geopolymer concrete recipe, casting, and curing

The mix design of P-GC and G-GC is shown in Table 6.1. This mix proportion was adopted after trial casting and testing to achieve a comparable compressive strength of POC based lightweight geopolymer concrete (P-GC) and granite-based normal weight geopolymer concrete (G-GC). The total paste volume in P-GC was required to keep

higher than G-GC. As stated in the introduction, lightweight aggregate requires more paste volume compared to normal weight aggregate for a specific strength grade. The water absorption of POC is about 7.5 times higher than that of the crushed granite aggregates. Therefore, higher water absorption of POC is necessitated pre-soaking for cement-based concrete to avoid the reduction of water content required for hydration process (Swamynadh & Muthumani, 2018). However, in this research, as geopolymeric reaction was involved, POC was not pre-soaked, and no additional water was added in P-GC mix for workability as additional water could affect geopolymeric reaction adversely at the POC-mortar interfacial zone. Due to numerous pores in POC, there is a tendency to fill the pores by geopolymer pastes that might results in a dry mix. Hence, to compensate the workability issue, a higher paste volume was required in P-GC compared to that of the paste used in G-GC.

Table 6.1: Mix proportions of P-GC and G-GC (kg/m^3)

Mix ID	Fly ash	M-sand	Granite	POC	Alkaline activator ($NaOH+Na_2SiO_3$)	Water
P-GC	643	482	0	482	276	0
G-GC	400	544	1,267	0	160	60

Six numbers of Ø100 mm × 200 mm cylinders were cast using P-GC and G-GC mixtures. The specimens were cured in an oven at 65°C temperature for 24 h, then the specimens were cured in laboratory ambient temperature (27±2°C) and humidity (~65%). Generally, geopolymer concrete in oven curing achieves strengths in early age (Bashar et al., 2016), and no significant change of strength was reported after 28-day age (Zhang et al., 2019).

6.2.3 Compression toughness test setup and data acquisition

The compressive toughness test-up of the cylindrical specimen under the actuator of the Instron 600 is shown in Figure 6.1. Three LVDTs were placed in the equal distance along the periphery of the specimen (Figure 6.2) to measure displacements. Then the deformation was calculated from the average of LVDT readings. The rate of the actuator

displacement was controlled at 0.25 mm/min. The load–displacement data was collected using a digital data logger. The cracks on the cylinder were observed visually. The images of the surface cracks of the broken specimens were taken using a high-resolution camera.

6.3 Results and discussions

6.3.1 Compressive load-deformation behaviour

The compressive load and deformation curves for P-GCs and G-GCs are plotted in Figure 6.3. The dotted black lines (LVDT-1, 2, 3) indicate the deformations at three equally distanced positions at cylinder periphery as shown in Figure 6.2.

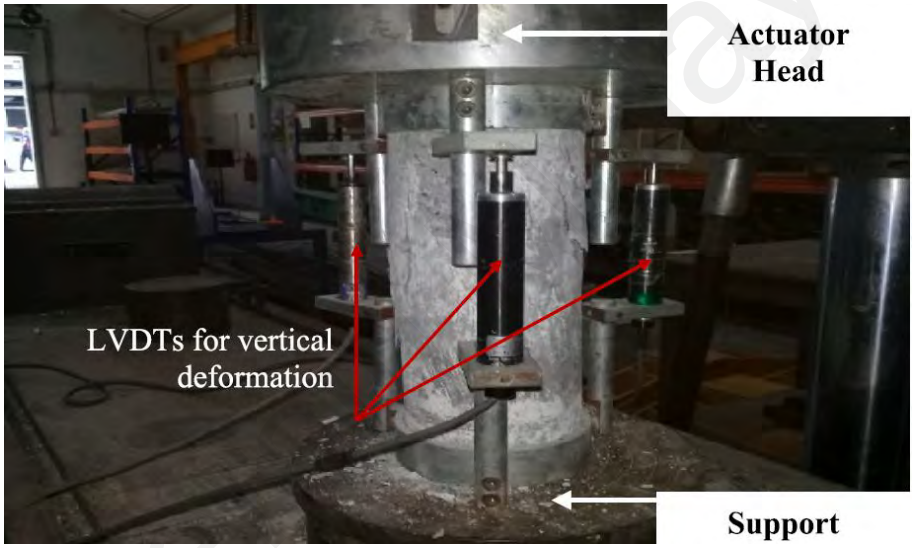

Figure 6.1: Test set-up for compression toughness experiment

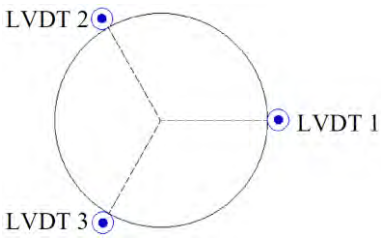

Figure 6.2: LVDT set up around periphery

The continuous line is the average of three LVDT measurements. The loading actuator of Instron was free to rotate. Therefore, deformation was measured from three equally distanced periphery of the cylinder and the average value was calculated for overall deformation of the cylinder under compression. The differences in the deformation

measured by three LVDTs indicate negligible difference for a particular loading point. An imaginary deformed plane at ultimate load is shown in Figure 6.3.

The compressive stress–strain plots of G-GC and P-GC are shown in Figure 6.4. After the elastic limit, the variation of stiffness of P-GC is less uniform (smooth) compared to G-GC. From the crack analysis, it can be understood that the crack path in P-GC followed through the POC aggregate whereas aggregate-matrix bond failure was noticed in G-GC.

Though the ultimate strength of both P-GC and G-GC were close to each other, P-GC deformed more than G-GC at the same stress level; it implies that P-GC absorbed more energy than G-GC. The energy absorption of lightweight aggregate concrete is higher than normal weight concrete material due to either less stiff aggregate material (Alengaram et al., 2016) or having pores in concrete (Amirrasouli, 2015) that enables mortar to compact under compression. Alengaram et al. (2016) investigated blast resistance of oil palm shell (OPS)-based concrete which could withstand blast pressure more than granite based normal weight concrete (G-NWC) of similar strength. Due to lower stiffness of OPS, the impact energy distributed through the concrete, thus multi-cracks were generated in concrete panel, whereas G-NWC was broken into two parts. G-NWC could not distribute impact/ blast energy due to higher stiffness of granite aggregates. Amirrasouli (2015) investigated energy absorption potential of fibre - reinforced cellular concrete. Cellular concrete comprised of pores that attributed to compact under pressure at compression zone, then reflected the air-blast pressure. In this research, P-GC is porous concrete like cellular due to porous physical property of POC, which increases energy absorption capacity of P-GC.

The hump at ultimate stress indicates that P-GC softens faster than GGC. The aggregate crushing value (ACV) may suggest the reason for the tapered hump shape of the stress–strain curve of P-GC. ACV of POC is about three times higher than that of granite.

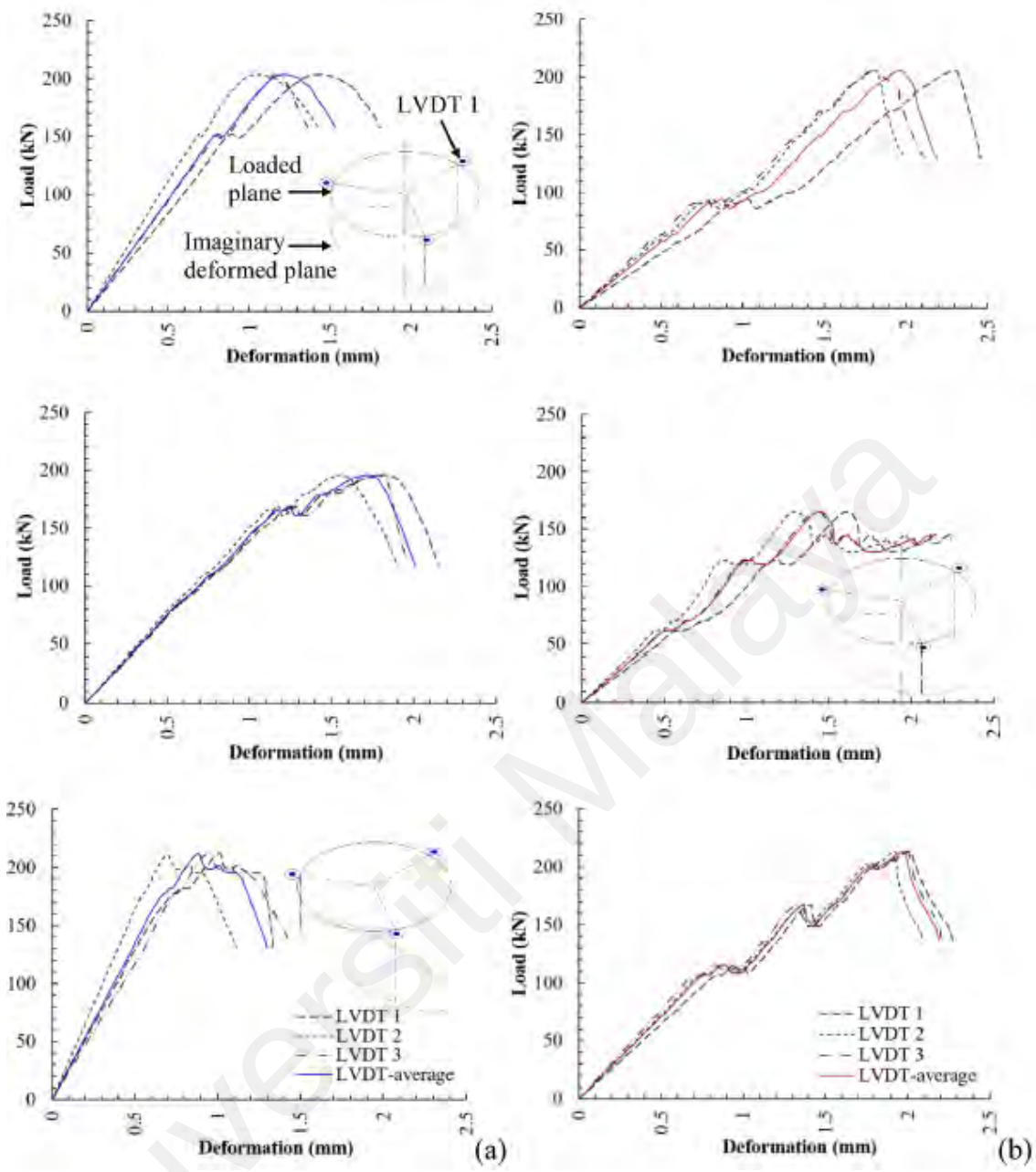

Figure 6.3: Compression load-deformation of (a) G-GC, (b) P-GC

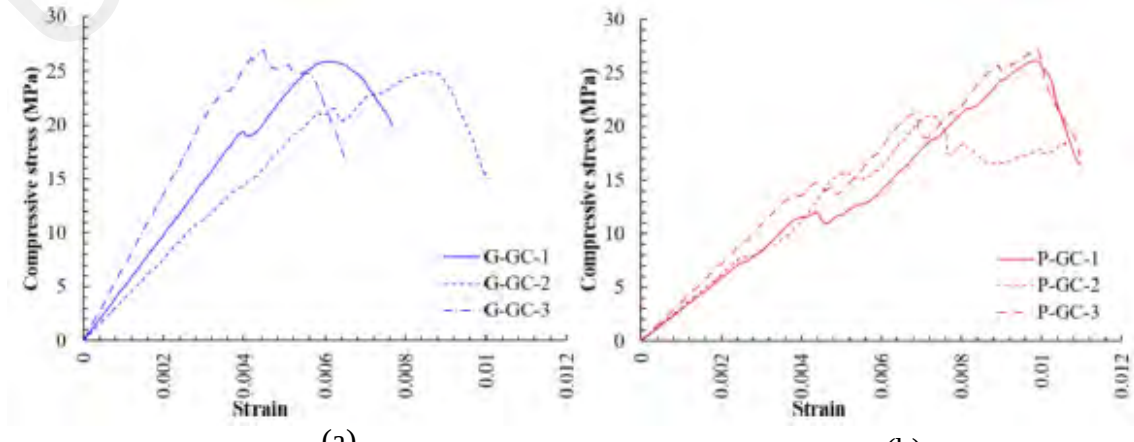

Figure 6.4: Compressive stress–strain of (a) G-GC and (b) P-GC

The higher crushing value means lower resistance of the aggregate. Since the cracks in the P-GC pass through the POC, after certain slip of adjacent cracked plane, it smoothens and causes rapid softening. However, for G-GC, the crack path propagates through the aggregate-matrix interfacial zone that keeps the adjacent cracked planes roughen (Figure 6.5). Due to this reason, after ultimate stress, the softening takes place by the gradual fall of stiffness that results in a smooth rounded stress–strain falling branch as shown in the stress–strain curve.

Figure 6.5: Crack propagation schematic diagram for P-GC and G-GC

6.3.2 Strain energy and strain energy density

The elastic and plastic behaviours of P-GC and G-GC under compression load are shown in Figure 6.6. The shape of the compressive load-deformation curve is shown by a schematic diagram as seen in Figure 6.6. Four points - A, B, C, and D are defined on the curve for elastic limit, critical point, ultimate point and failure point, respectively. When the compression load is applied on the cylinder top surface as shown in Figure 6.7, the concrete deforms with a constant stiffness ($K = dP / d\Delta$) until the elastic limit (A). A sudden drop of load can be noticed after the critical point B due to the first fracture that causes a release of stress resistance. However, immediately after this drop, the load increases gradually with a varied stiffness (ascending hardening) till the ultimate load point, C; then descending softening takes place and stress resistance capacity is reduced till the failure point D.

The concrete specimen stores potential energy due to the applied compression load. The amount of potential energy stored within the elastic limit is known as elastic strain energy, which can be mathematically expressed as given in Eq. (6.1).

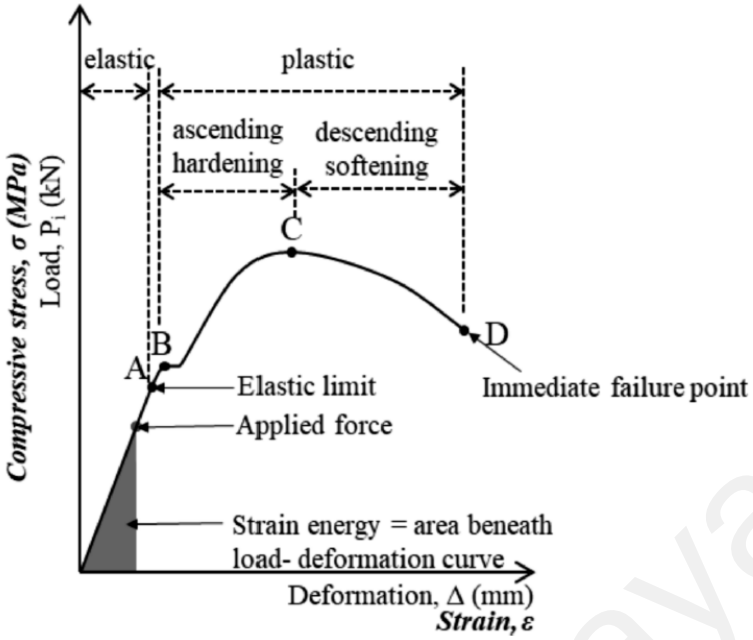

Figure 6.6: Schematic diagram of compressive load and deformation of concrete

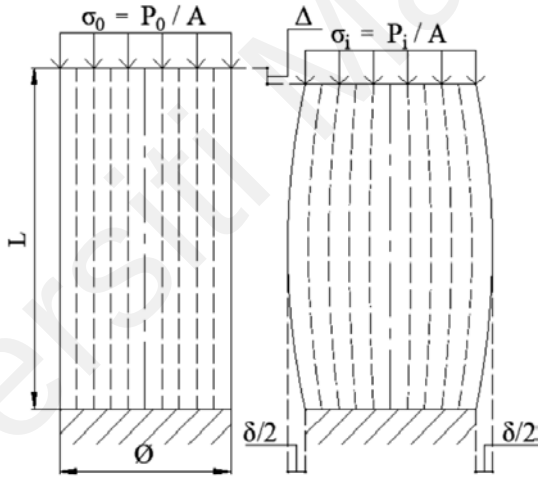

Figure 6.7: Applied compression force on a cylinder specimen – a schematic diagram

The total strain energy is the product of load and deformation beneath the curve (Eq. (6.2)). The strain energy per unit volume of concrete specimen is well-known as strain energy density and can be calculated as the area under the compressive stress–strain diagram (Eq. (6.4)). Total strain energy density and elastic strain energy density are called modulus of toughness (Eq. (6.4)) and modulus of rupture (Eq. (6.3)), respectively.

Elastic strain energy,

$$U_e = \frac{1}{2} P_i \Delta \tag{6.1}$$

Total strain energy,

$$U_t = \int_0^{\Delta} P d\Delta \tag{6.2}$$

Modulus of rupture (i.e., elastic strain energy density),

$$u_e = \int_0^{\varepsilon_e} \sigma d\varepsilon \tag{6.3}$$

Modulus of toughness (i.e., total strain energy density),

$$u_t = \int_0^{\varepsilon} \sigma d\varepsilon \tag{6.4}$$

Strain energy and strain energy density of G-GC and P-GC are given in Table 6.2 and Figure 6.8, respectively. The subscripts *e* and *t* represent elastic and total, respectively. The elastic strain energy of P-GC is less than that of G-GC. It represents that P-GC has less elastic strain compared to G-GC. In the P-GC, the mortar matrix fills the porous POC. Due to the high volume of pores in POC, the post-elastic stiffness variation of P-GC starts sooner than G-GC. The elastic energy of P-GC is 1/10 of the total energy, whereas this fraction is 1/4 for G-GC.

Table 6.2: Strain energy and strain energy density of G-GC and P-GC

		Strain energy (J)		Strain energy density ($\times 10^3$ J.m^{-3})	
		U_e	U_t	u_e	u_t
G-GC	1	55	235	35	149
	2	87	258	55	164
	3	55	179	35	114
P-GC	1	19	203	12	129
	2	20	213	12	136
	3	23	267	15	170

1 N.m = 1 kN.mm = 1 Joule (J); 1 N/mm^2 = 10^6 J.m^{-3}

Though a significant difference of elastic strain energy (U_e) and elastic strain energy density (u_e) exist between G-GC and P-GC, the total strain energy (U_t) and total strain energy density (u_t) are not significantly differed (Figure 6.8). Average total strain energy for G-GC and P-GC were found 224 and 228, respectively.

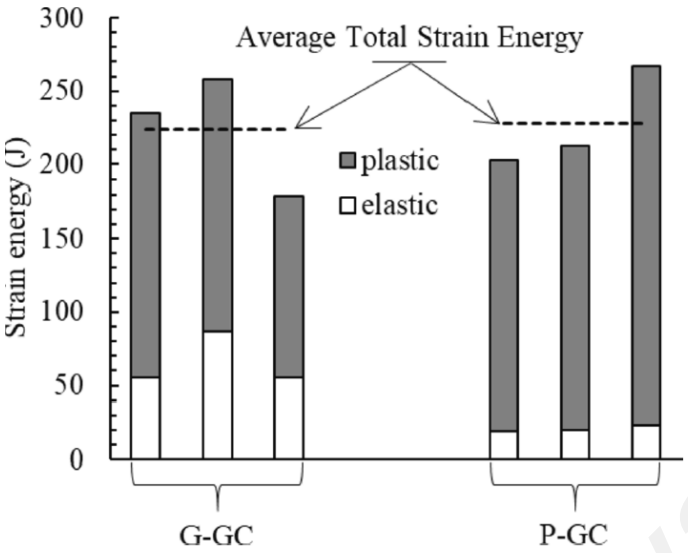

Figure 6.8: Strain energy of G-GC and P-GC

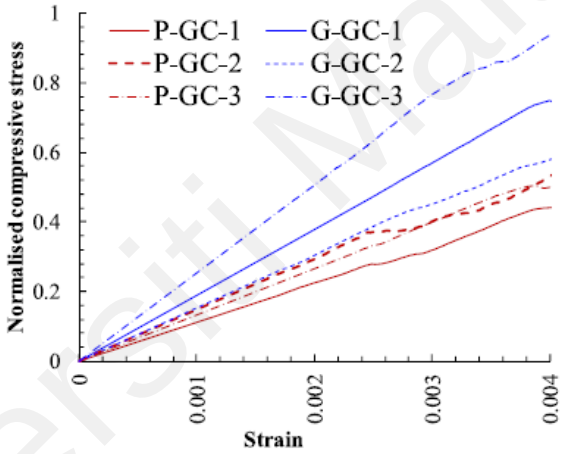

Figure 6.9: Normalised compressive stress–strain (elastic) of G-GC and P-GC

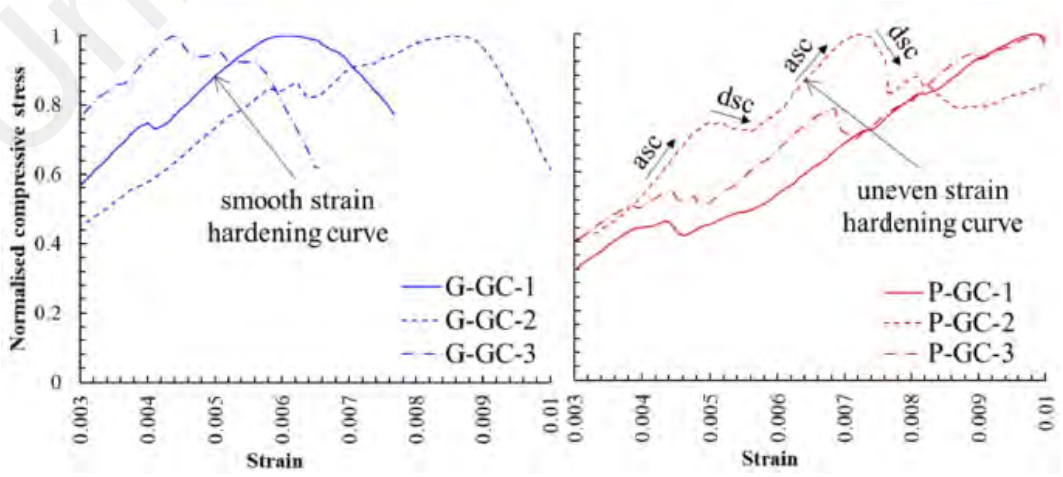

Figure 6.10: Normalised compressive stress–strain (plastic) of G-GC and P-GC

6.3.3 Energy absorption in elastic and plastic stages

A normalised compressive stress–strain relationship is shown in Figure 6.9 and 6.10 to analyse the percentage of energy absorption before and after the critical point B (Figure 6.6). The area beneath the curve represents the percentage of energy absorption and computed for pre-critical and postcritical stages (Table 6.3). It is noted that critical stage starts after a short interval at the end of the elastic state in G-GC, whereas in P-GC, the critical stage starts after a significant strain. This indicates that the mortar matrix that fills the pores of POC gradually enhances the stiffness of the P-GC before the critical stage. Nevertheless, due to brittle nature of G-GC compared to P-GC, the change of stiffness was insignificant before critical point B. Consequently, pre-, and post-critical energy absorptions are affected in both the G-GC and P-GC.

Table 6.3: Energy absorption (%) in elastic, pre-critical and post-critical stages

		0-A Up to elastic strain	0-B Pre-critical point	B-C-D Post-critical point
G-GC	1	23.5	26.3	73.7
	2	33.5	35.3	64.7
	3	30.7	39.4	60.6
P-GC	1	9.4	21.1	78.9
	2	9.4	22.5	77.5
	3	8.6	20.7	79.3

The toughness of P-GC was found lower than G-GC at the pre-critical stage (Figure 6.9). At the post-critical stage, the change of stiffness in G-GC produced a smooth ascending hardening and descending softening curve; however, an uneven curve in plastic state for P-GC indicates the crack propagation through the POC. In P-GC, while crack propagated through mortar-matrix interface, the stress released causing the softening descending (dsc) branch, before initiating fracture through subsequent POC aggregate in the P-GC; thus, the increase in the stress caused hardening of the ascending (asc) branch. This gradual crack propagation through POC led to developing an uneven plastic strain curve.

6.3.4 Cracking and failure mode

The failure pattern of G-GC and P-GC under compression load is shown in Figures 6.11 and 6.12. G-GC failed by multi cracks around the cylinder surface whereas P-GC cylinder failed in two to three segments (Figure 6.12). G-GC consisted of less volume of geopolymer paste compared to P-GC. When a fracture appeared in G-GC at certain compressive stress, the crack propagated through the granite-matrix interface (Figure 6.5). It led the crack path to travel more and generated multi-internal fractures, thus multi crack appeared around the cylinder surface.

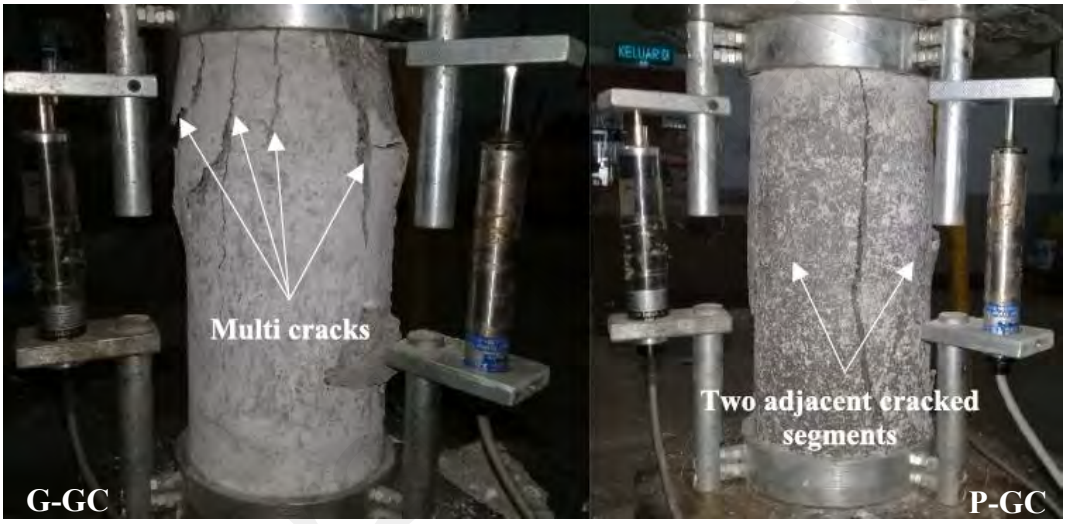

Figure 6.11: Crack pattern of G-GC and P-GC under compression

However, in PGC, after generating the fracture in the weakest portion, the crack propagated through the POC that caused the cylinder to split into two to three segments only. The close view of two adjacent cracked planes of PGC cylinder is shown in Figure 6.12. The splitting of POC is marked on the adjacent cracked planes.

6.3.5 Inherent mechanics in compressive ductility of P-GC and G-GC

The inherent mechanics of compression failure of P-GC and G-GC is attributed to the crack initiation and propagation by the fracture at the weakened portion. The fracture may initiate in the matrix, aggregates, or at matrix-aggregate interfaces. The propagation of

the crack path can be explained from the fundamental mechanics of plain concrete compression failure.

The primitive fundamental experiments using microscopic analysis (Hsu et al., 1963; Shah & Sankar, 1987) and acoustic emission test (holographic interferometry) revealed that fracture initiates at the interface and then propagate into the matrix (Maji & Shah, 1988). The concrete composition was used as conventional cement and granite/ sand in those research works. The initial crack initiation at the interface might occur in G-GC, which is a composition of geopolymer paste, M-sand and granite alike the cement-sand based mortar used by Maji and Shah (1988); however, there is a varied argument for P-GC due to POC is weaker than granite and POC is expected to be crushed before the interface failure. POC is a pozzolan and research proofed that POC participates in pozzolanic reaction actively (Karim et al., 2016). Therefore, in the presence of an alkaline environment, POC produces a strong bond between geopolymer paste and POC coarsen surface. The initial fracture in P-GC is coherent to instigate at the weaken plane of porous POC.

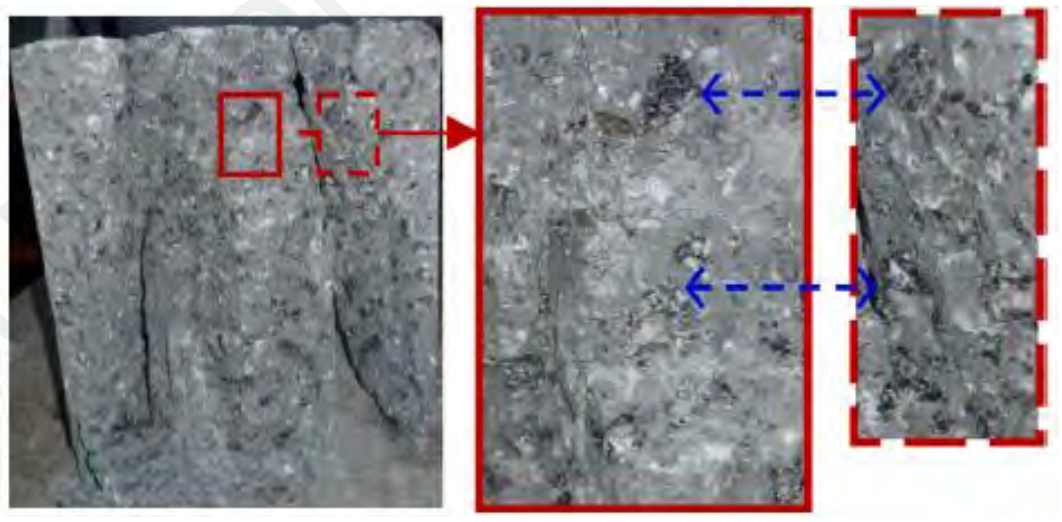

Figure 6.12: Close view on cracked plane of P-GC

As shown in Figure 6.13(a), concrete cylinder deforms in the uniaxial compressive stress. The bottom loading surface of universal testing machine displaces upward with a constant

rate while top support surface is fixed. Due to this movement, equal stress is applied on the cylinder specimen on its top and bottom surfaces, and this causes the specimens to deform axially and laterally. As a deformable body has tendency to either expand or shrink perpendicular to the axial loading direction as known as Poisson's effect and is defined by Poisson's ratio, v ($-1 < d\varepsilon_{transverse} / d\varepsilon_{axial} < 0.5$, for isotropic material) within the elastic limit (Shah & Sankar, 1987). P-GC and G-GC are considered isotropic material. However, the volumetric change of P-GC and G-GC cylinder is affected by porosity, aggregate crushing value and paste volume.

For an axial strain of ε_v, GCs deform laterally at a strain of ε_u. If the Poisson's ratio is defined as v, i.e., $v = \varepsilon_u / \varepsilon_v \Rightarrow \varepsilon_u = v.\varepsilon_v$, then the lateral strain and stress can be expressed as Eq. (6.5) and (6.6); whereas E is the modulus of elasticity of concrete.

$$\varepsilon_u = v.\frac{\varepsilon_v}{E} \tag{6.5}$$

$$\sigma_u = E\varepsilon_u = v\varepsilon_v \tag{6.6}$$

Eq. (6.6) represents the lateral stress induces for lateral strain. This should be noted that Eq. (6.5) and (6.6) valid until the elastic limit. It is seen in Figure 6.9 that modulus of elasticity of P-GC and G-GC are not same; G-GC is stiffer than P-GC. P-GC contains porous POC (Figure 6.14) and high volume of paste compared to G-GC.

Ahmmad et al. (2014) reported that modulus of elasticity of granite-based concrete was higher than POC based concrete of similar strength. That means granite-based concrete is stiffer than POC based concrete of similar strength due to high volume of paste containment and nature of aggregate porosity which agrees the experimental result presented in this research.

When concrete is in compression the lateral strain is not uniform (Haskett et al., 2011). The external point has more tendency to strain than the inner points as shown in Figure 6.13(b). This causes a relative strain difference at every infinitesimal segment in cylinder

specimen. An infinitesimal segment from cylinder is extracted and its free-body diagram is shown in Figure 6.13(d). The normal and shear stresses vary depending on the strain at the particular position. The diagonal lines as shown in Figure 6.13(d) is an imaginary line where the shear stresses reach to its ultimate limit and then ductile failure happens. However, Figure 6.11 shows that though G-GC had damage evenly distributed all-round, P-GC split into three parts. In P-GC, the lateral normal stress resistance at the cracked plane was weaker than shear stress. This might lead to fail P-GC cylinder into three parts.

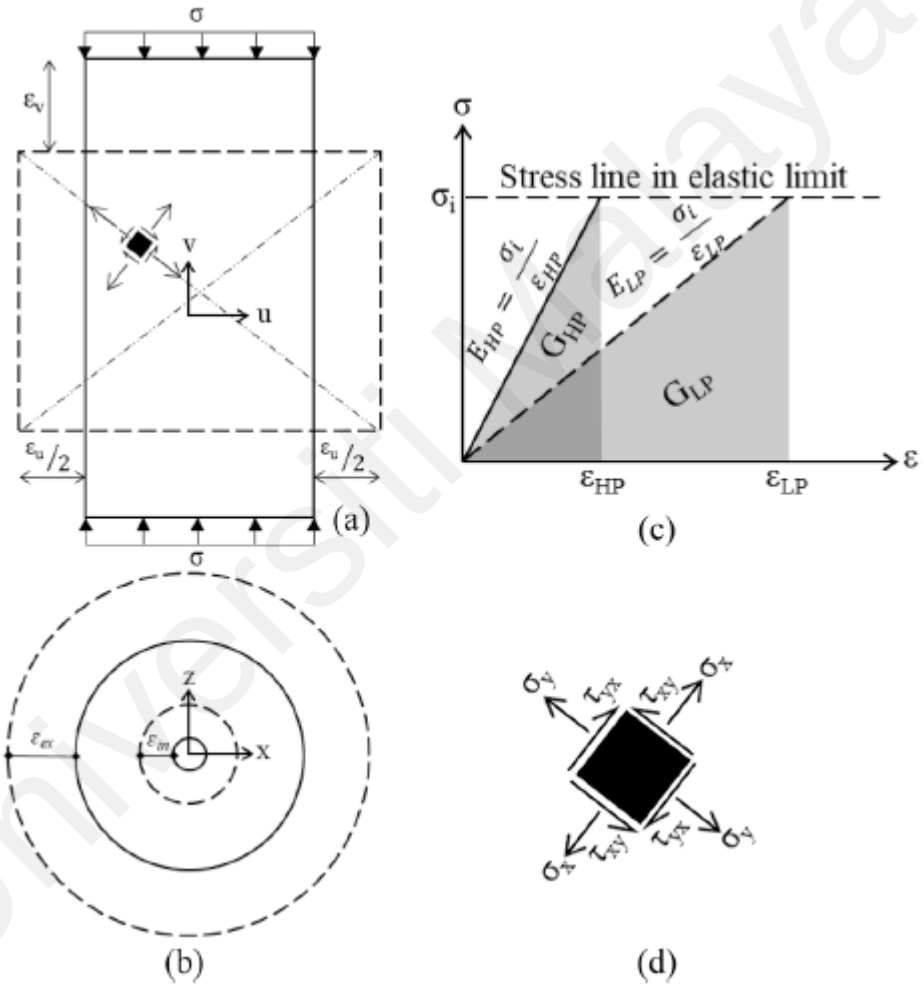

Figure 6.13: Inherent mechanics before fracture: (a) elevation view of a cylinder, (b) strain radius on plan view, (c) schematic graph of stress-strain relationship, (d) stresses at a finite element as shown in (a)

Figure 6.13(c) shows a graphical presentation of elastic strain energy of high (HSM) and low stiff materials (LSM). For a stress within the elastic range of both HSM and LSM, the elastic strain energy of HSM (GHP) is lower than that of LSM (GLP). However, from Table 6.2, it can be seen that $U_{e,G\text{-}GC}$ (i.e. GHP) is higher than $U_{e,P\text{-}GC}$ (i.e. GLP).

Notwithstanding being the higher stiff material, G-GC achieved higher strain energy due to the arise of first fracture at higher compressive stress than P-GC.

Figure 6.14: Pores in POC

Figure 6.4 shows that the critical points B (as defined in Figure 6.6) of G-GC and P-GC are at axial compressive stresses of 20 and 7 MPa (approximately) with a strain of 0.004 (approximately), respectively. Since the travel of strain is nearly same for both cases, induction of lateral stresses will be comparable according to Eq.(6.6). However, G-GC absorbs more energy than P-GC. This indicates that G-GC requires more internal stress to develop first fracture.

The relative displacements of imaginary points are shown in Figure 6.13(c), (d) and (e). Tasdemir et al. (1990) suggested the mixed-mode crack initiation and propagation from the aggregate-matrix interface in concrete under uniaxial compressive stress. Conventional normal weight granite was used in that experiment which is similar to G-GC. However, for P-GC, as explained in section 4.5, crack initiated in weaken part of POC plane, then propagated through that plane following the mixed mode crack initiation and propagation theory. Figure 6.15 represents the resultant stresses along separation direction at critical point B (Figure 6.6). Once the fracture appears, shear stress is induced with normal stress. The traction and separation continue until the complete failure. The concrete releases the energy absorption rate that causes ascending hardening and descending softening (Figure 6.6).

6.3.6 Analytical moment–curvature assessment

An analytical moment–curvature analysis was done to investigate the structural performance of P-GC and G-GC in reinforced concrete (RC) as a structural element. As the effects of compressive stress–strain of P-GC and G-GC are related, an over reinforced beam cross-section was adopted so that concrete at compression zone failed before the rebar yielded. Therefore, a beam cross section of width 100 mm × height 200 mm with a bottom reinforcement of cross-sectional area 226 mm^2 was adopted. The effective depth (d) of the rebar was taken as 164 mm. The beam was analysed applying the strain at its extreme compression fibre (ε_{0comp}) and corresponding moment–curvature was plotted. The flow diagram of this analysis is shown in Figure 6.16.

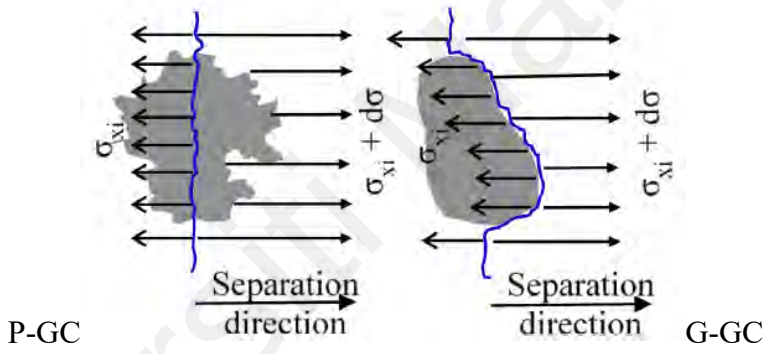

Figure 6.15: Schematic explanation of internal stress distribution in P-GC and G-GC

Four key points (A-D) were identified as shown in Figure 6.6 to describe the elastic, critical, ascending hardening, and descending softening branches of concrete compressive stress–strain relationship. The positions of neutral axis in elastic and plastic strain, stress distribution and moment–curvature are analysed for ε0comp at four stages of the points A-D.

Neutral axis: The depth of neutral axis changes in elastic and plastic strain of applied ε0comp at extreme compression fibre; it can be observed that until the elastic and critical strains, d_{NA} are equal. However, when ε_{0comp} is following the ascending hardening branch of concrete compression strain, d_{NA} shifts towards extreme compression fibre.

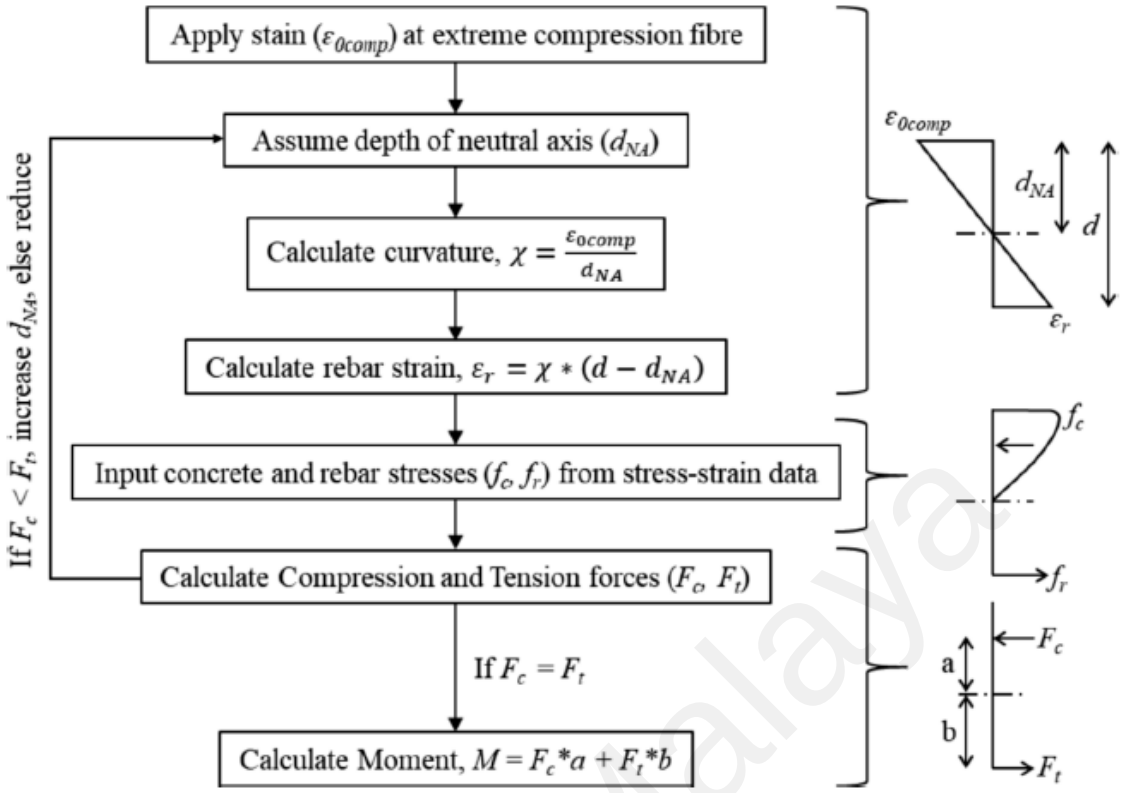

Figure 6.16: Flow of analysing moment–curvature from stress-strain experimental data

Due to the ascending strain hardening, the compression stress increases at the compression zone, and then at the equilibrium, the compression and tensile forces, d_{NA} is shifted near to the extreme compression fibre (Point D in Figure 6.17). At point D, concrete reaches to ultimate compression, afterwards softening starts. The concrete softening initiates at the extreme compression fibre and then gradually it moves towards the tension zone. Therefore, for equilibrium, the compression and tension forces in the beam section, d_{NA} shifts towards tension zone.

Figure 6.4 shows the compressive stress of G-GC is higher than of P-GC for an equal amount of strain until G-GC's ultimate strain hardening. Afterward, strain softening initiates in G-GC, but P-GC is at strain hardening stage. The effect of this strain variation in G-GC and P-GC, is reflected in the position of neutral axis as shown at ① in Figure 6.17. Within this region, d_{NA} of P-GC reduces whereas that of G-GC increases. Other than ① changes of d_{NA} for both P-GC and G-GC are in same direction.

Stress distribution at compression zone: The position of d_{NA} is affected by the concrete elastic property. The d_{NA} for the elastic and plastic design of a beam cross-section is shown in Figure 6.18. For both cases d_{NA} for G-GC is less than for P-GC. As D is the point after which the compressive strength of an unconfined cylinder strength can be neglected due to immediate failure (Figure 6.6), the compression stress distribution at compression zone of the beam section is significant.

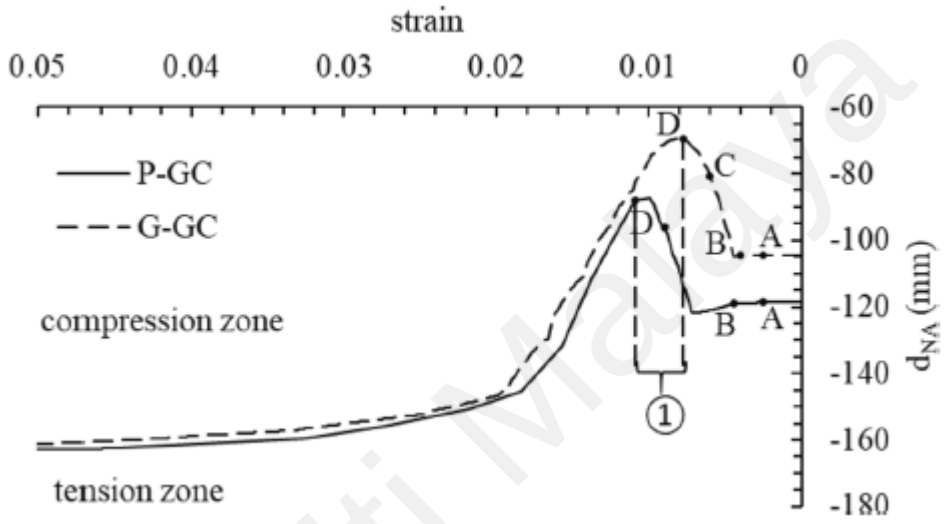

Figure 6.17: Variation neutral axis in elastic and plastic state

Figure 6.19 shows the compression stress distribution for P-GC and G-GC at their respective ε_{ocomp} at D as 0.0109 and 0.0077, respectively. The transition between ascending hardening and descending softening at ultimate compression load of G-GC is smoother than P-GC (Figure 6.4). That reflects in the stress distribution in Figure 6.19. G-GC has a smoother beam softening compared to P-GC. The total compression stress resisted by G-GC (172 MPa) is higher than P-GC (128 MPa). However, since d_{NA} of G-GC is less than P-GC, the resultant moment resistant (M) is comparable for both cases. M for G-GC (15.41 kN-m) is slightly higher than that for P-GC (14.84 MPa). In summary, since the ultimate compressive strengths of P-GC and G-GC are comparable, moment resistance for similar beam cross-section was found comparable. However, due to the difference of strain at equal moment, the curvatures of P-GC and G-GC are different.

Hence, it is important to analyse the moment–curvature of these two types of geopolymer concrete.

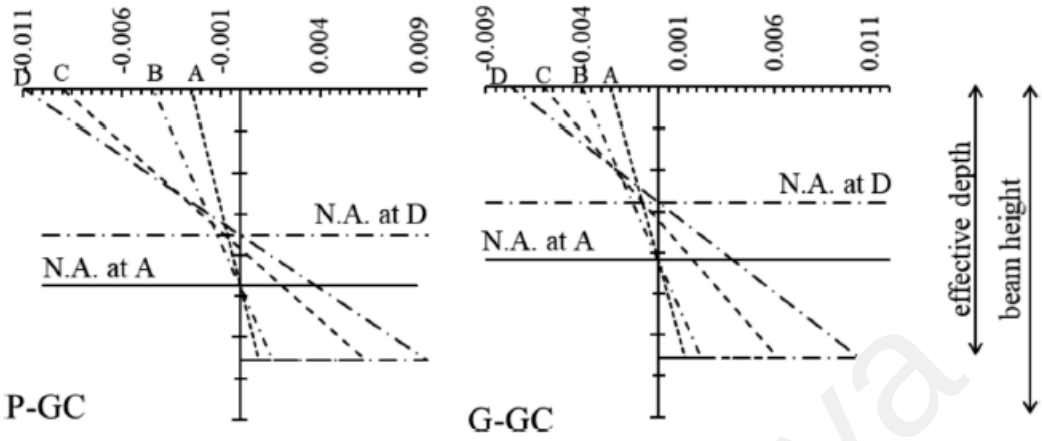

Figure 6.18: Position of neutral axis at elastic and plastic strain

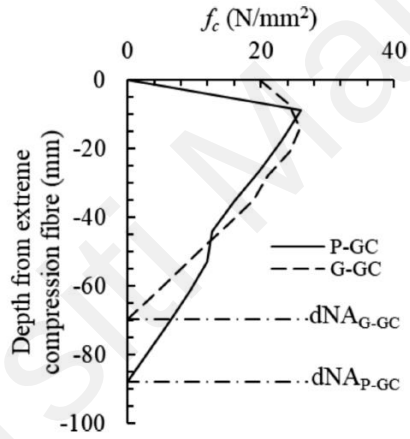

Figure 6.19: Compression stress distribution on beam cross section at point D

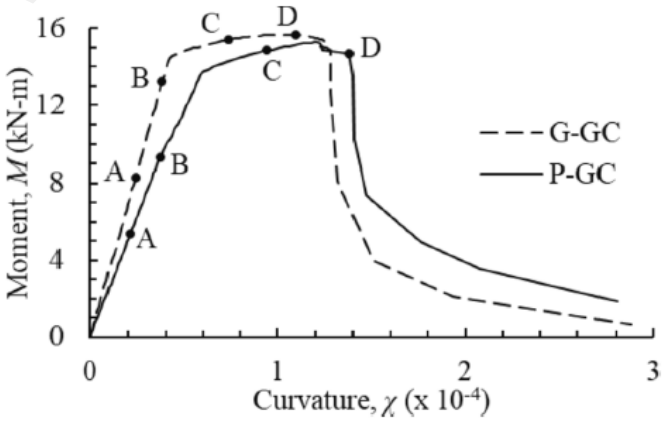

Figure 6.20: Moment-curvature analysis of an idealised beam section for P-GC and G-GC

Moment-curvature: The moment curvatures of P-GC and G-GC based reinforced geopolymer concrete beams are shown in Figure 6.20. A-D are the key points when the extreme compression fibre strain reaches to the same strain as identified for these key points in Figure 6.6. P-GC has higher value of curvature compared to G-GC for the same moment. This indicates that structural elements made of P-GC is likely to deflect more in bending than the element made of G-GC. The deflection at a structural element from the support is the cumulative sum of the deflection of all infinitesimal section calculated from the curvature also. Therefore, any structural member restricted to certain amount of deflection will require more cross-sectional effective moment of inertia for P-GC than G-GC. This will affect the beam size or quantity of rebar.

6.4 Summary

The compression toughness of P-GC and G-GC was investigated in this research. The failure modes and internal fracture mechanism were explored based on the physical properties of aggregates which supported the fundamental theories. The moment–curvature for an idealised beam section was analysed for both P-GC and G-GC which shows the serviceability state behaviour of P-GC and G-GC beams. The overall findings can be summarised as followings.

Compression fracture initiated at the weaker plane of porous POC in P-GC and at the interface of granite-GC matrix. The elastic strain energy of G-GC was higher than P-GC though the compression strengths of both concretes were within comparable range. The elastic limit of P-GC was lower than that of the G-GC, hence, the first crack initiated in P-GC sooner than G-GC. The deflection of P-GC reinforced concrete (RC) beam in bending was higher than that of G-GC RC beam. However, this deflection can be controlled adopting slightly higher beam cross-section that enables P-GC a suitable concrete for structural application like G-GC.

CHAPTER 7: REBAR PULLOUT-SLIP CHARACTERISTICS EMBEDDED IN P-GC AND G-GC

7.1 Introduction

The palm oil clinker (POC) is a by-product from the palm oil industry. It is produced abundantly in various shapes and sizes in the power generating boiler of Palm oil mill as an end-product of oil palm shell (OPS) and palm fruit fibre-bunch mixture after combustion at a high temperature (≈ 250°C). During the incineration process, plenty of micro and macro pores are created in POC resulting it lightweight. Currently, POC has no regulated use in large scale; it is either dumped for landfilling or stacked on the open field. Hence, the massive regular production of POC is a serious environmental issue. However, POC can be utilised as lightweight aggregate in concrete after crushing and grading it to the required size. Its potentiality as lightweight aggregate in concrete is suggested in numerous research articles (Hamada et al., 2020; Mohammed et al., 2013, 2014; Muthusamy et al., 2021; Sinoh et al., 2021).

The microstructural investigation of POC confirms it as pozzolan (Karim et al., 2016). Pozzolan has demand in concrete as it reacts with portlandite ($Ca(OH)_2$) and produces calcium silicate hydrate (C-S-H) or calcium aluminate hydrates (C-A-H), thus pozzolan attributes to form a harden product in concrete (Pavia et al., 2017). This comprehends the possibility of pozzolanic reaction at POC-binder interface. But the pozzolanic reaction is slow in hydration process; its advantage is realised at the matured age of concrete knowing the additional production of C-S-H or C-A-H as a result of pozzolan-portlandite reaction (Sata et al., 2007). The pozzolan is activated fast in the alkaline environment; hence, it has demand in the production of alkaline activated and geopolymer concrete. As POC is a pozzolan, the pozzolanic reaction at POC-geopolymer paste interface may initiate at the early age of geopolymer concrete and the product forms a homogeneous interfacial bridge between geopolymer matrix and POC. This attribution, thus expected,

eliminates the prospect of bond-shear failure in POC-geopolymer matrix interface; hence, instead of, the aggregate-paste interfacial damage due to compression or tension in concrete, crack propagates through POC (Bashar et al., 2022a). Thus, POC, due to be a porous material, influences the failure mechanism of concrete under compression, and tension. Also, due to be lightweight aggregate, it requires comparatively more paste than lightweight aggregate concrete to achieve similar range of compressive strength. Earlier research works reported that types, and quantity of aggregates in concrete significantly effects the elastic behaviour of concrete (Crouch et al., 2007; Hansen 1965; 1979; Neville, 1997; Stock et al., 1979).

The modulus of elasticity of materials (concrete and reinforcing bar) attributes to the distribution of bond shear stress along the concrete-steel interface of reinforced concrete under tension (Kabir and Islam, 2014). While the ribbed steel bar is embedded in concrete, ribs provide an additional bearing resistance that accumulate in the overall bond-slip mechanism (Kabir and Islam, 2014). The micro-cracks are generated at the concrete-rib interface when the bearing stress exceeds the concrete compressive resistance. The localised slip at the rib, also depends on the modulus of elasticity of concrete. Therefore, it is significant to investigate the bond shear stress-slip behaviour of reinforcing steel while embedded in POC-based lightweight geopolymer concrete (P-GC) before promoting this concrete material for structural application.

In the previous studies, the pull-out response of rebar from lightweight cement-based concrete was addressed (Al-Shannag & Charif, 2017; Hossain, 2008; Lachemi et al., 2009; Mo et al., 2015). Hossain (2008) investigated the influence of lightweight volcanic pumice aggregate (VPA) in pull-out response of rebar embedded in VPA-cement-based lightweight concrete. Lachemi et al., 2009 assessed the bond behaviour of reinforcing steel embedded in expanded shale-based lightweight self-consolidated concrete and the results were compared with the pull-out resistance of rebar embedded in

slag aggregate-based lightweight concrete. Mo et al. (2015) compared the bond properties of oil palm shell-cement-based concrete with normal weight cement-based concrete of 25, 35, and 45 MPa strength. Al-Shannag and Charif (2017) studied the bond strength of cement-based lightweight concrete made of lightweight scoria aggregate. Two strength grade concretes consisted of 350 and 500 kg/m^3 cement were used to investigate the bond strength of deformed reinforcing bar of nominal diameters of 12, 14, 16, 20, and 25 mm with an embedment length of 150 mm.

The adhesion of cement-based concrete is different from that of geopolymer concrete. The adhesion of geopolymer matrix was found comparatively stronger than cement-based matrix (Luo et al., 2021). Very little amount of research on bond strength of lightweight geopolymer concrete is available. Mo et al. (2018) evaluated the bond strength of palm oil fuel ash-based geopolymer concrete .

According to the authors review, no experimental research on the rebar pull-out from POC-based lightweight geopolymer concrete is available. Therefore, the experimental data and its investigation on the pull-out mechanism for this specific type of concrete (P-GC) are unique which is exclusively important to estimate the structural response of P-GC reinforced concrete under bending and tensile stress. The results have been compared with the bond shear stress-slip response of rebar embedded in normal weight geopolymer concrete (G-GC) of similar compressive strength. The local bond shear stress and slip properties have been extracted following the method suggested by International Federation for Structural Concrete (2010). The findings in this article will be beneficial for the structural engineers and construction regulatory bodies to utilize P-GC as structural concrete in reinforced concrete structure.

7.2 Rebar pull-out generic mechanism

It is necessary to discuss the pull-out generic mechanism to recognise the factors those influence the pull-out load-slip response of a rebar embedded in P-GC and G-GC. Three types of bond failure scenarios may be observed when pulling-out a rebar from concrete: (a) only pull-out, (b) concrete splitting, and (c) combined effect of (a) and (b) (Figure 7.1). The rebar pulls out without splitting the concrete when the distributed tensile stresses in the concrete as a result of pull-out force is lower than the tensile resistance of concrete (Gambarova et al., 1996; Maranan et al., 2015).

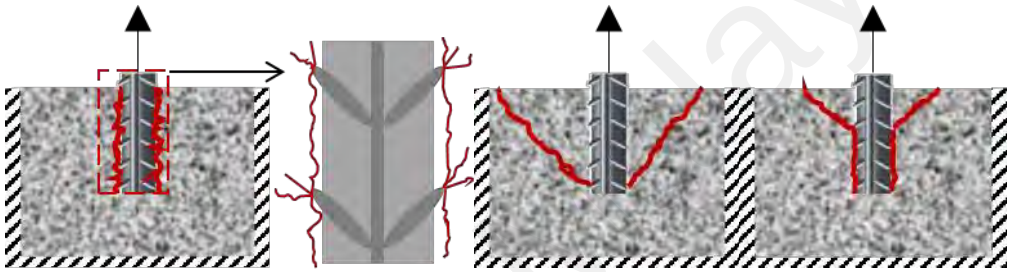

(a) (b) (c)

Figure 7.1: Bond failure scenarios – (a) concrete pull-out; (b) concrete spill; (c) combined effect of concrete pull-out and concrete splitting

Only pull-out (no concrete splitting) of rebar embedded in concrete is possible when sufficient concrete cover (rebar surface to concrete surface) and an appropriate embedment depth of the bonding zone from loading plane are adopted. When a rebar is pulled-out for the tensile force applied to the reinforcing bar, the interfacial slip initiates from the loading end. The bond-shear stress is thus resulted. Due to the differences of elastic properties of concrete, rebar, and interface, the localised slip along the rebar is different. So, the bond-shear stress along a plain rebar-concrete interface gradually varies. In case of a ribbed bar, rib provides additional pull-out resistance due to bearing resistance. The bearing resistance depends on the dimension of the rib (rib height, area), geometry (angle, continuity), quantity, and spacing. Figure 7.2 represents the forces

(/stresses) those act along the rebar-concrete interfaces during pull-out process. In Figure 7.2, the ribs are shown at both side of the rebar and the ribs are present at an interval along the rebar, because this figure is a longitudinal cross-section of the embedded rebar. Actually two ribs are present spirally along the rebar, so, the bearing resistance is available at two sides of the rebar at any position along the embedment length.

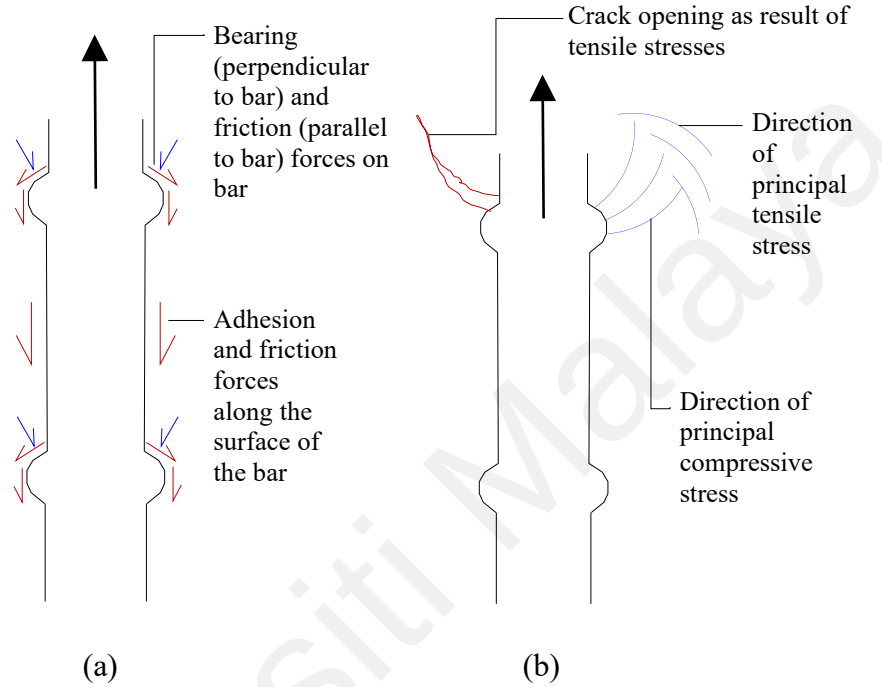

Figure 7.2: (a) Bearing resistance, Adhesion, and friction stress resistance; (b) Direction of principal axis (American Concrete Institute, 2003)

When the bonding zone is located at a sufficiently long depth and the concrete cover is sufficiently deep, those can distribute the pull-out reaction stresses in concrete within the range of concrete tensile capacity, there will be no concrete splitting for the pull-out of the rebar. In this situation, the active stresses can be anticipated as shown in Figure 7.2(a). The micro-cracks those appear at the rib due to bearing stresses, propagate through the weakest region along the rebar length due to concrete confinement (Figure 7.3). So, rebar slips either debonding the adhesion (possibility 1) or failing concrete near the interface for shear (possibility 2). The possibility 1 (debonding the adhesion) is possible when concrete is of high strength, and the aggregates near the crack path in concrete have high

shear resistance. The possibility 2 likely happens when bond shear stress is higher than concrete shear resistance.

For a low embedded region with insufficient concrete cover, concrete may split conically because of pull-out force. The micro-cracks generated at ribs propagate thorough weakest radial stress resistance zone of the hoops surrounding the rebar perimeter (American Concrete Institute, 2003). Due to difference of stress distribution at the conical shape of the loop, wedges form because of hoop tensile stress; thus, at an insufficient concrete cover, concrete splits for pull-out force in rebar (Saliba & Mezhoud, 2019).

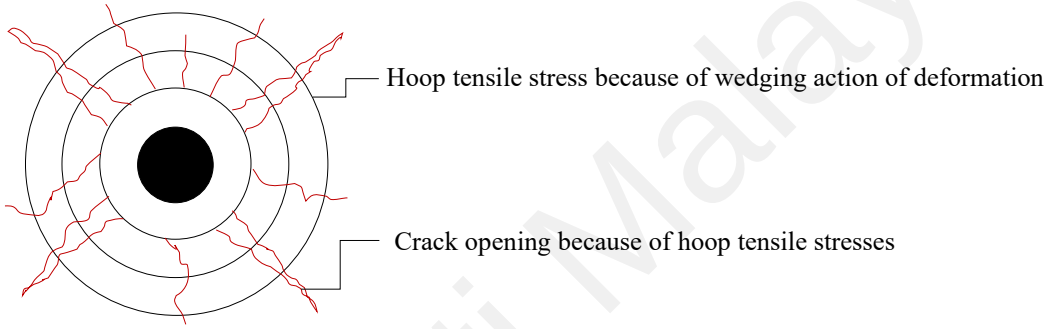

Figure 7.3: Crack opening, hoop stress surrounding a reinforcement in tension

The generic form of pull-out load and rebar slip relationship can be represented as shown in Figure 7.4. The response has divided into four stages: (i) elastic stage (⓪ to ①), (ii). strain hardening stage (① to ②), (iii) strain softening stage (② to ③), (iv) frictional stage (③ onwards).

Elastic stage: Before the debonding is initiated at the loading end, the whole embedded length is bonded elastically. The bond-shear stress along the interface gradually reduces from loading end to another end. The rib bearing resistance at this stage is not significant.

Strain hardening stage: The debonding at loading end is initiated after reaching the ultimate local bond stress (τ_{max}). The local bond stress at that point (loading end point) is then gradually reduced for more slips; the ultimate level of bond shear stress (τ_{max}) is

then moved to the next points towards end of the bonded zone. Thus, each infinitesimal point along the interfacial length experiences changes of local bond stress with local slip (which increases up to τ_{max}, then gradually reduced until zero bond-shear stress.). The total pull-out load (P) is equal to summation of forces contributed by the interfacial bond-shear stresses along the embedded length and rib bearing resistances. In the strain hardening stage (① to ②) of generic load-slip response (Figure 7.4), the combined contribution of resistance forces (force for bond shear stresses, and rib bearing resistance) increases nonlinearly.

Strain softening stage: This stage initiates after the ultimate pull-out load (P_{max}) and remains until the whole bonded zone is completely debonded. The combined contribution of resistance forces reduces for increasing slip. At the end of this stage, only friction stress contributes to P (③ onwards).

Frictional stage: At this stage, debonding is completed along the whole bonded zone. Only frictional resistance takes place. The total frictional surface area along the embedded length gradually reduces due to pulling-out from the embedded canal. This leads to reduction of P (③ onwards).

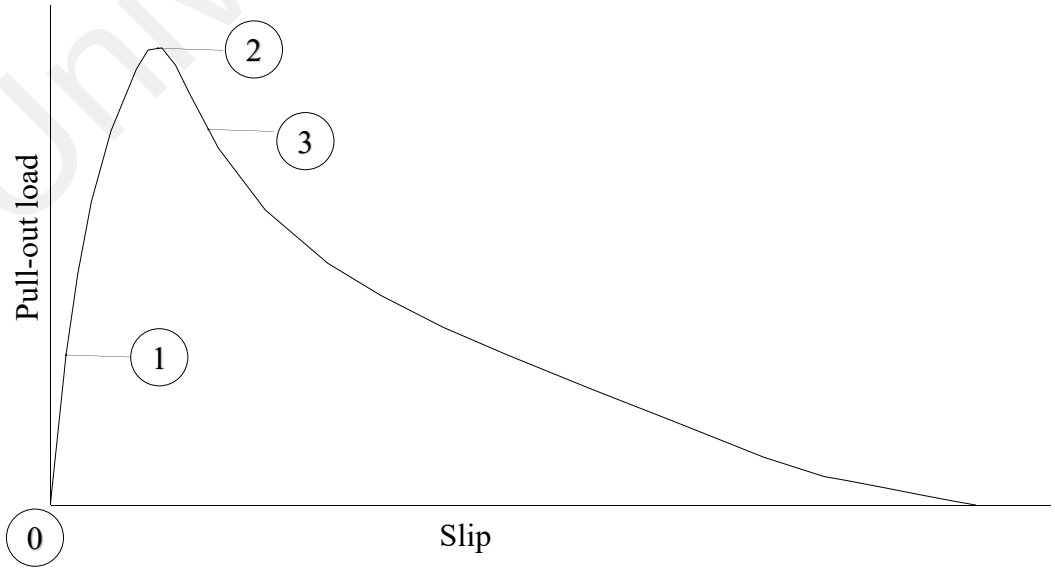

Figure 7.4: Generic pull-out load – slip response of rebar embedded in concrete

7.3 Experimental programme

7.3.1 Materials and preparation f specimens

The bond strengths of similar grade lightweight geopolymer concrete (P-GC) and normal weight geopolymer concrete (G-GC) were investigated pulling-out a high yield deformed steel bar of 12mm diameter embedded in P-GC and G-GC.

The paste ingredients in P-GC and G-GC were fly ash (FA), 14 *M* NaOH, liquid Na_2SiO_3 and water. The weight proportion of 14 *M* NaOH solution and liquid Na_2SiO_3 was 1:2.5. This alkaline environment helped to activate FA through geopolymer reaction process and this geopolymer paste was used as binding material for P-GC and G-GC.

The manufactured sand (M-sand) of size between 300μ and 4.75 mm was used as fine aggregate. M-sand is a processed fine aggregate from quarry dust (a by-product from the quarry industry) and was used in this research as a substitute for mining and river sand.

The lightweight palm oil clinker (POC) and crushed granites were used as the lightweight and normal-weight aggregates in P-GC and G-GC, respectively. The weight proportion of the constituents is shown in Table 7.1. The concrete mix design was adopted through numerous trial casting and strength tests to produce a similar strength grade. The average 28-day compressive strengths of P-GC and G-GC were found 25 MPa and 30 MPa, respectively. The compression toughness of P-GC and G-GC shows that P-GC was less ductile than G-GC due to presence of higher volume of paste in P-GC.

Table 7.1: Weight proportion of constituents used in P-GC and G-GC

	FA	M-sand	Granite	POC	AA	H_2O
P-GC	1	0.75	-	0.75	0.43	-
G-GC	1	1.36	3.17	-	0.40	0.15
FA = fly ash, M-sand = manufactured sand, AA = alkaline activator						

Three numbers of pull-out specimens (Figure 7.5) and their companion cylinder (Ø100 mm × 200 mm) specimens for compressive strength test were cast for each set of concrete.

Pull-out test specimen: A rebar was embedded at the centre of the cross-section of a concrete block of dimension 200 × 200 × 350 mm^3. The alignment of the rebar was carefully controlled during casting and shifting for curing to ensure it embedment direction is aligned with the loading direction. The nominal average diameter of rebar was 12 mm; the rib height, spacing and angle were measured as 0.8mm, 7.55mm and 45°, respectively.

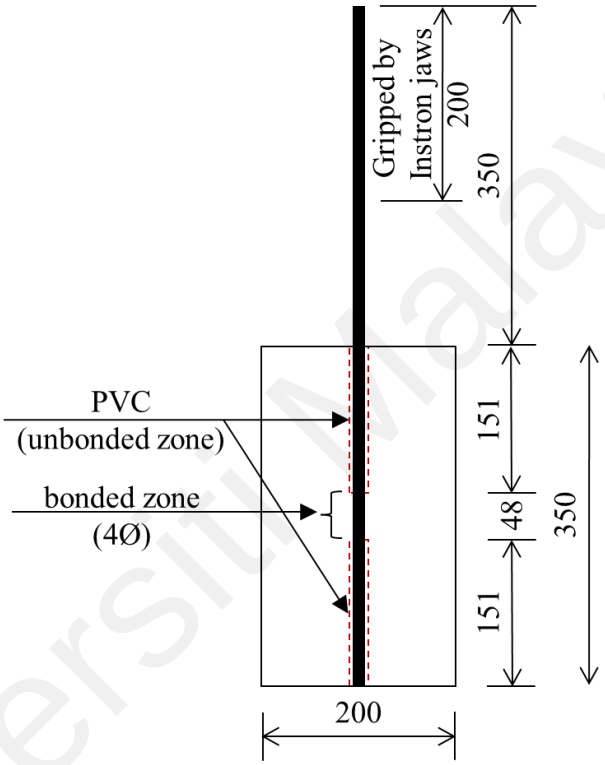

Figure 7.5: Pull-out specimen

The dimension of the concrete cross-section and depth of reinforcement-concrete bond inside the concrete block was adopted large enough to avoid splitting and to have the zero-compressive stress on the bonded zone due to support reaction at the loading face of the specimen. The bonded zone was taken four times the rebar diameter (i.e. 48mm). The PVC tube of Ø14mm was used at the unbonded zone to keep concrete and reinforcement separate always. A thin layer sponge was used at both ends of the PVC tube to avoid pouring concrete between rebar and PVC tube. The position of the bonded zone was at the middle of the prism length. Therefore, the height (350mm) from the loading face

ensured of not happening a conical failure due to the bearing resistance of the rebar ribs (American Concrete Institute, 2003; Arezoumandi et al., 2018).

The cast specimens were left at the casting place for about three hours before shifting to the curing chamber to avoid any damage at the rebar-concrete interface; then the specimens were cured at 65°C temperature for 24h. The balance time before the testing day, specimens were cured in the laboratory ambient temperature. All specimens were left in the same place to ensure the same curing condition for all specimens of both types of concrete.

7.3.2 Experimental set-up and data acquisition

The pull-out experimental set-up was designed following RILEM 7-II-128 and Mo, K.H. et al. (2015) testing procedure. The detail of the experimental set-up is shown in Figure 7.6.

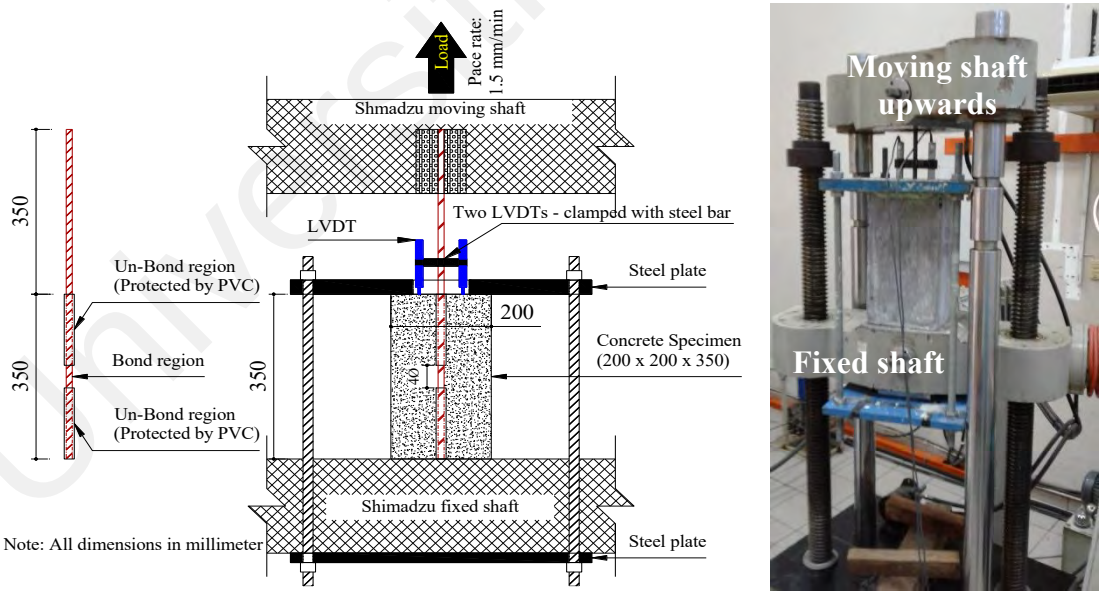

Figure 7.6: Pull-out test set-up

A steel frame was used to hold the specimen. The free unbonded length of the rebar was gripped firmly by the top jaws of the Shimadzu universal testing machine. The bottom part of the steel frame was fixed with the bottom jaws of the machine. A constant

displacement rate (1 mm/min) was applied for the movement of the load head upward direction.

The displacement reading of the INSTRON load head doesn't provide the actual slip of the rebar from the specimen since numerous uncertain variables such as mechanical elongations of all components connected between the loading head and hydraulic jack are involved. Therefore, the slip was measured using two linear variable displacement transducers (LVDT) fixed closely to the loading surface with the rebar using a tiny frame. The LVDT leads measured the displacement readings between the top surface of the concrete specimen and the LVDT connecting point on the rebar. A continuous every second load and slip readings were recorded using a data logger.

7.4 Results and discussion

7.4.1 Global pull-out load and slip response

The global pull-out load – slip behaviour of rebar embedment in P-GC and G-GC are represented in Figure 7.7. The dotted and straight lines represent LVDT readings and their average. The ultimate pull-out force for both P-GC and G-GC are comparable. However, there is a difference in experimental results among P-GC specimens, whereas G-GC specimens showed less difference in the pull-out response. The reasons of these differences can be revealed comparing the results with the generic pull-out and load behaviour as shown in Figure 7.4.

A sudden release of load in is marked in Figure 7.7 as [i] which is the point ① as shown in Figure 7.4. At this point, fracture was produced up to the first rib debonding the chemical adhesion. The rib bearing resistance at first rib was then initiated. As POC is a porous aggregate, it might be crushed near the first-rib interface due to the stress at rib. This caused a drop of pull-out load (P) in some P-GC specimens at ①. However, this drop of P was not noticed for G-GC specimens as granite is stronger aggregate than POC.

The improvement of *P* (strain hardening as shown in Figure 7.4) afterward is attributed to combined stress resistance by bond shear and rib bearing. The load-slip response of P-GC specimens between ① and ② points is approximately linear up to the ultimate pull-out load (P_{max}); but this response of G-GC is non-linear. This indicates that G-GC adhesion might be more ductile than P-GC adhesion.

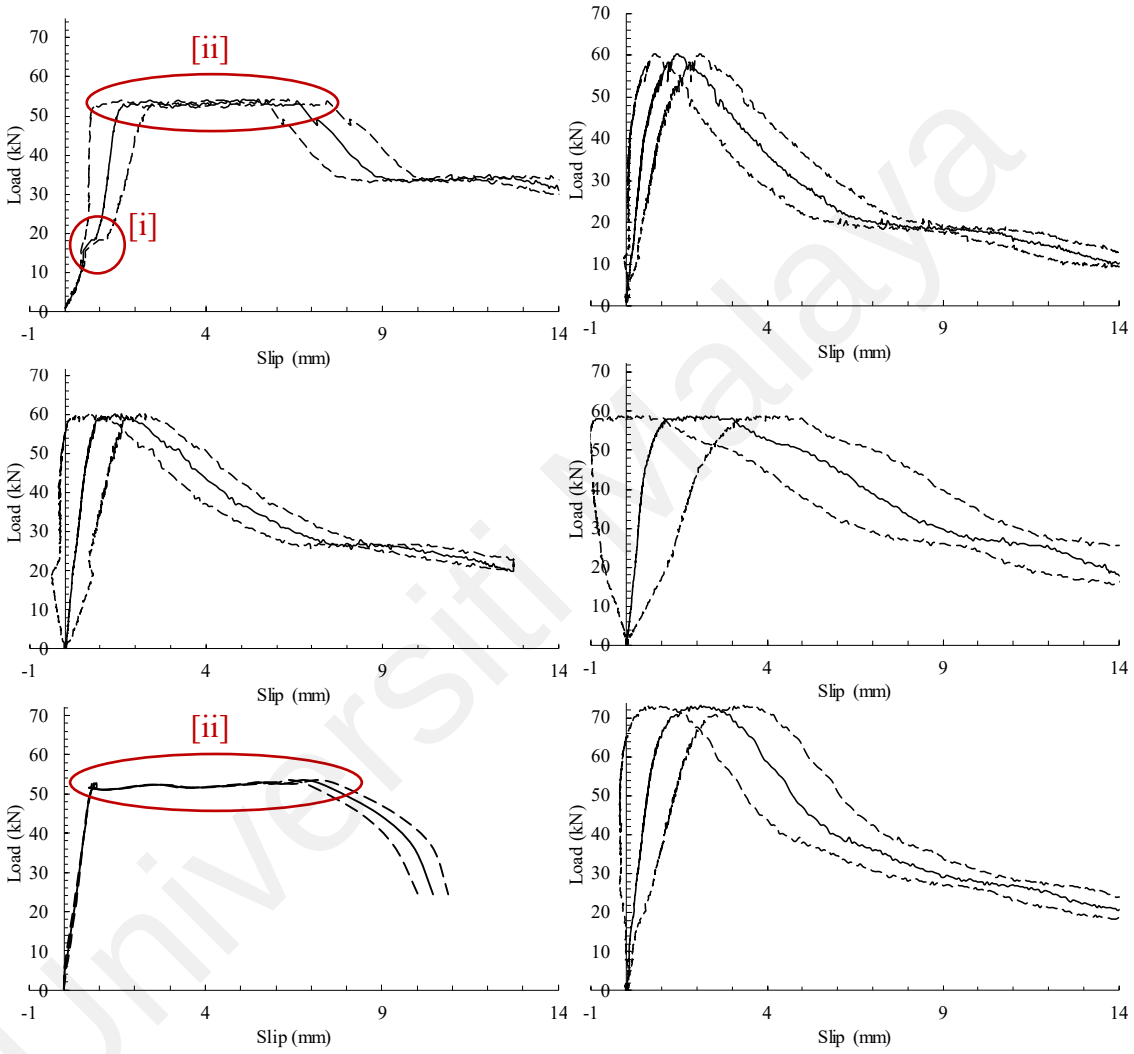

(a) (b)

Figure 7.7: Pull-out load and slip response of rebar embedded in (a) P-GC and (b) G-GC

Since adhesion is attributed to the effort of binding paste, the reason of linear (P-GC)/ non-linear (G-GC) response can be recognised reviewing the mix ingredients in binding

paste. An amount of water was added, and a slightly reduced amount of alkaline activator (AA) was used in G-GC whereas only AA was used in P-GC (Table 7.1)., the higher amount of AA in P-GC might cause brittle chemical adhesion.

The pull-out response of P-GC specimens consist of a flat response at point ② (marked as [ii] in Figure 7.7). The transition zone in P-GC is higher than G-GC. Because, at this point of ultimate pull-out load, POC near ribs might be crushed and local bond stresses were reduced at those localised points. However, the resultant effort of rib resistance and bond shear-stress resistance was comparable to the P_{max} up to a longer slip period than that of G-GC specimens. The change of the pull-out resistance of G-GC specimens was non-linearly varied from ultimate to reduced *P*.

7.4.2 Effect of modulus of elasticity of P-GC and G-GC in pull-out responses

The average pull-out load-slip responses for P-GC and G-GC are shown in Figure 7.8(a). The pull-out response is shown up to 70% reduced load from the ultimate pull-out load. The differences between the ultimate pull-out load and slip responses of P-GC and G-GC specimens can be noted in Figure 7.8(a). It should be noted that the geometrical arrangement, rib size and spacing, and steel properties of rebar embedded in both concrete were kept similar. There was a minor difference in the mix design of geopolymer paste. G-GC paste had a small quantity of water with AA whereas only AA was available in P-GC paste. However, in the matured age of strength development, this difference may not have any significant impact on the chemical adhesion as the compressive strengths of both concrete was comparable (≈ 25 - 30 MPa) at 28-day age which indicates that a similar strength grade adhesion took place at the rebar-concrete interface. Therefore, the difference of the pull-out stiffnesses in the elastic stage most likely caused by the elastic properties of materials. The global pull-out slip is the cumulative sum of the local slips, and the local slip-strains are the strain-difference between rebar and concrete at that

locality (Bashar et al., 2022b). Since identical rebars were pulled out from P-GC and G-GC, concrete elastic properties may be the only attributor to the differences of stiffness in the elastic stage of pull-out response. The elastic response of P-GC and G-GC under compression is shown in Figure 7.8(b). The ultimate compressive strengths of both concretes are within comparable range i.e., 25 to 30 MPa; however, their elasticity varies. The modulus of elasticity of G-GC is slightly higher than that of P-GC. The differences in paste volume and aggregate porous property might influence the elastic property of these concretes.

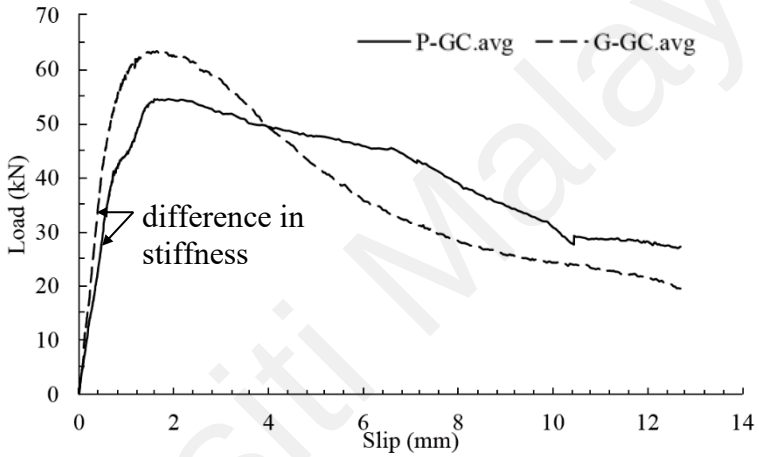

(a)

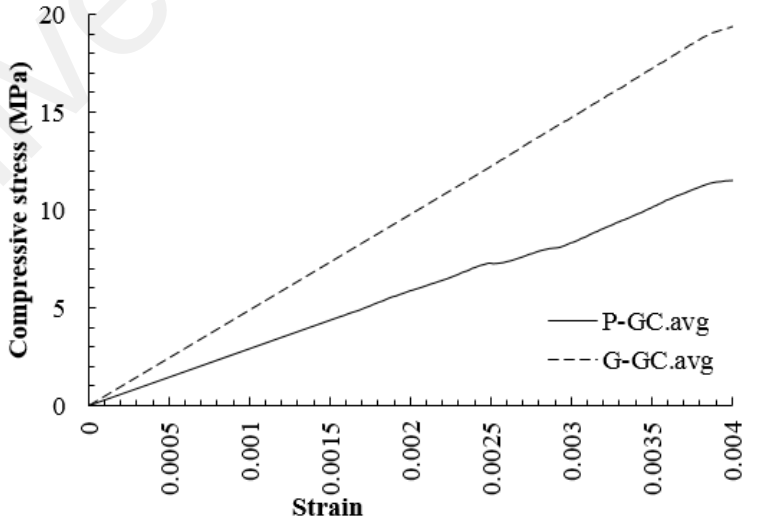

(b)

Figure 7.8: (a) average pull-out load-slip and (b) elastic behaviour of P-GC and G-GC under compressive stress

The debonding of chemical adhesion was attributed to the upward movement of rebar and downward shear resistance at interface during pull-out experiments. The difference of strains of rebar and concrete caused slip-strain at the interface. Therefore, for a higher value of modulus of elasticity of concrete, the slip is lower. The modulus of elasticity of G-GC is higher than that of P-GC (Figure 7.8(b)). Thus, the rebar slip for same amount of pull-out load, is less in G-GC specimen than P-GC specimens.

7.4.3 Effect of paste volume in post-elastic pull-out response

The difference in the post-elastic pull-out load-slip responses for identical rebars embedded in P-GC and G-GC is visible in Figure 7.8(a). A normalised response is presented in Figure 7.9 dividing the loads by P_{max} and slips by the embedded length of the bonded zone (48 mm) to identify the slight difference in post-elastic pull-out response (as dotted in Figure 7.9).

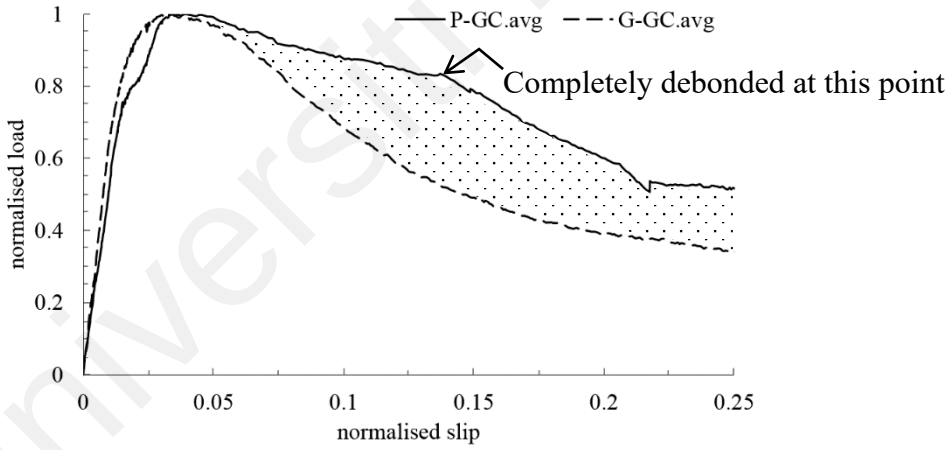

Figure 7.9: Normalized pull-out load-slip relationship

The descending branch of pull-out response after the ultimate pull-out load is smoother for G-GC than P-GC. The pull-out post-peak ductility of P-GC is higher than that of G-GC. As described earlier for Figure 7.3, the crack initiates at rib-concrete interface when the bearing resistance exceeds compressive strength of concrete. The propagation of cracks follows the weakest radial stress zone.

The crack propagation in P-GC and G-GC initiated from the rib-concrete interface; then it followed the weakest radial stress zone to reach to the closest aggregate particle. The stronger particle diverted the crack path through the weakest route. The volume of paste in P-GC was higher than that of G-GC; that means the quantity of aggregate particle in P-GC than G-GC. This led the cracks in P-GC to travel a longer path than the crack path in G-GC; thus, more pull-out post-peak energy could be absorbed in P-GC within ②-③ range as shown in Figure 7.4. The rebar was completely debonded after point ③. The point of complete debonding is identified in Figure 7.9 through an analytical analysis using model code 2010 (International Federation for Structural Concrete, 2010). It has been discussed in the following section.

7.4.4 Interfacial Local bond-slip properties of P-GC and G-GC

The experimental results from this research are based on identical rebar embedded in the same depth of P-GC and G-GC. However, by knowing the local bond shear stresses-slips extracting from this research experimental results, pull-out load-slip relationship for other embedment depth and rebar size can be predicted which will be useful to analyse structural elements. International Federation for Structural Concrete (2010) suggests a local bond shear stress (τ_b) -slip (s) relationship as shown in Figure 7.10(a). The τ_b-s can be divided in four regions: (1) ascending ($s < s_1$), (2) sustained ($s_1 < s < s_2$), (3) descending ($s_2 < s < s_3$) and (4) frictional region ($s_3 < s$) (International Federation for Structural Concrete, 2010), whereas s_1, s_2, and s_3 represent slips at ultimate bond shear stress (τ_{bmax}), at the end of sustained region (when τ_b starts reducing) and at the stage when only frictional stress (τ_{bf}) contributes to the pull-out resistance.

Ascending region ($s < s_1$): In the ascending branch, ribs of the rebar penetrate the concrete matrix that causes local crushing and microcracking. Due to this internal damage by ribs, this ascending branch is considered non-linear for rebar, and τ_b is equated as shown in Eq.

(7.1). A coefficient, α is used to address the non-linearity of the ascending branch. α is a value between 0 to 1. $\alpha \rightarrow 0$ refers to the constant stress, whereas $\alpha \rightarrow 1$ means linear bond-shear stress-slip relationship. International Federation for Structural Concrete (2010) suggests $\alpha = 0.40$, however, the most appropriate value can be calibrated from the experimental data for a specific type of concrete and rebar.

$$\tau_b = \tau_{bmax} * \left(\frac{s}{s_1}\right)^{\alpha} \qquad \text{for } 0 \leq s \leq s_1 \qquad (7.1)$$

Sustained region ($s_1 < s < s_2$): For a confined concrete, the sustained region may occur due to the gradual advancement of the crushing at rib bearing area and the occurrence of shearing off the concrete between ribs. This region represents the residual bond characteristics which maintain a constant resultant bond-shear stress equal to τ_{bmax} (Eq. 7.2).

$$\tau_b = \tau_{bmax} \qquad \text{for } s_1 \leq s \leq s_2 \qquad (7.2)$$

Descending region ($s_2 < s < s_3$): The descending region is the reduction of bond shear resistance due to the shear off the concrete corbels between ribs. As the cross-sectional area of the concrete pull-out specimen is sufficiently large to consider the rebar as confined in concrete, the gradual degradation of pull-out bond-shear resistance is expected. International Federation for Structural Concrete (2010) suggests a linear relationship for this region as:

$$\tau_b = \tau_{bmax} - \frac{(\tau_{bmax} - \tau_{bf})(s - s_2)}{s_3 - s_2} \qquad \text{for } s_2 \leq s \leq s_3 \qquad (7.3)$$

Frictional region ($s_3 < s$): When the bond-shear stress reaches to only frictional stress at the end of descending region. International Federation for Structural Concrete (2010) suggests a consistent frictional region as shown in Figure 7.10(a). Hence,

$$\tau_b = \tau_{bf} \qquad \text{for } s_3 < s \qquad (7.4)$$

The pull-out analysis has been conducted using model code 2010 and the local bond-slip properties have been calibrated comparing with the experimental data (Figure 7.10(b)).

The experimental bond-shear stress properties are shown in Table (7.2). The ascending-, sustained- and descending-region agree the experimental results; however, at frictional region, the global pull-out load and slip analysis result is linear though the experimental result suggests a non-linear behaviour. The linearity at the frictional resistance stage is caused due to the assumption of τ_{bf} as constant. There may have a gradual crushing of concrete at the rebar-concrete interface, that may cause degradation of frictional resistance during slipping at frictional stage. Hence, it might be more appropriate to consider a non-linear frictional stress resistance at local bond-slip relationship. A modified assumption of degraded friction stress is shown in Figure 7.10(a).

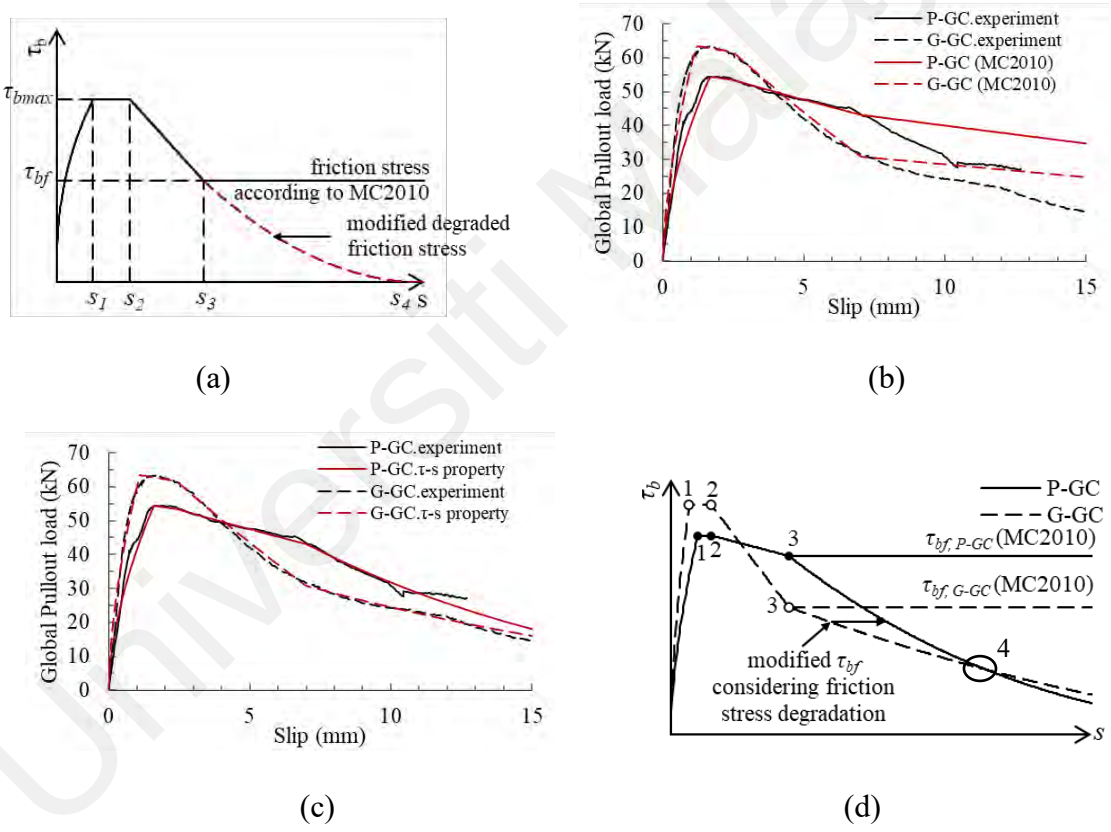

Figure 7.10: (a) Schematic diagram of τ_b-s property; (b) Global pull-out load-slip analysis using model code 2010; (c) Global pull-out load-slip analysis using modified τ_b-s; (d) τ_b-s for P-GC and G-GC

Based on this revision, Eq. (7.4) can be reformed as

$$\tau_b = \begin{cases} \tau_{bfmax} * \left(1 - \frac{s - s_3}{s_4 - s_3}\right)^{\alpha 1} & s_3 < s \leq s_4 \\ 0 & s_4 < s \end{cases} \quad (7.5)$$

Whereas α_1 is a non-linear coefficient and the value of it is more than 1. s_4 is the slip when the frictional stress becomes zero due to degradation. The analysis of pull-out load-slip response with the calibrated α_1, s_4 values as 3, 48 and 2, 48 for P-GC and G-GC, respectively are more comparable than model code 2010 (Figure 7.10(c)).

Table 7.2: Interfacial bond-slip properties of P-GC and G-GC

	τ_{bmax}	τ_{bf}	s_1	s_2	s_3
	(N/mm^2)		(mm)		
P-GC	31.2	28	1.6	2.4	7
G-GC	36	20	1.1	2.4	7

The calibrated τ_b-s for P-GC and G-GC are shown in Figure 7.10(d). The points as marked as 1, 2 and 3 correspond to τ_b-s values at slips s_1, s_2, and s_3. The stiffness at ascending region (τ_b/s) of P-GC is slightly less than G-GC and τ_{bmax} is higher for G-GC. This indicates that the chemical adhesion of G-GC might be higher and more brittle than that of P-GC. While the chemical adhesion was attributed by the binding paste to achieve τ_{bmax}, the interfacial local slip was the attribution of slip strain which is the difference of concrete and rebar strains. Due to the slip, ribs penetrated the concrete and might create microcracks. The modulus of elasticity of G-GC (E_{GGC}) is higher than that of P-GC (E_{PGC}) (Figure 7.8(b)). As the rebar strain was identical for both G-GC and P-GC, only modulus of elasticity of concrete in this experiment might influence the local slip-strains as well as local-slip.

The sustained region (between points 1 and 2 in Figure 7.10(d)) of G-GC remains slightly more slip (s_2-s_1) than that of P-GC. The residual local bond-shear stress ($\approx \tau_{bmax}$) is the resultant stress induced by progressive microcracking at ribbed area (rib bearing resistance) and shearing off the concrete between ribs. It is challenging to distinguish the percent of contribution rib-bearing resistance and concrete shearing off.

The ascending branch from point 2 to 3 (Figure 7.10(d)) is caused due to the reduction of the concrete shearing off resistance by concrete corbels between ribs. This reduction for

G-GC was higher than P-GC as the P-GC corbel shearing off resistance was eliminated sooner than G-GC corbel shearing off resistance. As the concrete corbel shearing off resistance eliminates, only friction resistance (τ_{bf}) initiates. Hence, the friction bond shear stress for P-GC ($\tau_{bf,\ P\text{-}GC}$) was found higher than that for G-GC ($\tau_{bf,\ G\text{-}GC}$) at s_3.

The friction bond shear stress resistance (τ_{bf}) degraded with slip for P-GC and G-GC (Figure 7.10(d)). However, the degradation was found higher for P-GC than G-GC. As P-GC mix contained less volume of aggregates, this might cause higher amount of frictional degradation.

7.5 Summary

The bond shear stress and slip responses of lightweight and normal weight geopolymer concretes of similar compressive strength have been investigated experimentally in this research and model code 2010 has been used to extract the interfacial bond-shear stress and slip relations. The role of aggregate, and past volume in bond shear resistance have been studied. The ultimate pull-out loads for identical rebar geometry, embedment length, concrete grade and loading condition were found comparable for P-GC and G-GC. The types and volume of aggregate in similar strength of concrete did not influence the ultimate pull-out load. However, there was influences in the pull-out load – slip stiffness in elastic and plastic range. The variation of pull-out load-slip stiffness can be related to the modulus of elasticity of P-GC and G-GC. The modulus of elasticity of G-GC was higher than that of P-GC; the stiffness of pull-out load and slip of G-GC was thus found higher than that of P-GC. At any applied pull-out load, the slip of rebar was more in P-GC than G-GC. That means, a reinforced structural member made of P-GC will have more deflection under bending than that made of G-GC.

CHAPTER 8: FLEXURAL AND SHEAR PERFORMANCE OF P-GC AND G-GC BEAMS

8.1 Introduction

The increment of world population has enhanced demand of new construction. As concrete is a construction material that enables the structure to shape in any form, and is required less maintenance for environmental corrosion, its demand has increased to its chronical stage (Mannan & Ganapathy, 2004). However, concrete requires cement and granites as the main constituents. Cement production proportionally releases CO_2 in the environment. The cement industries in the whole world emitted 576 million tons of CO_2 in 1990 which has been increased three time in 2014 with an amount of 2.083 billion tons (Benhelal et al., 2021; Boden et al., 2017). The yield of the CO_2 emission due to cement production at its current stage forecasts its increment at least 2.34 billion tons by 2050 (Cement roadmap, 2012). Therefore, cement industry demands at prime priority to find an alternative of cement. On the other hand, regular use of granite in concrete causes gradual depletion of natural resources which leads to ecological imbalance. Therefore, like cement, it is required to find alternative source of aggregates too, that would not require to compromise with the environmental benefits.

Manufacturing a new binding material like cement that has less zero-carbon emission might be a good option; but it may take hundreds of years to develop the chemistry, rather, it might be easiest way to utilize an existing technology that can produce a binding material, that acts similar manner of cement, but has less- or zero-carbon in production process. Davidovits (2008a) invented such technology known as geopolymer technology. The term, “Geopolymer” was named by Davidovits (2008a), similar type of binding material had been used in ancient Egypt to develop pyramids (Davidovits, 2008b). The geopolymer technology does not involve any high incineration process like cement production. It uses alkaline environment like combination of NaOH solution and liquid

Na_2SiO_3 to activate any pozzolanic material. The advantage of using cement over other pozzolans in producing binding paste is that it requires only water to initiate hydration, whereas many pozzolans do not activate in presence of water only. Such kind of pozzolans can be found as industrial by-product after burning in combustion chamber e.g., fly ash, ground granulated blast furnace slag, palm oil fuel ash, rice husk ash, palm oil clinker powder, etc. This burning process should not be considered while assessing environmental impact of geopolymer paste, because this combustion process is part of other industrial need. Generally, those combustion process is involved in energy production for other industrial necessity using their wastes; thus, pozzolans are produced from those combustion process as an industrial waste or by-product.

Fly ash is one of the most popular, and recently agreed by many authorities as acceptable pozzolan that can be used as substitute in cement. However, this substitution is limited to 10 to 30% of binding material for maintaining a structural grade of concrete; however, the usage of pozzolan is beneficial for long term, because its pozzolanic reaction attributes to produce more calcium silicate hydrate (which provides strength) replacing the CaOH (which has inverse contribution to strength development). Though a limited percent of fly ash is allowed to use in cement replacement, it helps to reduce CO_2 emission at an amount. Using geopolymer technology, fly ash is activated through chemical reaction in an alkaline environment. The product of the geopolymer reaction is Zeolite which achieves similar strength as Calcium silicate hydrate provides. There is no additional combustion is involved after collecting by-product fly ash from industry. So, no additional CO_2 is produced in manufacturing geopolymer concrete. Geopolymer concrete can be produced using other pozzolans like palm oil fuel ash, palm oil clinker powder, etc, as discussed in earlier chapters). But the characteristics of fly ash can be considered distinctive, because of its most consistency in physical and chemical properties. So, geopolymer concrete of

similar strength can be reproduced using fly ash activated by same amount and kind of alkaline. So, in this research, fly ash has been used as binding material only.

In south-east Asian countries, palm oil is an economically benefitted agriculture which is considered one of the main sources of economy in Malaysia, Indonesia, and Philippine. Indonesia and Malaysia are the leading countries in palm cultivation. The palm oil is extracted from the palm fruit bunch for human consumption in food preparation. Millions of tons of palm oil are extracted from palm fruit bunch, the leftovers of palm fruit bunch are the agricultural waste. These agricultural wastes are used in combustion chamber as fuel to generate energy for inhouse purpose in the mill. Two wastes, palm fiber and oil palm shell (OPS) are mixed in a proportion to use in chamber for burning properly. The combusted product from OPS and fibre composites are found in the burner as palm oil fuel ash (POFA) and palm oil clinker (POC). POFA is a powder material which can be used as pozzolanic replacement in concrete; and clinker is harden form of pozzolan. Due to combustion in high temperature (> 250°C) it consists of huge amount of micro and macro pores that makes POC lightweight.

POC are generally, dumped in open land, and no other authority approved usage of POC yet reported. But POC can be used as lightweight aggregate in concrete, especially in geopolymer concrete. Because POC is a pozzolan (Karim et al., 2016), it has additional benefit to develop a monolithic composite with geopolymer paste (Chapter 6). Very minimum scale of research has been conducted on the structural performance of POC-based reinforced concrete beam, and according to the candidate, no detail structural investigation is available on structural performance of POC-based geopolymer concrete. This investigation is important before promoting composition of POC and geopolymer in structural use. The purpose of this research is to investigate flexural and shear performance of reinforced beam made of POC-based geopolymer concrete (P-GC). As P-GC is lightweight structural grade concrete, its performance has been evaluated

comparing with the flexural and shear performance of the reinforced beam made of granite-based normal weight geopolymer concrete. The flexural and shear strengths of P-GC- and G-GC-based beams were found comparable, but the ductility of P-GC was found slightly higher than G-GC. This research outcome says that P-GC can be utilised as structural grade concrete in reinforced concrete structure. So, the investigations will be beneficial to the authorities to approve POC as lightweight and sustainable aggregate in construction industry.

8.2 Literature review

This section shows the gradual increase of interests on POC as lightweight aggregate among the research fellows. Zakaria (1986) might be the pioneer to develop a lightweight concrete using POC as aggregate. The short-term mechanical properties were investigated comparing the results with those of normal weight concrete. The research outcome suggested to use POC up to 20% as aggregate in cement-based concrete. But a question was raised by the researcher, whether the presence of sulphate in POC would be aversive in cement hydration process.

Researchers attempted to reduce the adverse effect of porous nature of POC adopting various techniques. Abutaha et al. (2016) used Department of Environment, UK's method of concrete mix design to design 40 grade concrete, where granite was substituted by POC partially, and fully. The workability, and compressive strength could be achieved comparatively of same as those of normal weight conventional concrete made of granite as aggregate. After finding the potentiality of POC as lightweight aggregate in concrete POC powder was introduced to fill the external pores of POC prior to casting. The adopted method improved the compressive strength of concrete because of the filling pores and better compaction.

Due to porous physical characteristics of POC, it causes the concrete less workable. Kanadasan & Razak (2014) thus, attempted to improve compressive strength and workability using particle packing principle. Feen et al. (2017) investigated a comparable study between 100% granite and 100% POC based self-consolidated concretes' fresh and harden properties. By using low dosage of superplasticiser, the internal friction of POC porous surface was minimised and flowability was increased. The flowability of POC self-consolidated concrete was found more than granite based self-consolidated concrete due to the aggregate particle weight. As Kim et al. (2010) commented that the flowability of normal weight aggregate self-consolidated concrete is less than lightweight aggregate self-consolidated concrete due to the constraint of the heavier matrix and greater collision between aggregates in the mixture.

The suitability of POC as lightweight aggregate is reported by many researchers based on the physical properties of POC. Ahmad & Noor (2007) examined the specific gravity, water absorption, moisture content, aggregate impact value, bulk density, crushing aggregate value. Various mix proportions were adopted to investigate the compressive strength of lightweight POC-based concrete. Structural grade lightweight concrete was able to produce using POC as aggregate. However, as POC is a porous material, it may consist of higher amount of moisture that influence the strength development in concrete. Thus, Ahmad & Noor (2007) suggested its higher moisture to be taken seriously while designing water quantity in the mix proportion.

Ahmmad et al. (2017) investigated the effect of binding material in compressive, flexural, splitting strength and modulus of elasticity of POC based light weight concrete. POC was used as complete substitute of conventional lightweight coarse aggregate. The binder properties were varied replacing cement with POC powder (POCP). Though 100% POC was used as coarse aggregate, the influence of POC powder as substitute of cement in strength development as pozzolanic material was the focus of investigation and its

influence in workability and strength development were addressed. However, the influence of POC aggregate in the fracture mechanism was not investigated in this research.

Like other lightweight concrete, POC-based concrete requires higher amount of paste compared to normal weight concrete. Higher amount of paste has adverse effect in crack initiation at early stage due to drying shrinkage. Ahmad et (2008) reported a higher drying shrinkage in concrete where POC was used as fine and coarse aggregate. The lower elastic property of POC attributes to higher drying shrinkage (Neville & Brooks, 2010).

The chloride penetration through concrete may seriously affect the overall ductility of reinforced concrete in long run due to corrosion on rebar surface that raises a question of existence of required level of strength. Mohammed et. (2011) found that POC-based cement concrete had higher amount of penetration of chloride ion due to porosity in POC aggregate. However, this penetration of chloride ion depends on the compactness of the concrete. In self-consolidated concrete, or in concrete with good workability, the external pores of POC is covered by matrix, that increases the compactness of the concrete. Kanadasan & Razak (2014) developed self-compacting concrete mix design where POC was used as lightweight aggregate. The particle packing concept was adopted to develop the mix proportions. The evaluation of fresh and harden properties of POC-based self-consolidated concrete suggested the suitability of POC as aggregate in structural grade concrete.

As POC is produced burning at high temperature (> 250°C), it may have less adversity in strength reduction while it is incorporated in concrete and that concrete experiences high temperature. Jumaat et al. (2015) investigated the temperature resistance of POC-based concrete. The weight loss, surface cracking, change of colours and the residual compressive strength were the evaluation criteria in this research. The experimental

results were compared with the results of a lightweight concrete made of another palm oil industrial and agricultural waste, oil palm shell (OPS) as aggregate. The weight loss of POC-based concrete was insignificant, the number of cracks due to high temperature was reduced while volume of POC was increased, i.e., when the volume of paste was reduced. The shrinkage of POC-based concrete was not significantly differed from the shrinkage of conventional concrete; but this finding was contradictory with the findings reported by Ahmad et (2008). The difference in paste volume might be caused in variation of shrinkage response.

Omar & Mohamed (2002), and Mohammed et al. (2014) studied the flexural strength of POC-cement-based reinforced concrete beam. Less than 0.5% (Omar & Mohamed, 2002), and 0.35 to 2.23% (Mohammed et al., 2014) reinforcement ratios were used in beam manufacturing. A typical flexural failure was observed. The use POC thus assumed that it had no detrimental effect on flexural strength of reinforced beam. Mohammed et al. (2014) found the ductility of POC-based beam less than the expected. The deflection was reported 10 to 45% less than the deflection suggested in British standard (1997) (This code has been withdrawn and replaced by Euro code 2 in recent years; but the old version cannot be completely ignored.). A contradictory to commentary can be found in Omar & Mohamed (2002)'s investigation. The mix proportion of concrete constituents may play significant role. Higher amount of paste volume in concrete, comparatively, reduces the ductility of concrete. In lightweight aggregate, generally requires high amount of paste; But if the paste volume is optimised, it may help to reduce the brittleness of concrete due to high volume of paste.

Mohammed et al. (2013) studied the shear behaviour of reinforced concrete beams made of POC as aggregate. Various strengths of POC-based concrete were used. The tension reinforcement ratio, shear span to effective depth ratio, were varied. The shear cracking response was comparatively similar to that of normal weight concrete made of granite as

aggregate. The variation of shear span to effective depth ratio did not provide any significant variation in responses of concretes made of POC or granite as aggregate. The variation of tension ratio, and compressive strengths of POC-based concrete had significant influence in shear strength of the beam. Mohammed et al. (2013) compared the experimental results with the prediction formulae suggested by British standard (1997), ACI committee 318, and Eurocode 2. The shear capacity of POC-based on concrete while checked using these building standards, was found overestimated. Therefore, additional safety precautions to be taken were suggested to avoid shear failure of POC-based concrete. This overestimation was meaningful for POC-based concrete. Because POC is porous in nature, and the shear properties vary significantly, when concrete contains large and unpredictable number of pores.

The above literature review addresses research on cement based lightweight concrete where POC was used as lightweight aggregate. The following review have been addressed research on POC-based lightweight geopolymer concrete.

Like Jumaat et al. (2015), Sharmin et al. (2015) investigated a comparison between OPS and POC-based geopolymer concrete. The difference between this two research is that, Sharmin et al. (2015) used geopolymer matrix, and OPS-POC blends in various proportion to investigate engineering properties of concrete, whereas Jumaat et al. (2015), used cement-based matrix, and OPS and POC were not blended. Overall Sharmin et al. (2015) used POC sand as fine aggregate in geopolymer matrix. 50 to 75% of mining sand was replaced by POC sand. The modulus of elasticity and splitting tensile strength was reduced with increment of substitution of mining sand by POC sand. The modulus of elasticity of geopolymer concrete made of 50% substituted POC sand was noticeably less (only 5 GPa) than geopolymer concrete made of mining sand without any substitution. The reasons of reduction of modulus of elasticity and tensile strength of concrete were attributed to OPS for its spongy physical property (Alengaram et al., 2011), and POC for

its porous physical nature. Multiple number of micro-cracks were generated while the tension stress was executed, these micro-cracks were appeared for low stiffness of POC (Shannag, 2011).

Above the major and significantly related research on POC-based concrete has been discussed. More research works on development of various mix proportion, and their mechanical properties are available; none of the research addressed the flexural and shear behaviour of geopolymer lightweight concrete where POC had been used as 100% lightweight aggregate. Moreover, the effect of variations of POC sizes in shear resistance of geopolymer beam had not been addressed in earlier research. The role of POC in flexural and shear response of beam is important to know before applying POC-based geopolymer concrete in structural application. Therefore, this research has been focused to evaluate the flexure and shear responses and the role of POC as lightweight aggregate has been discussed in relation to the discussion of Chapter 5, 6, and 7. The outcome of the finding in this research will be useful for structural engineers and authority to recognise the value of POC as aggregate in geopolymer concrete.

8.3 Experimental programme

8.3.1 Material properties and concrete recipe

Lightweight and normal weight geopolymer concrete was cast using POC, and granite as aggregate, respectively. The geopolymer matrix was prepared with an appropriate mix proportion so that both lightweight (P-GC), and normal weight (G-GC) concretes achieve compressive strengths within a comparable range.

Fly ash was used as binding material. 14*M* NaOH solution and liquid Na_2SiO_3 were used as activator to activate fly ash through geopolymer reaction process. Manufactured sand (M-sand) was used as fine aggregate. The general material properties have been discussed

in chapter 3. However, some characteristics of POC have been discussed below as these properties have major role in the influence of flexural and shear responses of beam.

POC is highly porous material since POC is generated after combustion in chamber at high temperature (250°C). The pores are developed externally, and internally at micro- and macro-level during incineration process. This causes POC to be lightweight. The bulk dry density of POC was measured as 780 kg/m^3. According to ASTM International (2017), this bulk-density of POC is appropriate to utilise as lightweight aggregate (< 880 kg/m^3) for structural lightweight aggregate concrete.

POC is 53% lighter than conventional granite. As it has pores, it is broken in fine particle easily. That's why, the aggregate crushing value of POC is about three times higher than conventional granite. The micro- and macro- pores of POC absorbs water and moisture about 7.5 times higher amount than granite. The detail mix design can be found in chapter 3, and 6. However, the weight proportion of constituents is reported in this chapter.

The weight proportion of fly ash, M-sand, coarse aggregate (100% POC or 100% granite), alkaline activator was used as 1:0.75:0.75(POC):0.43, and 1:1.36:3.17(granite):4, respectively, for P-GC, and G-GC. No water was used in P-GC, as it reduces the strength. So to compensate the workability issue, volume of geopolymer was increased compared to G-GC. An amount of water (0.15 of binder) was used in G-GC. The compressive strengths of developed geopolymer concretes were measured within 25 to 30 MPa. The average compressive strength-strain responses of P-GC and G-GC have been shown in Figure 8.1. The bond properties of P-GC and G-GC with the reinforcing bar is significant to analyse the flexural response of beam. The detail investigation of pull-out load and slip responses of rebar from P-GC and G-GC has been discussed in Chapter 7. The tensile stress-strain response of the rebar and the average pull-out load and slip of the rebar which is identical with the main rebar used in beam are shown in Figure 8.2, and 8. 3.

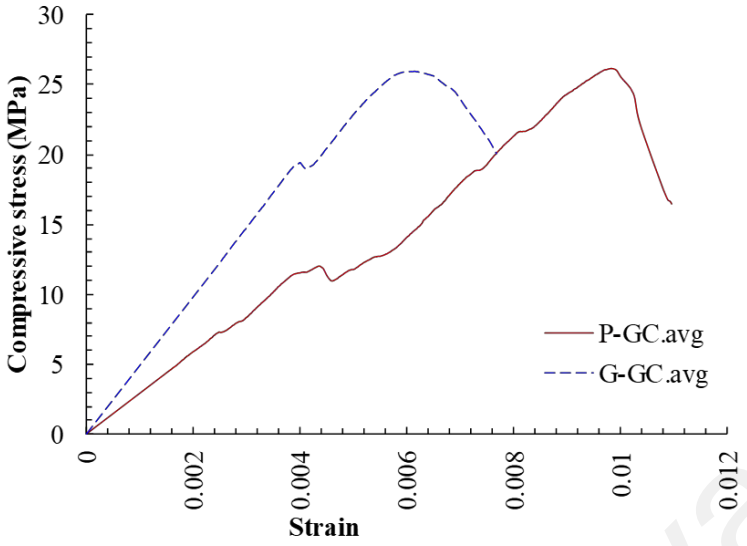

Figure 8.1: Average compressive stress-strain response of P-GC and G-GC

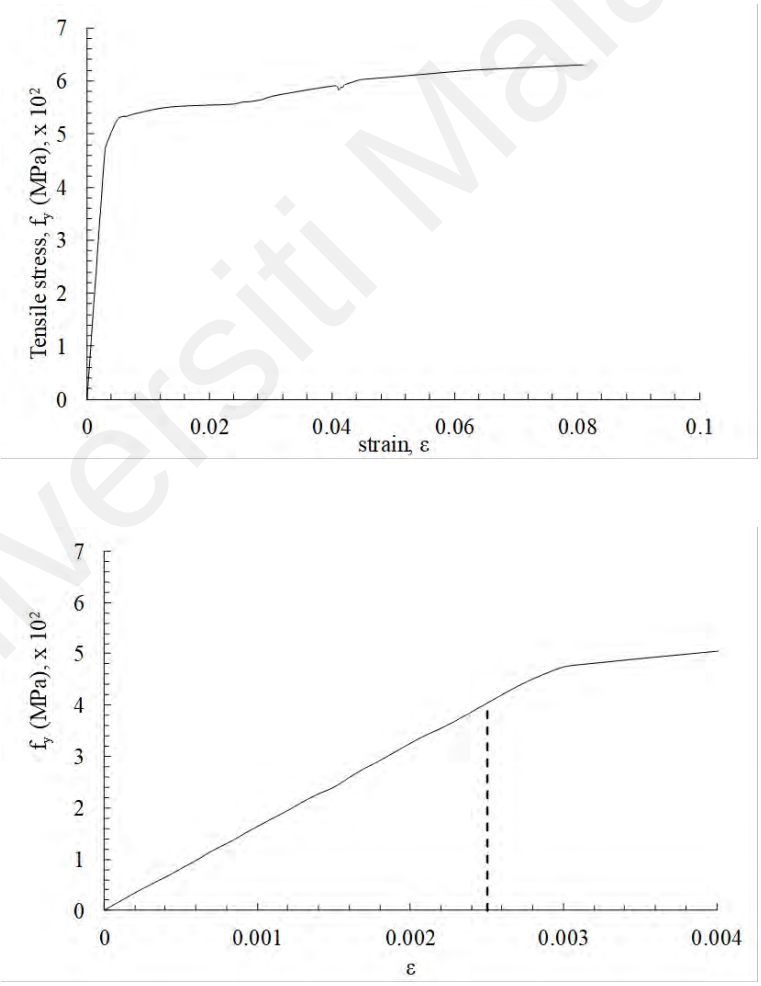

Figure 8.2: Tensile stress-strain response of Grade 500 reinforcement

8.3.2 Reinforcement detail, beam casting, and curing

The reinforcement details of flexural strength beam are shown in Figure 8.4. The middle span of length 700mm was designed as singly reinforced beam. This length of span is within the constant moment zone (CMZ) according to the loading set-up. The purpose of this flexural experiment is to evaluate the flexural response and discuss the result in relation to the concrete stress-strain behaviour (Figure 8.1), and rebar pull-out and slip responses (Figure 8.3). Because of this reason, singly reinforced beam was adopted at CMZ that simplify the analysis. The novelty of this research is to achieve a clear concept of the role of POC, while reinforced P-GC beam is under bending stress. However, the interactions of material properties (concrete compression stress-strain, steel stress-strain, and pull-out load-slip) have been discussed based on the conceptual development of moment rotation theory (Oehlers et al., 2014a,b). Two types of reinforcement ratio were used as variables in P-GC and G-GC reinforced beams. The bottom reinforcement was used 2T12, and 3T12, whereas no reinforcement at compression zone within CMZ, and 2T12 at compression zone outside CMZ. The shear links (Ø6 mm) was provided at 50 mm spacing at both side spans of CMZ. The link-spacing was determined following Eurocode 2 (EC2) so that the beam failed in flexure only and no failure occurred due to shear.

The cross-sectional dimension of beam was 250 x 150 mm^2 therefore, percentage of reinforcements for 2T12 and 3T12 at CMZ was 0.6 and 0.9% respectively. Grade 500 reinforcement was used in this research. According to EC2, minimum and maximum percentage of reinforcement were calculated as 0.182 and 4%, respectively. The beams are designated in this chapter as P2T12, P3T12, G2T12, and G3T12. P and G denote for P-GC and G-GC, respectively. Two specimens were cast for each type of four categories of beams.

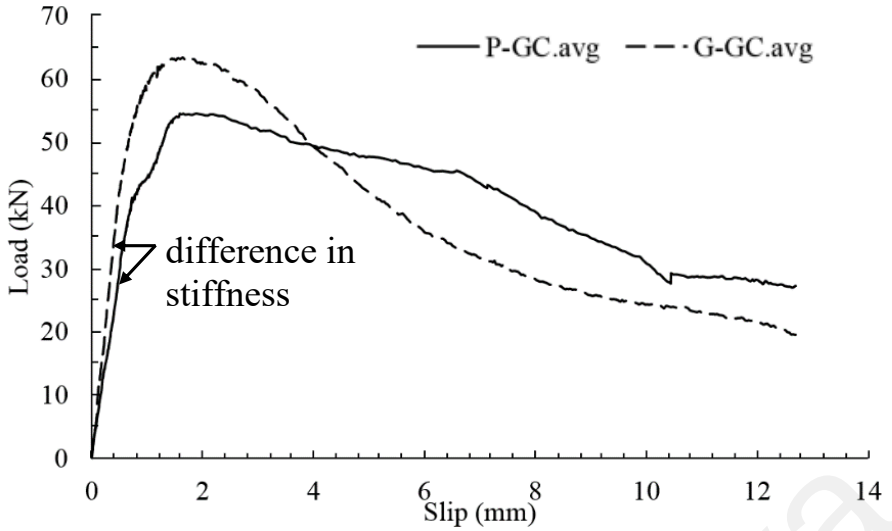

Figure 8.3: Pull-out load and slip responses of rebar from P-GC, and G-GC

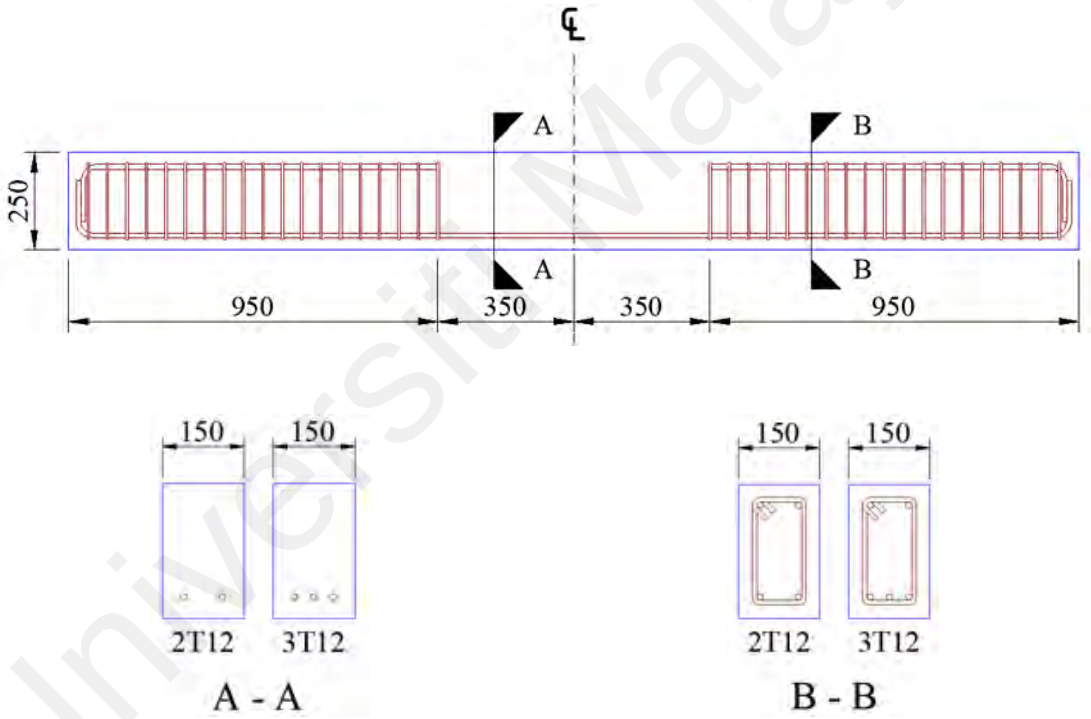

Figure 8.4: Reinforcement details of beams for flexural test

The minimum steel was calculated using the following formula suggested in Eurocode 2.

$A_{s,min} = 0.26\frac{f_{ctm}}{f_{yk}} b_t d; \; but \; not \; less \; than \; 0.0013 b_t d$; Whereas f_{ctm}, f_{yk} = 3.5 (for grade 35 concrete) and 500, respectively.

The concrete cover was provided 25mm all-around of the cross-section which was decided according to Eurocode 2 guideline for minimum concrete cover for a safe transmission of bond stresses.

$$c_{min} = max\{c_{min,b}; 10mm\}$$ Whereas c_{min} = 1.5Ø = 18 mm.

The beams were left in ambient temperature for three to four hours after casting. The beam specimens were then shifted to curing chamber including their steel moulds and companion specimens. The beams were cured at 65°C temperature for 24 hours. As geopolymer curing in high temperature, accelerates the early age strength development, the beams were sufficiently strong to demould after 24 hours of oven curing. However, another two days were waited to avoid any micro-cracking during handing the beams.

Another set of beams were cast for shear tests using four different aggregates such as: P5-14, P-5-10, P10-14, and G5-14. These concretes were used to cast beams with and without shear links. P5-14 refers to the P-GC that contained POC of 5 to 14mm sizes. Similarly, P10-14, and P5-10 refer to the same P-GC mix, but the POC sizes were within 10 to 14mm and 5 to 10mm. G5-14 refers to G-GC which had granite of sizes between 5 and 14mm. The reinforcement details of 150mm × 150mm × 1300mm beam for shear test is shown in Figure 8.5. Two bottom and two top reinforcements of 12mm diameter was used in the cross-section of beams with Ø6 mm stirrups/ shear links at 50mm spacing. Only two bottom reinforcements were provided for beams without shear links. The concrete cover (25mm all-around) and size of main reinforcements were decided following Eurocode 2 guideline. The length of shear beams was shorter than the flexural testing beams. The lengths were decided based on the availability of spreader beam sizes, support distances below INSTRON machine.

The shear beams were cast following the same casting and curing as adopted for flexural testing beams.

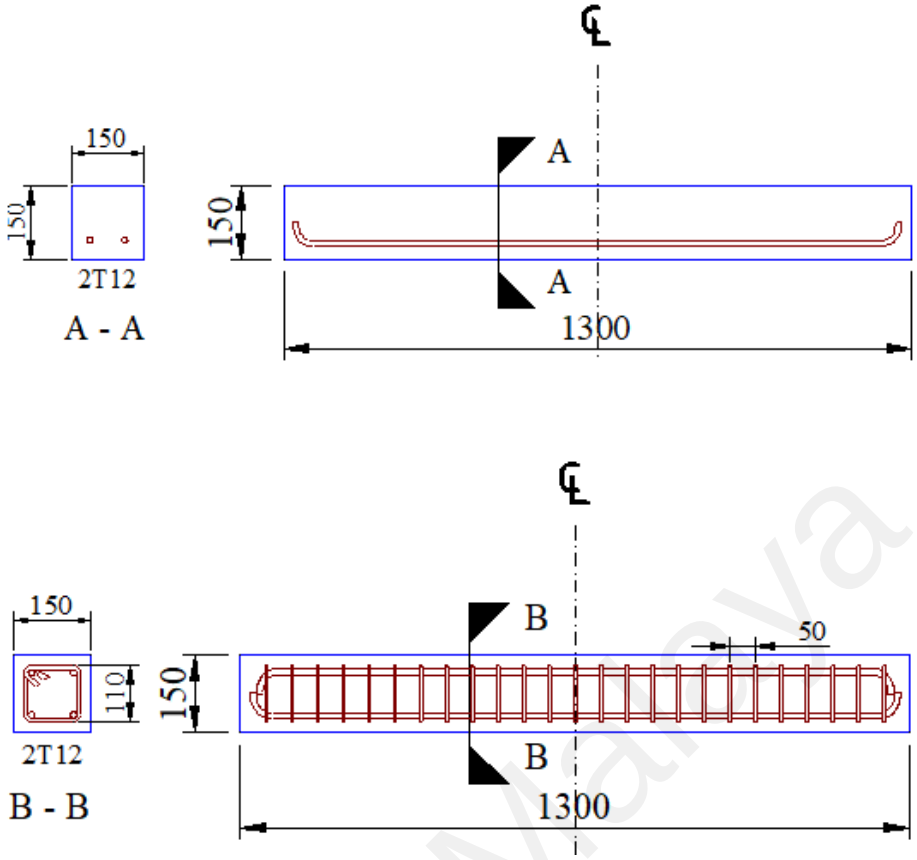

Figure 8.5: Reinforcement details of beams for shear test: beams without shear link (top beam); beams with shear links (bottom beam).

8.3.3 Flexural test set-up and data acquisition

The beam of 2,600mm of length was supported beneath the loading actuator of INSTRON. The supports were 2,300mm distance from each other. This is the span of simply supported beam. There was 150mm over hanged at opposite side of the span. This overhanging was kept additionally for avoiding any kind of slip during the testing. A spreader beam was placed above beam which was symmetrically positioned beneath loading actuator. The distance of the loading points was considered as 700 mm which was less than ⅓ of the span; therefore, the constant moment zone was within that 700mm length of beam. The four-point static bending test was employed to investigate the flexural performance of P-GC and G-GC reinforced concrete beams. The experimental set-up is shown in Figure 8.6.

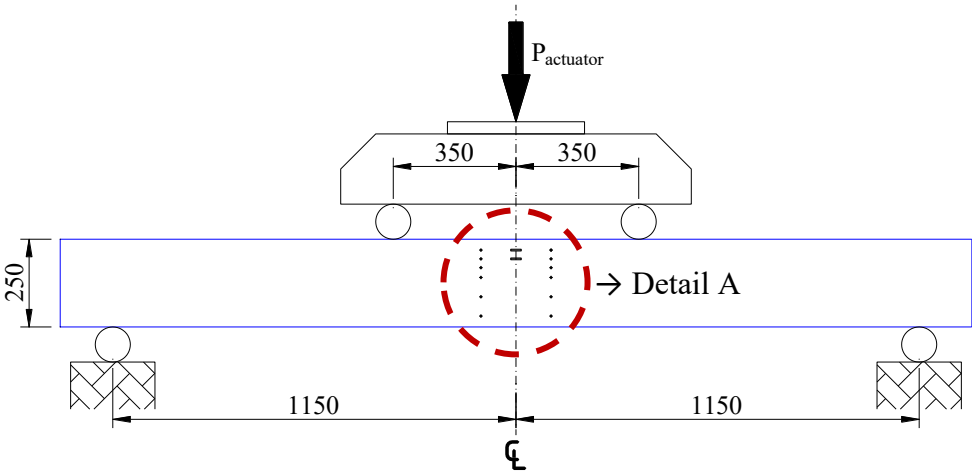

(a) Positions of beam, supports and spreader beam

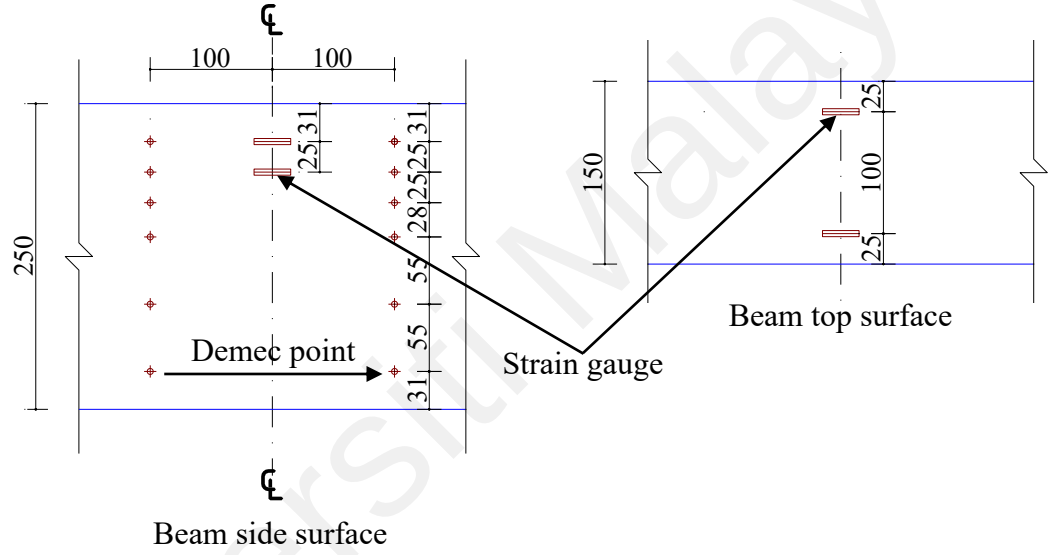

(b) Detail A – Positions of demec points and strain gauges

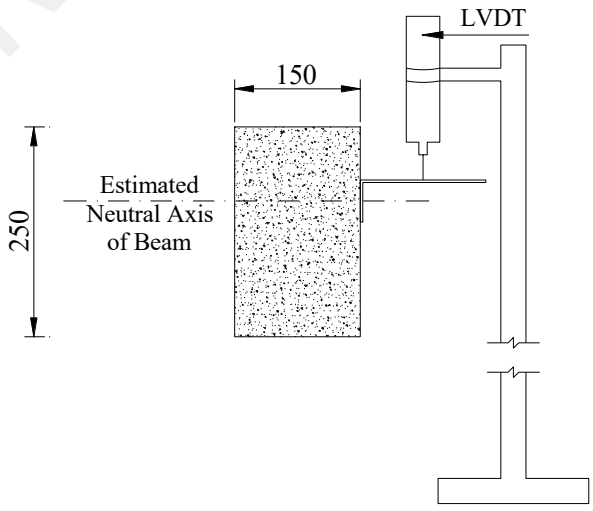

(c) Position of LVDT at mid-span for deflection measurement

Figure 8.6: Beam set-up for flexural test (dimensions are in mm)

Figure 8.7: Photographs of Beam set-up for flexural test

(a)

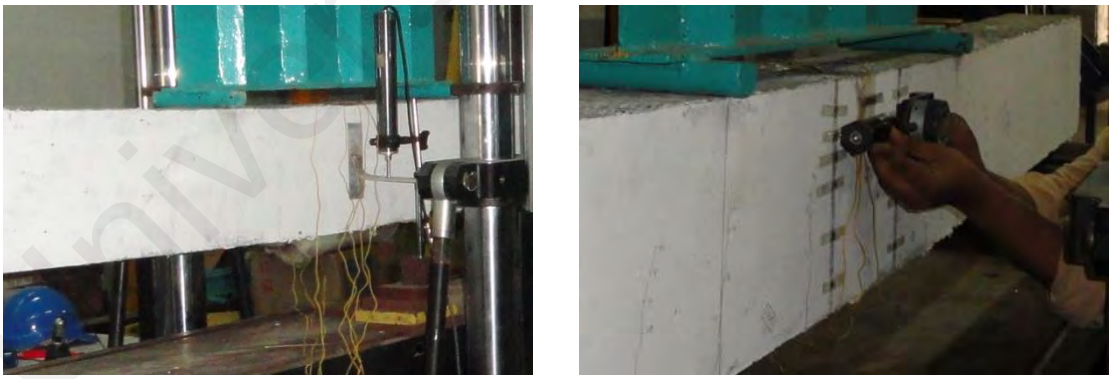

(b) (c)

Figure 8.8: Instrumentation: (a) strain gauges at side surface and top surface of beam; (b) LVDT for deflection measurement at mid-span; (c) Demec measurement

The load was applied from INSTRON actuator to the mid-span of spreader beam at a displacement control pace rate of 5mm/min. A linear variable differential transformer (LVDT) was placed at mid-span to monitor the beam deflection.

Demec and electrical-resistance strain gauges were fixed at the mid-span of the beam side surface and top surface. The detail of positions of demec points and strain gauges are shown in Figure 8.6(b).

The load measured from INSTRON, deflection from LVDT, and strain reading were collected using a datalogger. The data was recorded in every second.

In summary, applied load, deflection at mid-span, concrete strains at side and top surfaces of beam, and Demec measurements were taken frequently. These data were analysed with the material properties to investigate the role of POC in P-GC under bending stress.

8.3.4 Shear test set-up and data acquisition

The shear test set-up was comparatively simpler than flexural test set-up. The beam length was shorter than that of flexural test. The shear testing set-up is shown in Figure 8.9.

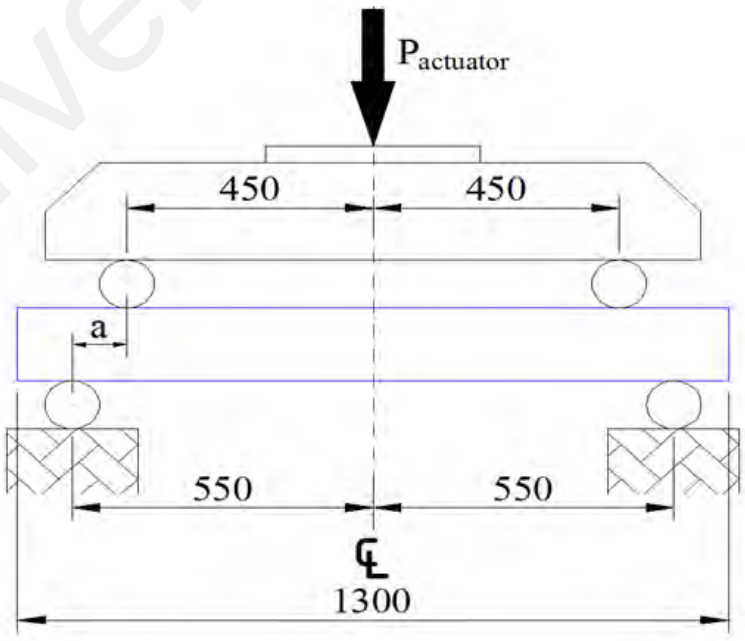

Figure 8.9: Shear test set-up

The shear beam of length 1300mm was supported on two pin supports distanced at 1100mm from each other. The spreader beam was placed at the middle top of the beam symmetrically so that loading point to closest support distance (a) remains equal, and the loading actuator of INSTRON provides load at mid-span of the spreader beam. The distance between loading points from the spreader beam was 900mm; therefore, the value of *a* was 100mm which was close to the effective depth of beam (150 – 37 = 113mm). This *a*/effective depth ratio is important to achieve shear failure in beam; this value of this ratio needs less than or equal to 1 to achieve shear failure; otherwise, the beam may fail for flexure, theoretically. The load and mid-span displacement were measured following same procedure adopted for flexural test, i.e., loads, and mid-span deflection from LVDT; and both data was collected in a common datalogger.

8.4 Results and discussion

8.4.1 Generic theory of stress-strain distribution across a section in bending

Before entering to the detail investigation of the experimental result, let's review, the generic theory of stress-strain distribution across a cross-section of a beam under bending stress. According to the theory of bending for reinforced concrete, it is assumed that concrete will crack in the regions of tensile strains and then, tensile resistance will be carried out by the reinforcement only (Figure 8.10). According to this theory, plane sections of a structural member is considered plane after straining; thus, the strains distribute across the plane is considered linear. However, from the concrete stress-strain response (Figure 8.1), stress-strain relationship can be found non-linear after a certain strain. And this non-linearity and concrete elasticity, vary depending on the constituents in concrete.

For a strain at compression extreme fibre, the plane is assumed to be rotated along neutral axis; and the tension extreme fibre achieves strain proportionally. As concrete is weak in tension, immediate after reaching tensile capacity of concrete after a short strain, the total

tensile stress is transferred to reinforcement. The moment of compression and tension resistance at neutral axis is the moment capacity of that section.

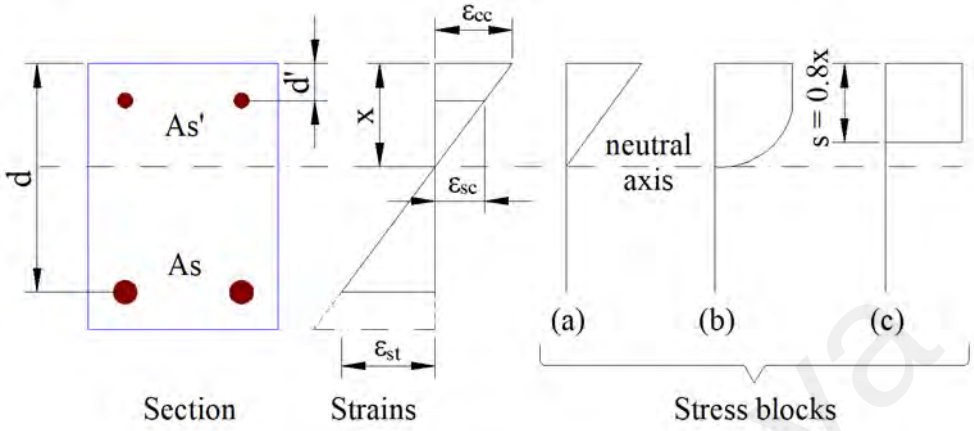

(a)

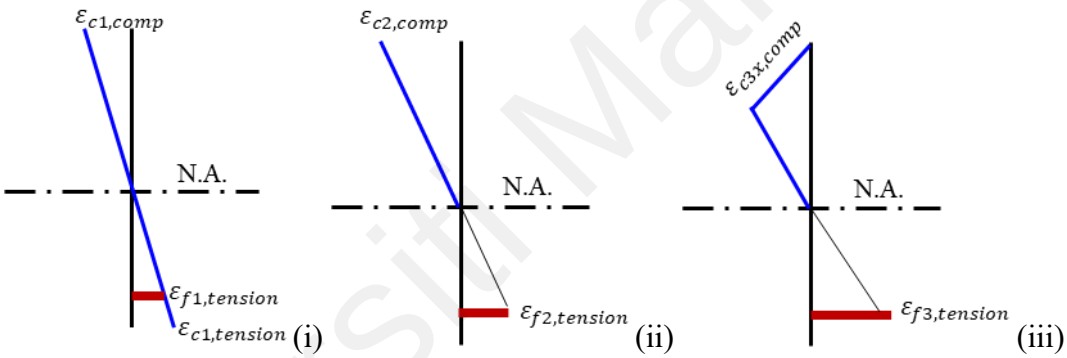

(b) Strain profile of beam cross section at CMZ

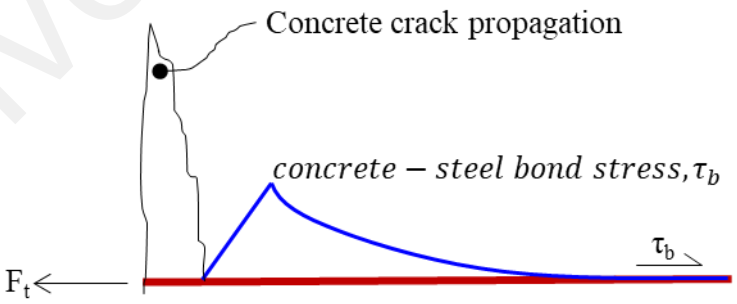

(c) Steel-Concrete bond failure and crack propagation in beam cross-section

Figure 8.10: Generic stress-strain distribution across beam cross-section

When the compression strain gradually increases, the compression and tensile stresses in compression zone and tension zone will be based on the material stress-strain responses: for concrete Figure 8.1, and for rebar Figure 8.2, and 8.3. Thus, computing the moment-

curvature for each strain at compression zone, a historical load-displacement curve can be adopted for the section, which will be able to show the response in elastic, and plastic stage of reinforced concrete section.

For structural application, beam is generally designed to be under-reinforced; that means, steel will yield before compression extreme of section reaches to maximum strain of concrete. The reinforcement details those have been shown in Figures 8.4, and 8.5 are designed as under-reinforced. That means, the crack at tension extreme fibre will appear due to yielding of steel before the compression extreme fibre reaches to its ultimate strains of P-GC/ G-GC. The ultimate strains of G-GC, and P-GC are 0.006, and 0.01, respectively (Figure 8.1). So, from the theoretical explanation, it can be assumed that until the strain of 0.006 at compression extreme fibre, both P-GC and G-GC are able to withstand the equal amount stress that is resisted by the tension reinforcements. At this stage, tension reinforcement should already be started yielding. So, the rebar is assumed to be able to resist tensile stresses of amount 500 MPa. It should be noted that concrete has been cracked and tension forces are transferred to the rebar only. So, the crack width of at the extreme tension fibre of the beam is the summation of steel elongation for the strain, and the slip occurs due to tensile force on steel bar. Thus, pull-out load-slip properties are required to know to analyse the crack-width, and load-displacement of a beam until its damage.

Now let's consider, that the strain at compression extreme fibre reaches to 0.01. At this stage P-GC will resist stress of an amount of its ultimate compressive stress. However, compression resistance of G-GC at this strain level will start reducing; because, according to it stress-strain relationship (Figure 8.1) starts weakening. So, implementing the material properties into the stress-strain distribution across the cross-section of beam, a detail analysis of beam until damage level can be found.

An analytical approach of this analysis is shown in Chapter 6 to develop a moment curvature response of P-GC and G-GC until their damage level.

Now we will see the experimental results in the following section. The accuracy of above assumption can be clearly understood from the discussion.

8.4.2 Investigation of flexural response

8.4.2.1 Neutral axis

The neutral axis of the cross-section was determined from the demec measurements. The strains of Demec points at a specific load (50 kN) are shown in Figure 8.11. The position of neutral axes of P2T12, P3T12, G2T12, and G3T12 were found 195, 205, 180, and 185mm, respectively. At this force, the statistical moment can be calculated as 40 kN-m (approximately, only actuator load is considered). The neutral axes of G-GC beams are at closer to the extreme fibre of compression zone than that of P-GC beams. So, it can be said that to withstand moment 40 kN-m, G-GC beams require less cross-sectional area in compression zone than the beam made of P-GC. In Figure 8.1, it is seen that before the ultimate strength, for a same amount of strain, G-GC resisted more stress than P-GC which justifies the accuracy of the above explanation regarding the neutral axes.

Figure 8.12 represents the strain variations measured by Demec points at various depth of beam at different loads. The strain variations at various loads are linear at the extreme fibres (Dem1, Dem2), whereas, at a high load, a non-linearity of strain variations can be noticed for Demec points those are positioned between neutral axis and extreme fibre (Dem3, Dem4). So, an important finding is found from this observation is that the assumption of linearity of cross-sectional plane, that is used to generalise the stress-strain across the beam cross-section, is not exactly linear. However, this non-linearity is very minor before the beam reaches to its ultimate resistance.

From the earlier investigation in Chapter 6, it was found that the neutral axis tends to move towards the extreme fibre of the compression zone when the concrete weakening at that fibre is initiated.

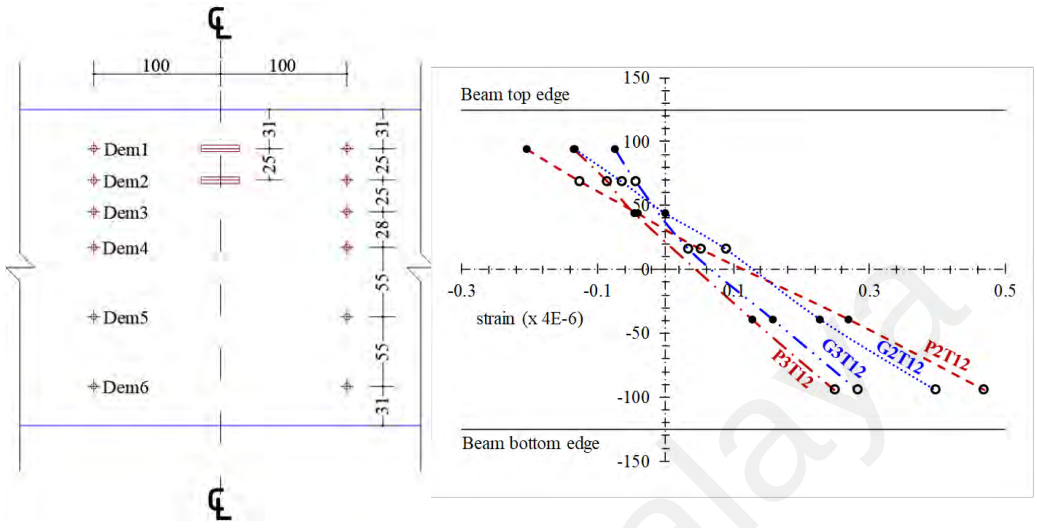

(a) (b)

Figure 8.11: (a) Demec point designation and position on beam side surface; (b) Strain of Demec points at load 50 kN

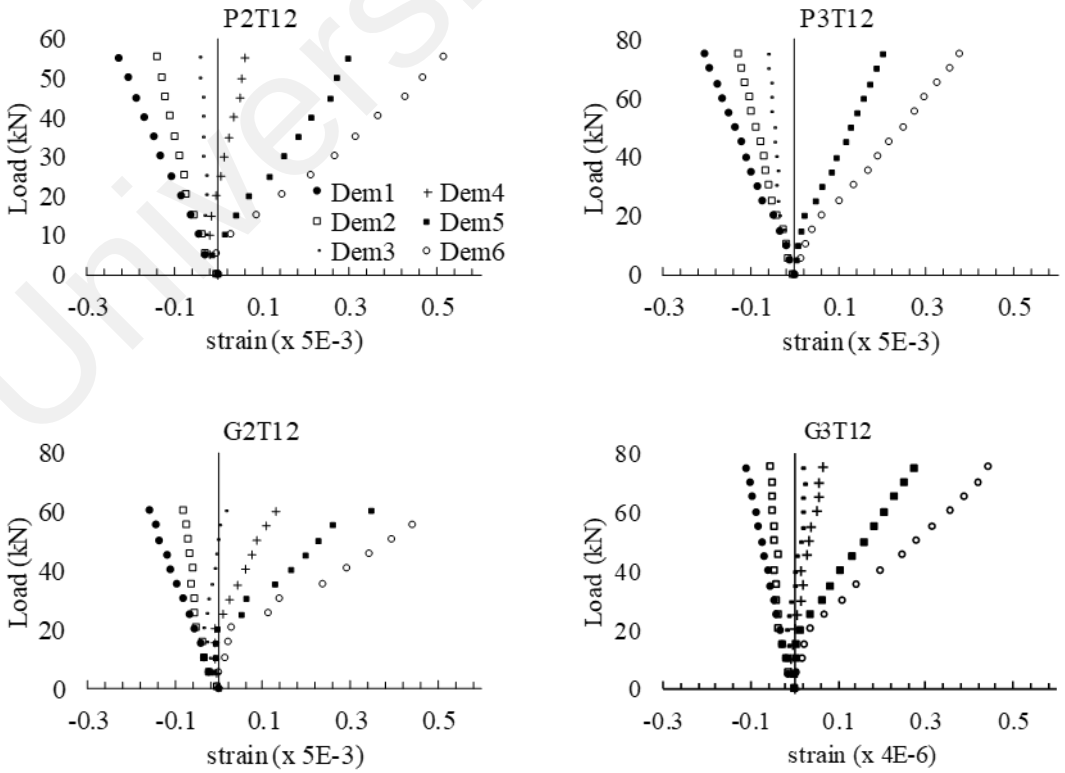

Figure 8.12: Variation of concrete strain along cross section

8.4.2.2 Load and deflection responses

The average responses of load and deflection at mid-span of P2T12, P3T12, G2T12, and G3T12 beams are shown in Figure 8.13. The responses have been divided into three sections 0-1, 1-2, 2-3 as shown the key points in Figure 8.13(a), and (b). However, for explanation purpose, distribution of stresses across the beam section is required to discuss concurrently. An analytical Moment-curvature relationship has been calculated (as shown in Figure 8.14) based on the interaction properties (concrete compression stress-strain and rebar pull-out -slip relationship). The profiles in Figure 8.13, and 8.14 can be compared and the key points can be recognised on Figure 8.14. After recognition of key points on Figure, 8.14, corresponding sectional stresses can be plotted as shown in Figure 8.15, and 8.16. The method of this analysis has been described in Chapter 6.

At point 1, the tension extreme of section reached to the tensile stress equivalent to the concrete ultimate tensile stress. Therefore, the crack initiates from tension zone. The estimated strains, and stresses at point 1 has been mentioned in Table 8.1. The strains at extreme tension fibres of P-GC beams are relatively higher than G-GC beams. This indicates that, P-GC had more curvature than G-GC at the first cracking. The visual crack width was measured using Dino capture microscopic camera. The first cracking load, and crack widths are recorded in Table 8.2. The visual records of first cracking loads match the analytically recognised first cracking loads (10kN (P2T12), 20kN (G2T12), 20 kN (P3T12, G3T12)).

At the load of first cracking, P-GC at tension zone (Figure 8.15(a), 8.16(a)) had initiated cracking; however, a little amount of tensile stress was taken by P-GC. However, tension zone of G-GC beams was fully resisted by concrete tensile resistance.

Concrete tension zone gradually separated widening the cracks gradually between point 1 and 2 in (Figure 8.13, 8.15(b,e), 8.16(b,e)). At point 2, P-GC at extreme compression

zone (Figure 8.15(b), 8.16(b)) started softening before G-GC (Figure 8.15(e), 8.16(e)). Because strains at extreme compression of P-GC beams, were almost double of strains of G-GC beams (Table 8.1). At point 3, both P-GC, and G-GC beams were softened completely; the strains of both type of concrete beams at their compression extreme fibre, were exceeded the maximum strain which can be found in concrete compression stress-strain relationship.

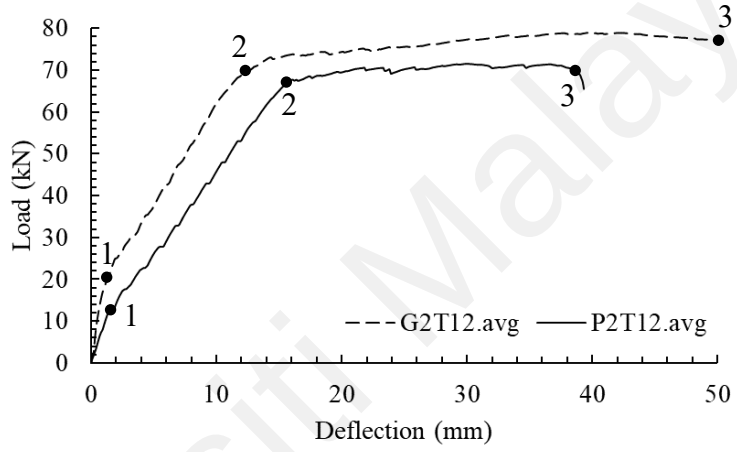

(a)

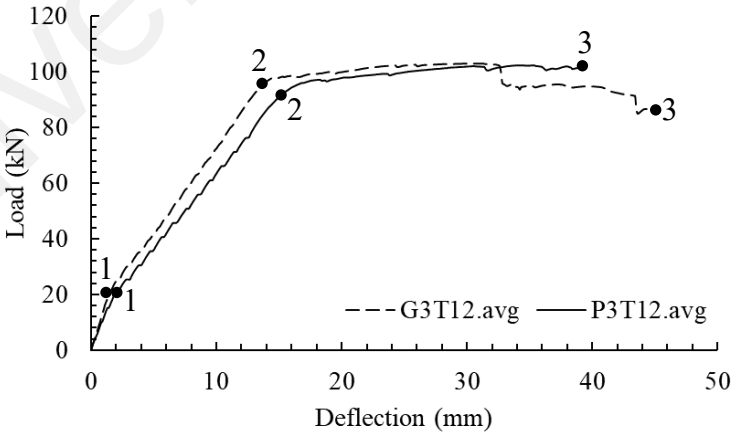

(b)

Figure 8.13: Load-deflection response of G-GC and P-GC beams with reinforcements (a) 2T12, and (b) 3T12 at tension zone within CMZ

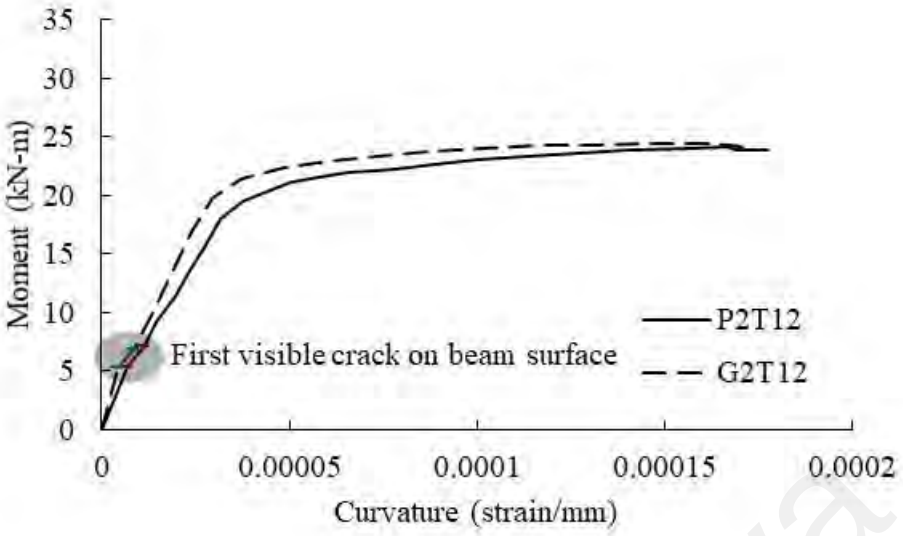

(a)

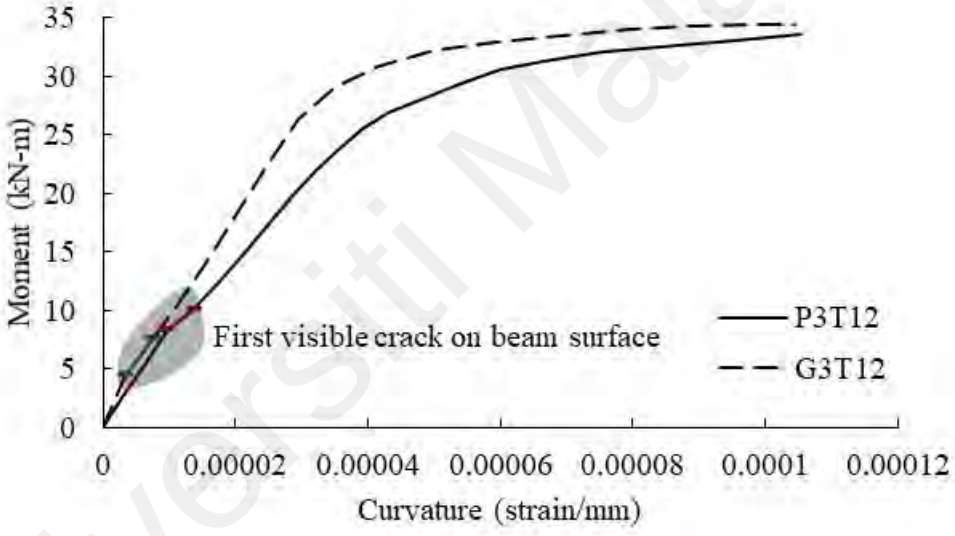

(b)

Figure 8.14: Moment capacity of beams at CMZ and curvature behaviour of (a) P2T12 & G2T12, and (b) P3T12 & G3T12 (analytically derived using material properties)

Table 8.1: Stress and strain of concrete at compression zone and rebar at tension zone at key points shown in Figure 8.13

Beam designation	Key points as shown in Figure 8.12											
	1				2				3			
	ε_c	ε_r	$\sigma_{c,avg}$	σ_r	ε_c	ε_r	$\sigma_{c,avg}$	σ_r	ε_c	ε_r	$\sigma_{c,avg}$	σ_r
P2T12	0.0010	0.0006	1.56	100	0.0060	0.0063	7.84	532	0.0115	0.0263	11.85	560
G2T12	0.0005	0.0002	1.22	42.84	0.0030	0.0032	7.36	482	0.0100	0.0269	13.35	561
P3T12	0.0015	0.0007	2.19	115	0.0055	0.0028	7.36	453	0.0100	0.0124	13.04	548
G3T12	0.0005	0.0002	1.22	37.83	0.0035	0.0027	8.59	444	0.0080	0.0142	15.57	550
ε_c = strain at extreme compression fibre; ε_r = strain at rebar; $\sigma_{c,avg}$ = avegare compressive stress on concrete at compression zone (MPa); σ_r = stress on rebar (MPa)												

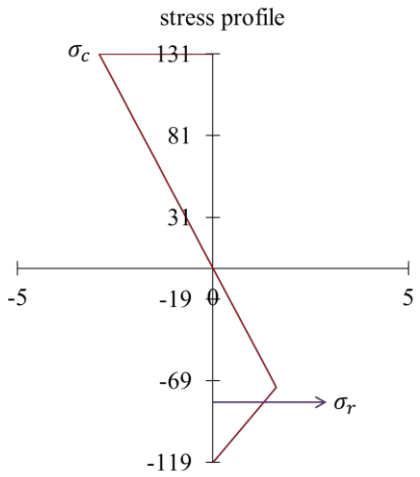

(a) P2T12 at key point ①

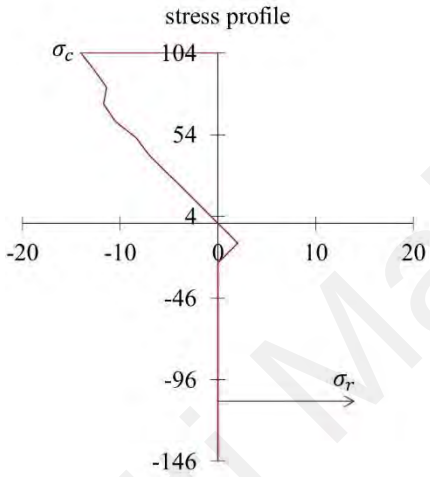

(b) P2T12 at key point ②

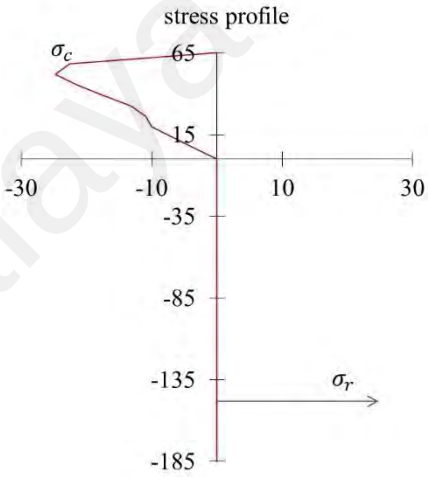

(c) P2T12 at key point ③

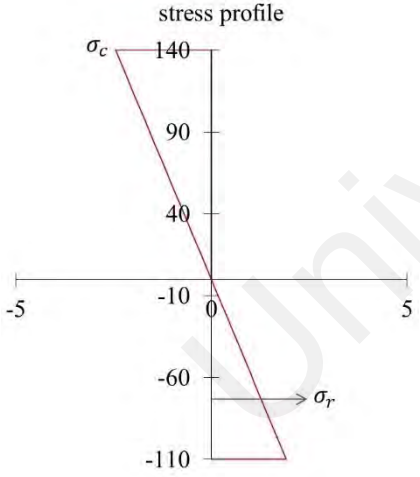

(d) G2T12 at key point ①

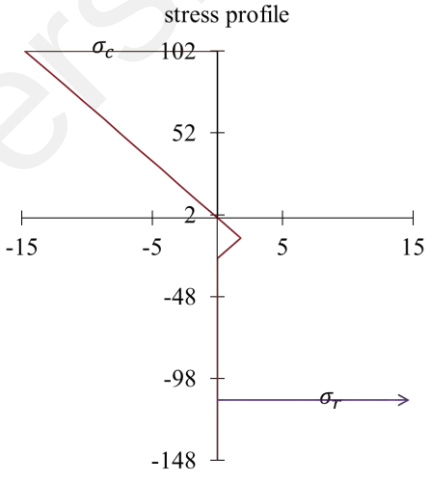

(e) G2T12 at key point ②

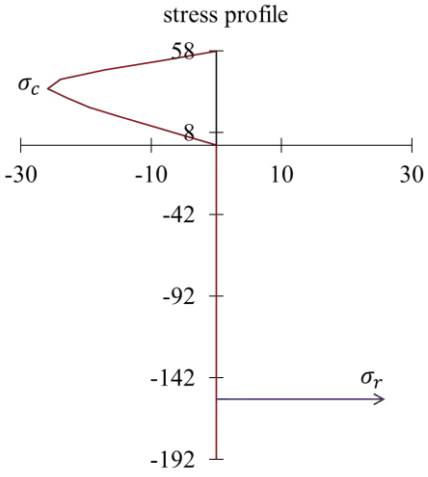

(f) G2T12 at key point ③

Figure 8.15: Stress profile along beam cross-sections of P2T12 and G2T12 at key points shown in Figure 8.12

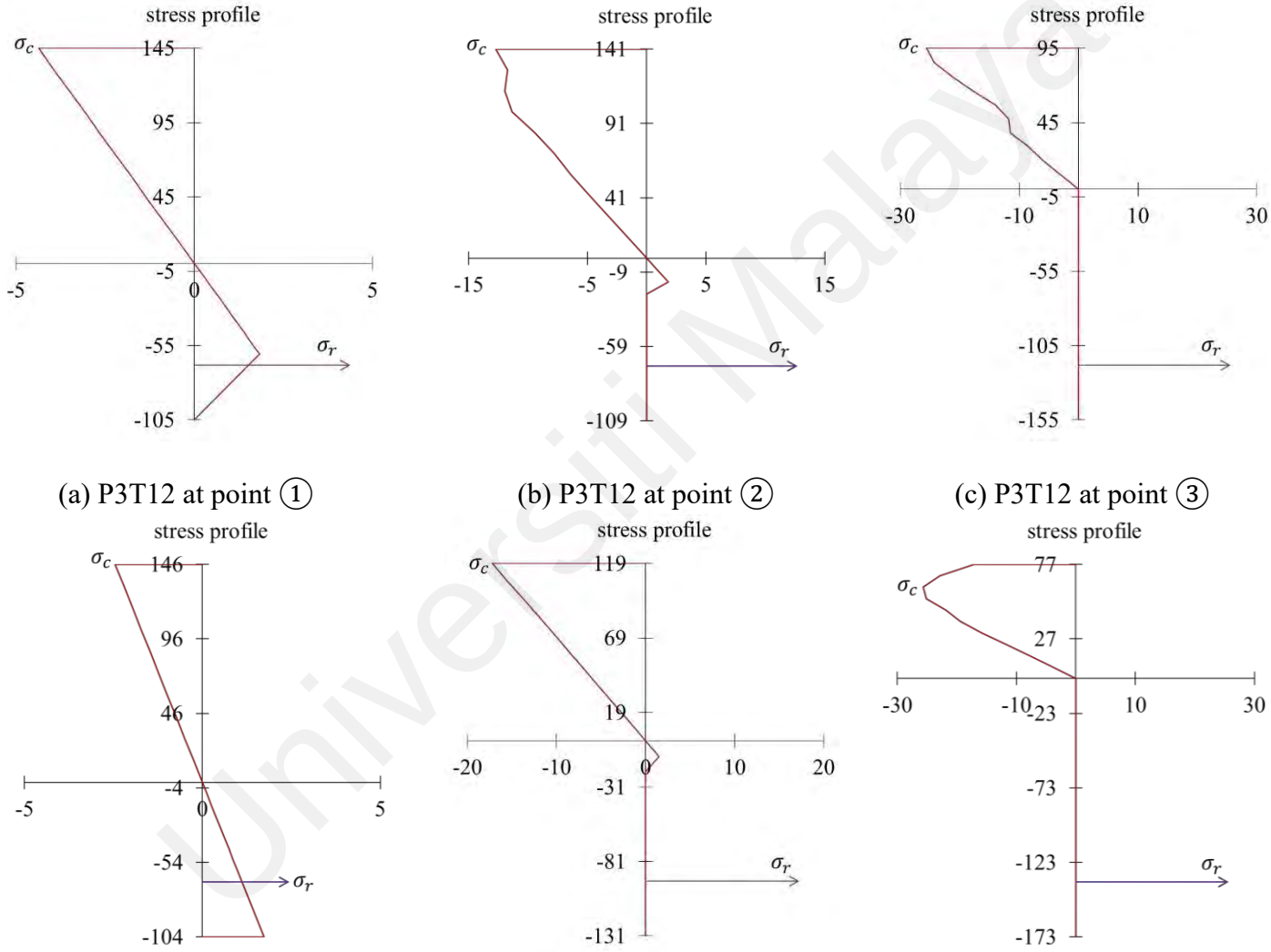

(a) P3T12 at point ①

(b) P3T12 at point ②

(c) P3T12 at point ③

(d) G3T12 at point ①

(e) G3T12 at point ②

(f) G3T12 at point ③

Figure 8.16: Stress profile along beam cross-sections of P3T12 and G3T12 at key points shown in Figure 8.12

Figure 8.17 shows the analytical assessment of change of depth of neutral axis. The depth of neutral axis has been reduced with increase of curvature. For a short strain, when the crosse section is uncracked condition, the depth of neutral axis is the highest depth from top of beam. However, this depth gradually reduces because the concrete softening was started at compression zone. The tendency of concrete softening is likely higher in P-GC compared to G-GC.

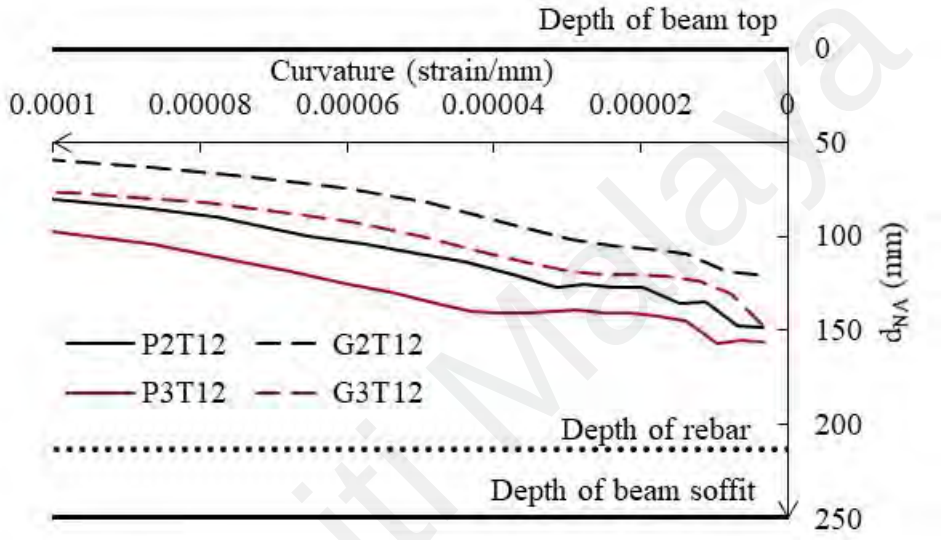

Figure 8.17: Variation of neutral axes of P2T12, G2T12, P3T12, and G3T12 beams with increments of curvature

The crack width, and crack spacings were measured during flexural test of the concrete beams. The crack widths at 50kN applied load have been tabulated (Table 8.2) to understand the effect of type of concrete. Crack width of G-GC beams were higher than P-GC beams. Again, the crack spacing in P-GC concrete was found less with high number of cracks. This indicated that P-GC absorbed more energy than G-GC. Similar findings were reported earlier in Chapter 6. Thus, P-GC showed more ductile than G-GC concrete. The wedge development for P2T12, G2T12, P3T12, and G3T12 has been shown in Figure 8.17 at ultimate failure. As geopolymer concrete material is very brittle, lots of crack can be found near to wedge at failure time.

Table 8.2: Crack widths and crack spacings of P2T12, G2T12, P3T12, G3T12 beams under bending action

Designation		First visible crack at load (kN)	Width (mm) of 1st crack at 50 kN	Avg crack spacing (mm)	Number of visible cracks
P2T12	1	13	0.330	15.0	18
	2	17	0.317	10.0	18
P3T12	1	25	0.165	13.0	20
	2	25	0.170	9.0	17
G2T12	1	18.6	0.445	19.0	11
	2	13.0	0.523	12.8	12
G3T12	1	25.0	0.219	18.0	12
	2	24.9	0.256	20.0	10

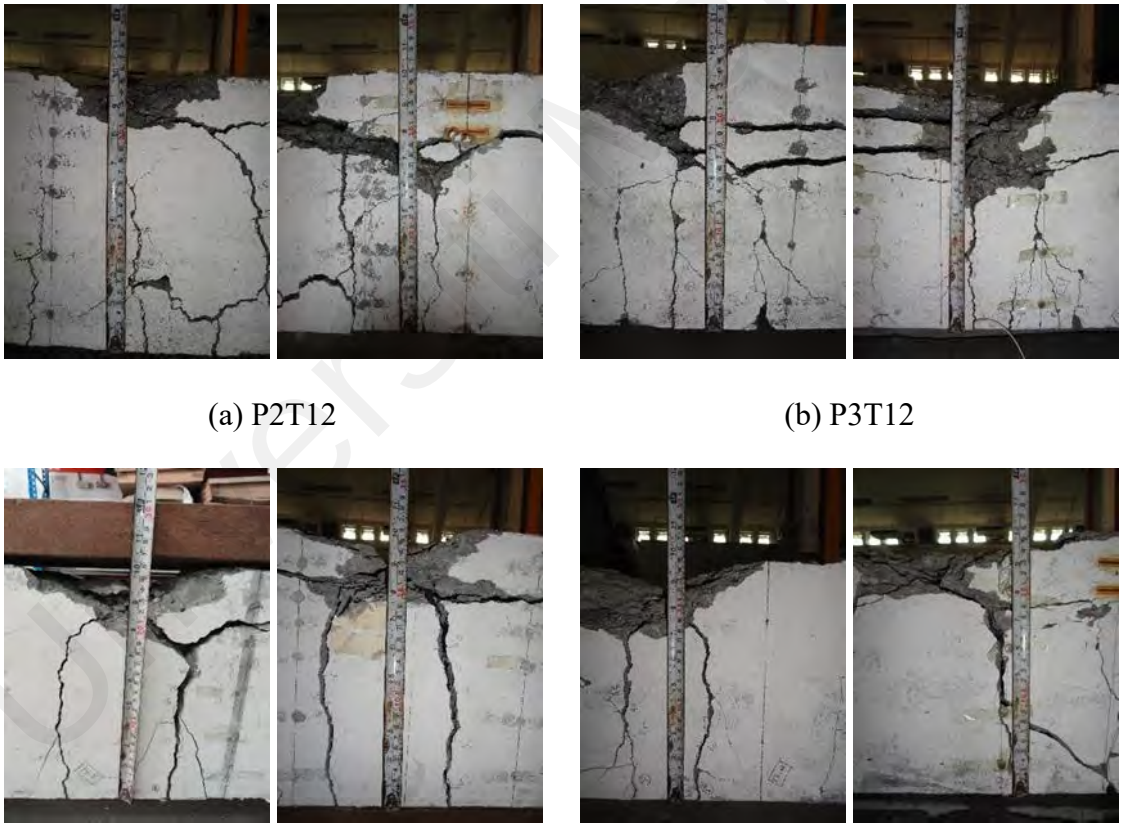

(a) P2T12 (b) P3T12

(c) G2T12 (d) G3T12

Figure 8.18: Wedge development at ultimate failure

The beam shear resistance for both P-GC, and G-GC beams with and without shear links are shown in Figure 8.19. No significant difference can be seen at the ultimate shear

resistance of beams made of either P-GC, or G-GC. The beams with links showed higher resistance than the beams without shear links. The pattern of shear failure of both type of beams were found comparable.

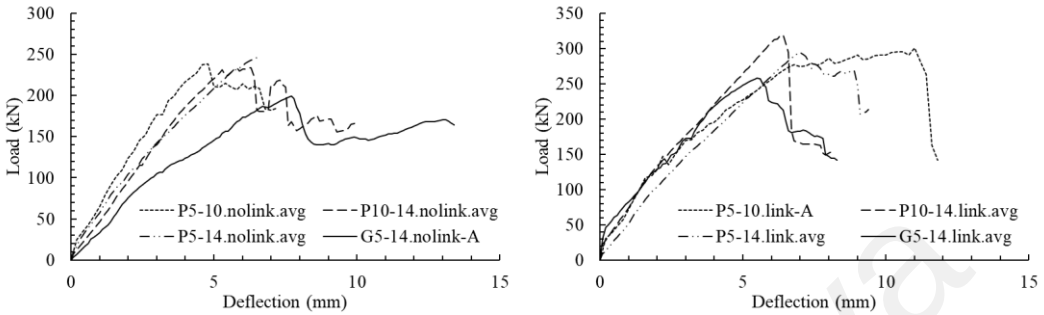

Figure 8.19: Beam shear test results (average of two beams)

8.5 Summary

The beams made of P-GC and G-GC concrete has been investigated for flexure and shear in this chapter. It has been found that the material property and partial interaction properties significantly influence the overall characteristics of the beam. The beam analysis technique using partial interaction concept, shows comparable results with the experimental result.

Both flexural and shear beams were investigated. P-GC beams found more ductile compared to G-GC beams, the concretes modulus of elasticity can be related to this nature. The overall failure of both beams under flexural load is comparable. The ultimate, shear strength of beams made of both types of concrete are comparable.

CHAPTER 9: CONCLUSIONS

The whole project investigated the suitability of Palm oil clinker based geopolymer concrete as structural grade lightweight concrete. All ingredients were chosen from the industrial wastes to produce a low-carbon and environment friendly geopolymer concrete. Fly ash, M-sand, and POC have been finalized based for the mix design used to investigate the structural performance. All aspects of the research can be summarised in the following sections:

M-sand is a comparable substitute of mining sand. The use of M-sand is recommended as a potential replacement for conventional N-sand in concrete as it produced comparable strength in the geopolymer mortar. The shape and water demand of fine aggregates in mortar affected the strength development of POFA-FA based geopolymer mortar. The high ratio of SiO_2/Al_2O_3 and CaO/Al_2O_3 attributed to the development of high compressive strength of geopolymer mortar. The fineness of pozzolans could also influence the development of compressive strength. The geopolymer mortar of binary mix of equal weight proportion of POFA and BFS as binding materials and M-sand as fine aggregate produced a 28-day compressive strength of about 56 MPa. Based on this investigation, POFA could be considered as an ideal pozzolan in the development of geopolymer concrete.

Oil palm shell (OPS) enhances ductility properties of geopolymer concrete due to its physical spongy property. The use of high volume POFA in the development of OPSGC was investigated, in addition, the effect of volume fraction and aspect ratio (AR) of steel fibre on the mechanical properties of OPSGC and fracture behaviour of fibre reinforced OPSGC and NWGC was also investigated and reported in this research. Based on the experimental investigation, the following conclusions are drawn:

The volume fraction and aspect ratio (AR) of steel fibre had little or no influence on the compressive strength of both OPSGC and NWGC. The use of steel fibres with higher aspect ratio enhanced the flexural and splitting tensile strengths and this could be attributed to due to the capability of fibres with longer lengths in delaying crack propagation in concrete. The bonding between steel fibre and binder influenced the development of flexural and splitting tensile strengths and this is in turn related to the surface area of the steel fibre. It has been observed from the failure mode of OPSGC, bond failure of OPS along the convex surface governed the failure of flexural specimens; however, the flexural and splitting tensile strengths of OPSGC were found higher than that of the corresponding NWGC. This could be attributed to the effect of stronger bond on the concave face and along the rougher surfaces of the crushed OPS. The mixes with fibres of AR65 showed higher ductility than the corresponding mixes with AR80, as the former had higher number of fibres compared to the latter for a given volume of fibres; the lower number of fibres in the AR80 mixes reduced the ductility. Though the addition of fibres in OPSGC slightly influenced the modulus of elasticity of the concrete, it was significantly lower than the corresponding NWGC. On the other hand, lower modulus of elasticity had higher ductility characteristics. The addition of high volume of steel fibre with low aspect ratio in OPSGC showed higher energy absorption. The toughness and equivalent flexural strength ratio of OPSGC were found higher than the corresponding NWGC and this could be attributed to ductility of OPS. The values of residual load and residual strength in two deflection limits of L/600 and L/150 indicated the progressive failure, which reflects the ductility of fibred OPSGC. OPSGC produced higher residual load and strengths than the corresponding NWGC which signified the better ductile property of OPSGC.

However, OPS was not finalised as aggregate in final mix design. As OPS is organic material, it has tendency to be degraded in corrosive environment. Geopolymer concrete

requires high dosage of alkaline solution during casting. Therefore from the durability aspect, OPS was not finalised, instead, palm oil clinker was used as aggregate in final mix design.

POC has better compressive ductility than granite. The compression toughness of P-GC and G-GC was investigated in this research. The failure modes and internal fracture mechanism were explored based on the physical properties of aggregates which supported the fundamental theories. The moment–curvature for an idealised beam section was analysed for both P-GC and G-GC which shows the serviceability state behaviour of P-GC and G-GC beams. The overall findings can be summarised as followings.

Compression fracture initiated at the weaker plane of porous POC in P-GC and at the interface of granite-GC matrix. The elastic strain energy of G-GC was higher than P-GC though the compression strengths of both concretes were within comparable range. The elastic limit of P-GC was lower than that of the G-GC, hence, the first crack initiated in P-GC sooner than G-GC. The deflection of P-GC reinforced concrete (RC) beam in bending was higher than that of G-GC RC beam. However, this deflection can be controlled adopting slightly higher beam cross-section that enables P-GC a suitable concrete for structural application like G-GC.

Aggregate influences bond properties; the influence of aggregate is measurable indirectly extracting the bond properties from rebar pull-out and slip response. The bond shear stress and slip responses of lightweight and normal weight geopolymer concretes of similar compressive strength have been investigated experimentally in this research and model code 2010 has been used to extract the interfacial bond-shear stress and slip relations. The role of aggregate, and past volume in bond shear resistance have been studied. The ultimate pull-out loads for identical rebar geometry, embedment length, concrete grade and loading condition were found comparable for P-GC and G-GC. The

types and volume of aggregate in similar strength of concrete did not influence the ultimate pull-out load. However, there was influences in the pull-out load – slip stiffness in elastic and plastic range. The variation of pull-out load-slip stiffness can be related to the modulus of elasticity of P-GC and G-GC. The modulus of elasticity of G-GC was higher than that of P-GC; the stiffness of pull-out load and slip of G-GC was thus found higher than that of P-GC. At any applied pull-out load, the slip of rebar was more in P-GC than G-GC. That means, a reinforced structural member made of P-GC will have more deflection under bending than that made of G-GC.

POC based geopolymer concrete is suitable for structural use; the ultimate strength is comparable with granite based geopolymer concrete; however, serviceability state design is affected. The beams made of P-GC and G-GC concrete has been investigated for flexure and shear in this chapter. It has been found that the material property and partial interaction properties significantly influence the overall characteristics of the beam. The beam analysis technique using partial interaction concept, shows comparable results with the experimental result.

Both flexural and shear beams were investigated. P-GC beams found more ductile compared to G-GC beams, the concretes modulus of elasticity can be related to this nature. The overall failure of both beams under flexural load is comparable. The ultimate, shear strength of beams made of both types of concrete are comparable.

An application of the developed product was demonstrated in a house constructed in the Universiti Malaya campus.

A long term experiment is recommended for future research to know the creep and durability performance of POC-based geopolymer concrete.

REFERENCES

Mo, K. H., Alengaram, U. J., Jumaat, M. Z., & Yap, S. P. (2015). Feasibility study of high-volume slag as cement replacement for sustainable structural lightweight oil palm shell concrete. *Journal of Cleaner Production, 91*, 297-304.

Abdullah, A. A. (1996). Palm oil shell aggregate for lightweight concrete. In Waste Materials Used in Concrete Manufacturing (pp. 624-636). William Andrew Publishing.

Abdullah, I., Mahmood, W. H. W., Fauadi, M. H. F. M., Ab Rahman, M. N., & Jali, F. A. A. (2015). Sustainability in Malaysian Palm Oil: A Review on Manufacturing Perspective. Polish Journal of Environmental Studies, 24(4).

Abdullah, N., and F. Sulaiman. The oil palm wastes in Malaysia. Biomass now-sustainable growth and use 1.3 (2013): 75-93.

Abutaha, F., Abdul Razak, H., & Ibrahim, H. A. (2017). Effect of coating palm oil clinker aggregate on the engineering properties of normal grade concrete. Coatings, 7(10), 175.

Abutaha, F., Razak, H. A., & Kanadasan, J. (2016). Effect of palm oil clinker (POC) aggregates on fresh and hardened properties of concrete. Construction and Building Materials, 112, 416-423.

Abutaha, F., Razak, H. A., Ibrahim, H. A., & Ghayeb, H. H. (2018). Adopting particle-packing method to develop high strength palm oil clinker concrete. Resources, conservation and Recycling, 131, 247-258.

ACI Committee 213 (2014). Lightweight Concrete (ACI PRC-213-14). American Concrete Institute, Farmington Hills, MI.

ACI committee 318. Building code requirements for structural concrete and commentary (ACI 318).

Ahmad, M. H., & Noor, N. M. (2007, December). Physical properties of local palm oil clinker and fly ash. Proceedings of EnCon2007 1st Engineering conference on energy and environment, Kuching, Sarawak

Ahmad, M. H., Mohd Noor, N., & Adnan, S. H. (2008). Shrinkage of Malaysian palm oil clinker concrete. International Conference on Civil Engineering Practice, Kuantan.

Ahmad, M. N., Mokhtar, M. N., Baharuddin, A. S., Hock, L. S., Ali, S. R. A., Abd-Aziz, S., ... & Hassan, M. A. (2011). Changes in physicochemical and microbial community during co-composting of oil palm frond with palm oil mill effluent anaerobic sludge. BioResources, 6(4), 4762-4780.

Ahmmad, R., Alengaram, U. J., Jumaat, M. Z., Sulong, N. R., Yusuf, M. O., & Rehman, M. A. (2017). Feasibility study on the use of high-volume palm oil clinker waste in environmental friendly lightweight concrete. Construction and Building Materials, 135, 94-103.

Ahmmad, R., Jumaat, M. Z., Alengaram, U. J., Bahri, S., Rehman, M. A., & bin Hashim, H. (2016). Performance evaluation of palm oil clinker as coarse aggregate in high strength lightweight concrete. Journal of Cleaner Production, 112, 566-574.

Ahmmad, R., Jumaat, M. Z., Alengaram, U. J., Bahri, S., Rehman, M. A., & bin Hashim, H. (2016). Performance evaluation of palm oil clinker as coarse aggregate in high strength lightweight concrete. Journal of Cleaner Production, 112, 566-574.

Ahmmad, R., Jumaat, M. Z., Bahri, S., & Islam, A. S. (2014). Ductility performance of lightweight concrete element containing massive palm shell clinker. Construction and Building Materials, 63, 234-241.

Aja, O. C., Al-Kayiem, H. H., Zewge, M. G., & Joo, M. S. (2016). Overview of hazardous waste management status in Malaysia. Management of Hazardous Wastes, (October).

Alavi-Fard, M., & Marzouk, H. (2004). Bond of high-strength concrete under monotonic pull-out loading. Magazine of Concrete Research, 56(9), 545-557.

Alderete, N. M., Joseph, A. M., Van den Heede, P., Matthys, S., & De Belie, N. (2021). Effective and sustainable use of municipal solid waste incineration bottom ash in concrete regarding strength and durability. Resources, Conservation and Recycling, 167, 105356.

Alengaram, U. J., Al Muhit, B. A., & bin Jumaat, M. Z. (2013a). Utilization of oil palm kernel shell as lightweight aggregate in concrete–A review. Construction and Building Materials, 38, 161-172.

Alengaram, U. J., Al Muhit, B. A., bin Jumaat, M. Z., & Jing, M. L. Y. (2013b). A comparison of the thermal conductivity of oil palm shell foamed concrete with conventional materials. Materials & Design, 51, 522-529.

Alengaram, U. J., Jumaat, M. Z., & Mahmud, H. (2008). Ductility behaviour of reinforced palm kernel shell concrete beams. European Journal of Scientific Research, 23(3), 406-420.

Alengaram, U. J., Jumaat, M. Z., & Mahmud, H. (2008). Influence of sand content and silica fume on mechanical properties of palm kernel shell concrete. In International conference on construction and building technology ICCBT (pp. 251-262).

Alengaram, U. J., Jumaat, M. Z., Mahmud, H., & Fayyadh, M. M. (2011b). Shear behaviour of reinforced palm kernel shell concrete beams. Construction and Building Materials, 25(6), 2918-2927.

Alengaram, U. J., Mahmud, H., & Jumaat, M. Z. (2010, November). Development of lightweight concrete using industrial waste material, palm kernel shell as lightweight aggregate and its properties. In 2010 2nd International Conference on Chemical, Biological and Environmental Engineering (pp. 277-281). IEEE.

Alengaram, U. J., Mahmud, H., & Jumaat, M. Z. (2011). Enhancement and prediction of modulus of elasticity of palm kernel shell concrete. Materials & Design, 32(4), 2143-2148.

Alengaram, U. J., Mohottige, N. H., Wu, C., Jumaat, M. Z., Poh, Y. S., & Wang, Z. (2016). Response of oil palm shell concrete slabs subjected to quasi-static and blast loads. Construction and Building Materials, 116, 391-402.

Alengaram, U. J., Salam, A., Jumaat, M. Z., Jaafar, F. F., & Saad, H. B. (2011a). Properties of high-workability concrete with recycled concrete aggregate. Materials Research, 14, 248-255.

Alghazali, H. H., & Myers, J. J. (2019). Bond performance of high-volume fly ash self-consolidating concrete in full-scale beams. ACI Structural Journal, 116(1), 161.

Alhasanat, M. B., Al Qadi, A. N., Haddad, M., & Al-Mattarneh, H. (2017). Effect of Aggregate Size on the Engineering Properties of Palm Oil Clinker Concrete. GSTF Journal of Engineering Technology (JET), 3(4).

Al-mulali, M. Z., Awang, H., Khalil, H. A., & Aljoumaily, Z. S. (2015). The incorporation of oil palm ash in concrete as a means of recycling: A review. Cement and Concrete Composites, 55, 129-138.

Almutairi, A. L., Tayeh, B. A., Adesina, A., Isleem, H. F., & Zeyad, A. M. (2021). Potential applications of geopolymer concrete in construction: A review. Case Studies in Construction Materials, 15, e00733.

Al-Shannag, M. J., & Charif, A. (2017). Bond behavior of steel bars embedded in concretes made with natural lightweight aggregates. Journal of King Saud University-Engineering Sciences, 29(4), 365-372.

American concrete Institute. (2003). Bond and development of straight reinforcing bars in tension. (ACI 408R-03). American Concrete Institute.

American Concrete Institute. (2014). Guide for Structural Lightweight-Aggregate Concrete. (ACI 213R-14).

Amirrasouli, B. (2015). Mechanical Properties of Low-Density Fibre-Reinforced Cellular Concrete and its Energy Absorption Potential against Air Blast. The University of Manchester (United Kingdom).

Andrew, R. M. (2020). A comparison of estimates of global carbon dioxide emissions from fossil carbon sources. Earth System Science Data, 12(2), 1437-1465.

Appukutty, P., & Murugesan, R. (2009). Substitution of quarry dust to sand for mortar in brick masonry works. International Journal on Design and Manufacturing Technologies, 3(1), 59-63.

Arezoumandi, M., Steele, A. R., & Volz, J. S. (2018, November). Evaluation of the bond strengths between concrete and reinforcement as a function of recycled concrete aggregate replacement level. In Structures (Vol. 16, pp. 73-81). Elsevier.

Aslam, M., Shafigh, P., & Jumaat, M. Z. (2017a). High strength lightweight aggregate concrete using blended coarse lightweight aggregate origin from palm oil industry. Sains Malaysiana, 46(4), 667-675.

Aslam, M., Shafigh, P., Nomeli, M. A., & Jumaat, M. Z. (2017b). Manufacturing of high-strength lightweight aggregate concrete using blended coarse lightweight aggregates. Journal of building engineering, 13, 53-62.

ASTM International. (2012a). Standard Test Method for Density, Relative Density (Specific Gravity), and Absorption of Coarse Aggregate. (ASTM C127-12). ASTM International, West Conshohocken, PA.

ASTM International. (2012b). Standard test method for flexural performance of fiber-reinforced concrete (using beam with third-point loading). (ASTM C1609/C1609M-12). ASTM International, West Conshohocken, PA.

ASTM International. (2014). Standard specification for lightweight aggregates for structural concrete (ASTM C330/C330M-14). ASTM International.

ASTM International. (2014). Standard Test Method for Static Modulus of Elasticity and Poisson's Ratio of Concrete in Compression. (ASTM C469/C469M-14). ASTM International, West Conshohocken, PA.

ASTM International. (2019). Standard Specification for Coal Fly Ash and Raw or Calcined Natural Pozzolan for Use in Concrete (ASTM C618-19). West Conshohocken, PA.

ASTM International. (2019a). Standard Test Method for Sieve Analysis of Fine and Coarse Aggregates. (ASTM C136/C136M-19). ASTM International, West Conshohocken, PA.

ASTM International. (2019c). Standard Test Method for Flexural Performance of Fiber-Reinforced Concrete (Using Beam With Third-Point Loading). (ASTM C 1609/C1609M-19a). ASTM International, West Conshohocken, PA.

ASTM International. (2020). Standard Test Method for Compressive Strength of Hydraulic Cement Mortars (Using 2-in. or [50-mm] Cube Specimens). (ASTM C109/C109M-20). ASTM International, West Conshohocken, PA.

ASTM International. (2020). Standard Test Method for Resistance to Degradation of Small-Size Coarse Aggregate by Abrasion and Impact in the Los Angeles Machine. (ASTM C131/C131M-20). ASTM International, West Conshohocken, PA.

Atiş, C. D., & Karahan, O. (2009). Properties of steel fiber reinforced fly ash concrete. Construction and Building Materials, 23(1), 392-399.

Atnaw, S. M., Sulaiman, S. A., & Yusup, S. (2013). Syngas production from downdraft gasification of oil palm fronds. Energy, 61, 491-501.

Ayompe, L. M., Schaafsma, M., & Egoh, B. N. (2021). Towards sustainable palm oil production: The positive and negative impacts on ecosystem services and human wellbeing. Journal of cleaner production, 278, 123914.

Azizinamini, A., Stark, M., Roller, J. J., & Ghosh, S. K. (1993). Bond performance of reinforcing bars embedded in high-strength concrete. Structural Journal, 90(5), 554-561.

Balamurugan, G., & Perumal, P. (2013). Use of quarry dust to replace sand in concrete–An experimental study. International Journal of Scientific and Research Publications, 3(12), 1.

Barham, S., & Darwin, D. (1999). Effects of Aggregate Type, Water-to-Cementitious Material Ratio, and age on mechanical and fracture properties of concrete. University of Kansas Center for Research, Inc..

Bashar, I. I., Alengaram, U. J., & Jumaat, M. Z. (2022). Enunciation of embryonic palm oil clinker based geopolymer concrete and its engineering properties. Construction and Building Materials, 318, 125975.

Bashar, I. I., Alengaram, U. J., Jumaat, M. Z., & Islam, A. (2014). The effect of variation of molarity of alkali activator and fine aggregate content on the compressive strength of the fly ash: palm oil fuel ash based geopolymer mortar. Advances in Materials Science and Engineering, 2014.

Bashar, I. I., Alengaram, U. J., Jumaat, M. Z., & Islam, A. (2016b). Development of sustainable geopolymer mortar using industrial waste materials. Materials Today: Proceedings, 3(2), 125-129.

Bashar, I. I., Alengaram, U. J., Jumaat, M. Z., Islam, A., Santhi, H., & Sharmin, A. (2016a). Engineering properties and fracture behaviour of high-volume palm oil fuel ash-based fibre reinforced geopolymer concrete. Construction and Building Materials, 111, 286-297.

Bashar, I. I., Strum, A. B., Visintin, P., & Sheikh, A. H. (2022b). Analytical approach to quantify the pull-out behaviour of steel hooked fibre [Manuscript submitted for Publication]. School of Civil, Environmental & Mining Engineering, The University of Adelaide SA5005.

Bateman, I. J., Fisher, B., Fitzherbert, E., Glew, D., & Naidoo, R. (2010). Tigers, markets and palm oil: market potential for conservation. Oryx, 44(2), 230-234.

Benhelal, E., Shamsaei, E., & Rashid, M. I. (2021). Challenges against CO2 abatement strategies in cement industry: A review. Journal of Environmental Sciences, 104, 84-101.

Boden, T. A., Marland, G., & Andres, R. J. (2017). National CO2 emissions from fossil-fuel burning, cement manufacture, and gas flaring: 1751-2014. Carbon Dioxide Information Analysis Center, Oak Ridge National Laboratory, US Department of Energy.

Boel, V., Helincks, P., Desnerck, P., & De Schutter, G. (2010). Bond behaviour and shear capacity of self-compacting concrete. In Design, Production and Placement of Self-Consolidating Concrete (pp. 343-353). Springer, Dordrecht.

Bouazaoui, L., & Li, A. (2008). Analysis of steel/concrete interfacial shear stress by means of pull out test. International journal of adhesion and adhesives, 28(3), 101-108.

British Standard (1997). (withdrawn, 2010, April and replaced by BS EN 1992-1-1:2004+A1:2014). Structural use of concrete. Code of practice for design and construction (BS 8110-1:1997). British Standard Institute

British Standards Institution (2012). Tests for geometrical properties of aggregates – Part 8: Assessment of fines – sand equivalent test (BS EN 933-8:2012). British Standards Institution.

British Standards Institution. (2004). Eurocode 2: Design of concrete structures - General rules and rules for buildings. (BS EN 1992-1-1:2004).

British Standards Institution. (2009). Testing hardened concrete - Tensile splitting strength of test specimens. (BS EN 12390-6:2009).

British Standards Institution. (2019a). Testing hardened concrete - Compressive strength of test specimens. (BS EN 12390-3:2019).

British Standards Institution. (2019a). Testing hardened concrete - Flexural strength of test specimens. (BS EN 12390-5:2019).

Carter, C., Finley, W., Fry, J., Jackson, D., & Willis, L. (2007). Palm oil markets and future supply. European Journal of Lipid Science and Technology, 109(4), 307-314.

Castel, A., & Foster, S. J. (2015). Bond strength between blended slag and Class F fly ash geopolymer concrete with steel reinforcement. Cement and Concrete Research, 72, 48-53.

Castel, A., Vidal, T., Viriyametanont, K., & Francois, R. (2006). Effect of reinforcing bar orientation and location on bond with self-consolidating concrete. ACI Materials Journal, 103(4), 559.

Cement roadmap, 2012. International energy agency (IEA) and world business council for sustainable development (WBCSD). Available: www.iea.org/papers/2009/Cement_Roadmap_Foldout_WEB.pdf. Accessed 20/07/2020.

Chan, C. M., & Shamsuddin, A. (2012). Developing a Sustainability Framework for the Second Life of Palm Oil Clinker. International Journal of Agriculture Innovations and Research, 1(1), 19-25.

Chan, Y. W., Chen, Y. S., & Liu, Y. S. (2003). Development of bond strength of reinforcement steel in self-consolidating concrete. Structural Journal, 100(4), 490-498.

Chiew, Y. L., Iwata, T., & Shimada, S. (2011). System analysis for effective use of palm oil waste as energy resources. Biomass and Bioenergy, 35(7), 2925-2935.

Choong, C. G., & McKay, A. (2014). Sustainability in the Malaysian palm oil industry. Journal of Cleaner Production, 85, 258-264.

Criswell, M. E. (1986). Design of columns. J. Mater. Ed, 8, 305-315."

Crouch, L. K., Pitt, J., & Hewitt, R. (2007). Aggregate effects on pervious Portland cement concrete static modulus of elasticity. Journal of materials in civil engineering, 19(7), 561-568.

Crow, J. M. (2008). The concrete conundrum. Chemistry World, 5(3), 62-66.

Cui, Y., Zhang, P., & Bao, J. (2020). Bond Stress between Steel-Reinforced Bars and Fly Ash-Based Geopolymer Concrete. Advances in Materials Science and Engineering, 2020, Article 9812526. https://doi.org/10.1155/2020/9812526

Datamonitor. (2010). Palm Oil Case Study: How Consumer Activism Led the Push for Sustainable Sourcing. London, UK: Datamonitor Plc.

Davidovits, J. (1991). Geopolymers: inorganic polymeric new materials. Journal of Thermal Analysis and calorimetry, 37(8), 1633-1656.

Davidovits, J. (1994, October). Properties of geopolymer cements. In First international conference on alkaline cements and concretes (Vol. 1, pp. 131-149). Kiev State Technical University, Ukraine: Scientific Research Institute on Binders and Materials.

Davidovits, J. (2008A). Geopolymer chemistry & application (3rd ed.). 16 rule Galilee, F-02100 Saint-Quentin, France: Institute Géopolymèr.

Davidovits, J. (2008b). They built the Pyramids. Geopolymer Institute.

Dayang Norwana, A. A. B., Kanjappan, R., Chin, M., Schoneveld, G. C., Potter, L., & Andriani, R. (2011). The local impacts of oil palm expansion in Malaysia; An assessment based on a case study in Sabah State. Center for International Forestry Research (CIFOR) Working Paper, 78, 1-17.

De Larrard, F., Shaller, I., & Fuchs, J. (1993). Effect of the bar diameter on the bond strength of passive reinforcement in high-performance concrete. Materials Journal, 90(4), 333-339.

Department of Environment Malaysia. (2015). Current practice of recycling and treatment of hazardous wastes in Malaysia.

Department of Statistics Malaysia. (2016). Selected Agricultural Indicators, Malaysia, Production of Agricultural Sector in 2015.

Desnerck, P., De Schutter, G., & Taerwe, L. (2010). Bond behaviour of reinforcing bars in self-compacting concrete: experimental determination by using beam tests. Materials and Structures, 43(1), 53-62.

Diab, A. M., Elyamany, H. E., Hussein, M. A., & Al Ashy, H. M. (2014). Bond behavior and assessment of design ultimate bond stress of normal and high strength concrete. Alexandria Engineering Journal, 53(2), 355-371. doi: 10.1016/j.conbuildmat.2015.03.040.

Dumitru, I., Zdrilic, T., & Smorchevsky, G. (1999, April). The use of manufactured quarry fines in concrete. In Proceedings of the 7th Annual Symposium on Aggregates-Concrete, Bases and Fines (pp. C1-5). International Centre for Aggregates Research (ICAR).

Dybeł, P., & Furtak, K. (2017). Influence of silica fume content on the quality of bond conditions in high-performance concrete specimens. Archives of civil and mechanical engineering, 17(4), 795-805.

Feen, O. S., Mohamed, R. N., & Mohamed, A. (2017). Fresh and hardened properties of self-compacting lightweight concrete using coarse palm oil clinker. Malaysian Journal of Civil Engineering, 29.

Fitzherbert, E. B., Struebig, M. J., Morel, A., Danielsen, F., Brühl, C. A., Donald, P. F., & Phalan, B. (2008). How will oil palm expansion affect biodiversity?. Trends in ecology & evolution, 23(10), 538-545.

Foo, K. Y., & Hameed, B. H. (2010). Insight into the applications of palm oil mill effluent: a renewable utilization of the industrial agricultural waste. Renewable and Sustainable Energy Reviews, 14(5), 1445-1452.

Food and Agriculture Organization of the United Nations. (n.d.). Crops and livestock products. Data retrieved July 23, 2021, from faostat website.

Galloway, J. E. (1994). Grading, shape, and surface properties. ASTM special technical publication, 169, 401-410.

Gambarova, P. G., & Rosati, G. (1996). Bond and splitting in reinforced concrete: test results on bar pull-out. Materials and Structures, 29(5), 267-276.

Gao, J., Sun, W., & Morino, K. (1997). Mechanical properties of steel fiber-reinforced, high-strength, lightweight concrete. Cement and Concrete Composites, 19(4), 307-313.

Gencel, O., Brostow, W., Datashvili, T., & Thedford, M. (2011). Workability and mechanical performance of steel fiber-reinforced self-compacting concrete with fly ash. Composite interfaces, 18(2), 169-184.

Guangul, F. M., Sulaiman, S. A., & Ramli, A. (2014). Study of the effects of operating factors on the resulting producer gas of oil palm fronds gasification with a single throat downdraft gasifier. Renewable energy, 72, 271-283.

Guo, Y. C., Zhang, J. H., Chen, G. M., & Xie, Z. H. (2014). Compressive behaviour of concrete structures incorporating recycled concrete aggregates, rubber crumb and reinforced with steel fibre, subjected to elevated temperatures. Journal of cleaner production, 72, 193-203.

Halim, N. I., Newman, A., Sidek, M. N. M., Saman, H. M., & Suliman, N. H. (2021). Effect of Utilization of Nano POFA on Performance of Self-Consolidating High-Performance Concrete (SCHPC). Scientific Research Journal, 18(2), 103-117.

Hamada, H. M., Alya'a, A., Yahaya, F. M., Muthusamy, K., Tayeh, B. A., & Humada, A. M. (2020b). Effect of high-volume ultrafine palm oil fuel ash on the engineering and transport properties of concrete. Case Studies in Construction Materials, 12, e00318.

Hamada, H. M., Jokhio, G. A., Al-Attar, A. A., Yahaya, F. M., Muthusamy, K., Humada, A. M., & Gul, Y. (2020). The use of palm oil clinker as a sustainable construction material: A review. Cement and Concrete Composites, 106, 103447.

Hamada, H. M., Tayeh, B., Yahaya, F., Muthusamy, K., & Al-Attar, A. (2020a). Effects of nano-palm oil fuel ash and nano-eggshell powder on concrete. Construction and Building Materials, 261, 119790.

Hamada, H. M., Tayeh, B., Yahaya, F., Muthusamy, K., & Al-Attar, A. (2020a). Effects of nano-palm oil fuel ash and nano-eggshell powder on concrete. Construction and Building Materials, 261, 119790.

Hamada, H. M., Thomas, B. S., Tayeh, B., Yahaya, F. M., Muthusamy, K., & Yang, J. (2020c). Use of oil palm shell as an aggregate in cement concrete: A review. Construction and Building Materials, 265, 120357.

Hamada, H. M., Thomas, B. S., Tayeh, B., Yahaya, F. M., Muthusamy, K., & Yang, J. (2020c). Use of oil palm shell as an aggregate in cement concrete: A review. Construction and Building Materials, 265, 120357.

Hambali, E., & Rivai, M. (2017, May). The potential of palm oil waste biomass in Indonesia in 2020 and 2030. In IOP Conference Series: Earth and Environmental Science (Vol. 65, No. 1, p. 012050). IOP Publishing.

Hansen, S. B., Padfield, R., Syayuti, K., Evers, S., Zakariah, Z., & Mastura, S. (2015). Trends in global palm oil sustainability research. Journal of cleaner Production, 100, 140-149.

Hansen, T. C. (1965, February). Influence of aggregate and voids on modulus of elasticity of concrete, cement mortar, and cement paste. In Journal Proceedings (Vol. 62, No. 2, pp. 193-216).

Hardjito, D., & Rangan, B. V. (2005). Development and properties of low-calcium fly ash-based geopolymer concrete.

Haskett, M., Oehlers, D. J., Ali, M. M., & Sharma, S. K. (2011). Evaluating the shear-friction resistance across sliding planes in concrete. Engineering Structures, 33(4), 1357-1364.

Hassan, A. A. A., Hossain, K. M. A., & Lachemi, M. (2010). Bond strength of deformed bars in large reinforced concrete members cast with industrial self-consolidating concrete mixture. Construction and Building Materials, 24(4), 520-530.

Hassan, O. A., Ishida, M., Shukri, I. M., & Tajuddin, Z. A. (1994). Oil-palm fronds as a roughage feed source for ruminants in Malaysia. Livestock Research Division, Malaysian Agriculture Research and Development Institute (MARDI), Kuala Lumpur, Malaysia, 1-8.

Hegazy, S. S., & Aref, I. M. (2010). Suitability of some fast-growing trees and date palm fronds for particleboard production. Forest products journal, 60(7-8), 599-604.

Hossain, K. M. A. (2008). Bond characteristics of plain and deformed bars in lightweight pumice concrete. Construction and Building Materials, 22(7), 1491-1499.

Hoyle, R. J. (1984). Design of composite beams. J. Mater. Ed, 6, 927-938.

Hsu, T. T., Slate, F. O., Sturman, G. M., & Winter, G. (1963, February). Microcracking of plain concrete and the shape of the stress-strain curve. In Journal Proceedings (Vol. 60, No. 2, pp. 209-224).

Huang, H., & Talreja, R. (2006). Numerical simulation of matrix micro-cracking in short fiber reinforced polymer composites: initiation and propagation. Composites science and technology, 66(15), 2743-2757.

Huda, M. N. (2017). Behavior of flexural members made from oil palm shell and clinker concrete [Master's dissertation, University of Malaya].

Huda, M. N., Jumaat, M. Z., & Islam, A. S. (2016). Flexural performance of reinforced oil palm shell & palm oil clinker concrete (PSCC) beam. Construction and Building Materials, 127, 18-25.

Huda, M. N., Jumaat, M. Z., Islam, A. S., & Soeb, M. R. (2015). Ductility performance of high strength lightweight concrete produced from a mixture of oil palm shell and

palm oil clinker. In Proceedings of the 1st International Conference on Advances in Civil Infrastructure and Construction Materials, Dhaka, Bangladesh, December.

Huda, M. N., Jumat, M. Z. B., & Islam, A. S. (2016). Flexural performance of reinforced oil palm shell & palm oil clinker concrete (PSCC) beam. Construction and Building Materials, 127, 18-25.

Hudson, B. P. (1999). Concrete workability with high fines content sands. URL: http://www. agmman. com/Pages/Agg, 200299.

Hwang, S. J., Lee, Y. Y., & Lee, C. S. (1994). Effect of silica fume on the splice strength of deformed bars of high-performance concrete. Structural Journal, 91(3), 294-302.

Ibrahim, H. A., & Razak, H. A. (2016). Effect of palm oil clinker incorporation on properties of pervious concrete. Construction and Building Materials, 115, 70-77.

Ibrahim, M. W., Mangi, S. A., Burhanudin, M. K., Ridzuan, M. B., Jamaluddin, N., Shahidan, S., ... & Othman, N. H. (2017, November). Compressive and flexural strength of concrete containing palm oil biomass clinker and polypropylene fibres. In IOP Conference Series: Materials Science and Engineering (Vol. 271, No. 1, p. 012011). IOP Publishing.

Ihekwaba, N., Hope, B., & Hansson, C. (1996). Pull-out and bond degradation of steel rebars in ECE concrete. Cement and concrete research, 26(2), 267-282.

International Federation for Structural Concrete. (2010). fib Model Code for Concrete Structures 2010. (MC2010). International Federation for Structural Concrete (fib).

Islam, A., Alengaram, U. J., Jumaat, M. Z., Bashar, I. I., & Kabir, S. A. (2015). Engineering properties and carbon footprint of ground granulated blast-furnace slag-palm oil fuel ash-based structural geopolymer concrete. Construction and building materials, 101, 503-521.

Islam, A., Alengaram, U. J., Jumaat, M. Z., Ghazali, N. B., Yusoff, S., & Bashar, I. I. (2017). Influence of steel fibers on the mechanical properties and impact resistance of lightweight geopolymer concrete. Construction and Building Materials, 152, 964-977.

Issa, C. A., & Assaad, J. J. (2015). Bond of tension bars in underwater concrete: effect of bar diameter and cover. Materials and Structures, 48(11), 3457-3471.

Jakarta Directorate General of Estate Crops (2016). Tree crop estate statistics of Indonesia 2015–2016 palm oil. Ministry of Agriculture of Republic Indonesia.

Ji, T., Chen, C. Y., Zhuang, Y. Z., & Chen, J. F. (2013). A mix proportion design method of manufactured sand concrete based on minimum paste theory. Construction and Building Materials, 44, 422-426.

Joohari, I., Mohamed, R. N., & Joohari, M. I. (2018). Development of Self-compacting Concrete Using Palm Oil Clinker as Lightweight Aggregate. In Regional Conference on Science, Technology and Social Sciences (RCSTSS 2016) (pp. 309-316). Springer, Singapore.

Jumaat, M. Z., Alengaram, U. J., Ahmmad, R., Bahri, S., & Islam, A. S. (2015). Characteristics of palm oil clinker as replacement for oil palm shell in lightweight concrete subjected to elevated temperature. Construction and Building Materials, 101, 942-951.

Köksal, F., Altun, F., Yiğit, İ., & Şahin, Y. (2008). Combined effect of silica fume and steel fiber on the mechanical properties of high strength concretes. Construction and building materials, 22(8), 1874-1880.

Kabir, M. R., & Islam, M. M. (2014). Bond stress behavior between concrete and steel rebar: Critical investigation of pull-out test via Finite Element Modeling. International Journal of Civil Structural Engineering, 5(1), 80-90.

Kabir, S. A., Alengaram, U. J., Jumaat, M. Z., Yusoff, S., Sharmin, A., & Bashar, I. I. (2017). Performance evaluation and some durability characteristics of environmental friendly palm oil clinker based geopolymer concrete. Journal of cleaner production, 161, 477-492.

Kala, D. R., Rosenani, A. B., Fauziah, C. I., & Thohirah, L. A. (2009). Composting oil palm wastes and sewage sludge for use in potting media of ornamental plants. Malaysian Journal of Soil Science, 13(1), 77-91.

Kanadasan, J. (2016). Feasibility study of palm oil clinker as environmentally friendly self-compacting concrete. [Doctoral thesis, University of Malaya].

Kanadasan, J., & Razak, H. A. (2014). Fresh properties of self-compacting concrete incorporating palm oil clinker. In InCIEC 2013 (pp. 249-259). Springer, Singapore.

Kanadasan, J., & Razak, H. A. (2015). Engineering and sustainability performance of self-compacting palm oil mill incinerated waste concrete. Journal of Cleaner Production, 89, 78-86.

Kaplan, M. F. (1959, May). Flexural and compressive strength of concrete as affected by the properties of coarse aggregates. In Journal Proceedings (Vol. 55, No. 5, pp. 1193-1208).

Karim, M. R., Hashim, H., & Razak, H. A. (2016). Assessment of pozzolanic activity of palm oil clinker powder. Construction and building materials, 127, 335-343.

Karim, M. R., Hashim, H., & Razak, H. A. (2016). Assessment of pozzolanic activity of palm oil clinker powder. Construction and building materials, 127, 335-343.

Karim, M. R., Hashim, H., & Razak, H. A. (2016). Thermal activation effect on palm oil clinker properties and their influence on strength development in cement mortar. Construction and Building Materials, 125, 670-678.

Karim, M. R., Hashim, H., Razak, H. A., & Yusoff, S. (2017). Characterization of palm oil clinker powder for utilization in cement-based applications. Construction and Building Materials, 135, 21-29.

Karim, M. R., Hashim, H., Razak, H. A., & Yusoff, S. (2017). Characterization of palm oil clinker powder for utilization in cement-based applications. Construction and Building Materials, 135, 21-29.

Khatun, R., Reza, M. I. H., Moniruzzaman, M., & Yaakob, Z. (2017). Sustainable oil palm industry: The possibilities. Renewable and Sustainable Energy Reviews, 76, 608-619.

Kidalova, L., Stevulova, N., Terpakova, E., & Sicakova, A. (2012). Utilization of alternative materials in lightweight composites. Journal of Cleaner Production, 34, 116-119.

Kim, Y. H., Kim, H. Y., Yang, K. H., & Ha, J. S. (2021). Effect of concrete unit weight on the mechanical properties of bottom ash aggregate concrete. Construction and Building Materials, 273, 121998.

Kimura, H. (1993). Effects of bar deformation and concrete strength on bond of reinforcing steel to concrete. Transactions of JCI, 15(2), 117-122.

Knight, D., Visintin, P., Oehlers, D. J., & Jumaat, M. Z. (2013). Incorporating residual strains in the flexural rigidity of RC members with varying degrees of prestress and cracking. Advances in Structural Engineering, 16(10), 1701-1718.

Konda, R. E., Sulaiman, S. A., & Bambang, A. (2012). Syngas production from gasification of oil palm fronds with an updraft gasifier. Journal of Applied Sciences, 12(24), 2555-2561.

Kramanandita, R., Bantacut, T., Romli, M., & Makmoen, M. (2014). Utilizations of palm oil mills wastes as source of energy and water in the production process of crude palm oil. Chemistry and Materials Research, 6(8), 46-53.

Kupaei, R. H., Alengaram, U. J., Jumaat, M. Z. B., & Nikraz, H. (2013). Mix design for fly ash based oil palm shell geopolymer lightweight concrete. Construction and Building Materials, 43, 490-496.

Kurugöl, S., Tanaçan, L., & Ersoy, H. Y. (2008). Young's modulus of fiber-reinforced and polymer-modified lightweight concrete composites. Construction and Building Materials, 22(6), 1019-1028.

Lachemi, M., Bae, S., Hossain, K. M. A., & Sahmaran, M. (2009). Steel–concrete bond strength of lightweight self-consolidating concrete. Materials and Structures, 42(7), 1015-1023.

Lamb, W. F., Wiedmann, T., Pongratz, J., Andrew, R., Crippa, M., Olivier, J. G., ... & Minx, J. C. (2021). A review of trends and drivers of greenhouse gas emissions by sector from 1990 to 2018. Environmental research letters, 16, 073005.

Lee, J. C. (2018). Engineering properties and shear behaviour of high strength lightweight aggregate concrete incorporating oil-palm-boiler clinker/Lee Jin Chai (Doctoral dissertation, University of Malaya).

Li, T. M. (2015). Social impacts of oil palm in Indonesia: A gendered perspective from West Kalimantan (Vol. 124). CIFOR.

Lim, C. I., & Biswas, W. (2015). An evaluation of holistic sustainability assessment framework for palm oil production in Malaysia. Sustainability, 7(12), 16561-16587.

Liu, M. Y. J., Alengaram, U. J., Jumaat, M. Z., & Mo, K. H. (2014b). Evaluation of thermal conductivity, mechanical and transport properties of lightweight aggregate foamed geopolymer concrete. Energy and Buildings, 72, 238-245.

Liu, M. Y. J., Alengaram, U. J., Jumaat, M. Z., & Mo, K. H. (2014b). Evaluation of thermal conductivity, mechanical and transport properties of lightweight aggregate foamed geopolymer concrete. Energy and Buildings, 72, 238-245.

Liu, M. Y. J., Chua, C. P., Alengaram, U. J., & Jumaat, M. Z. (2014a). Utilization of palm oil fuel ash as binder in lightweight oil palm shell geopolymer concrete. Advances in Materials Science and Engineering, 2014.

Lloyd, N., & Rangan, V. (2009). Geopolymer concrete-sustainable cementless concrete. In Proceedings of Tenth ACI International Conference (pp. 33-53). American Concrete Institute.

Loh, S. K. (2017). The potential of the Malaysian oil palm biomass as a renewable energy source. Energy conversion and management, 141, 285-298.

Looney, T. J., Arezoumandi, M., Volz, J. S., & Myers, J. J. (2012). An experimental study on bond strength of reinforcing steel in self-consolidating concrete. International journal of concrete structures and materials, 6(3), 187-197.

Luo, Z., Li, W., Wang, K., Castel, A., & Shah, S. P. (2021). Comparison on the properties of ITZs in fly ash-based geopolymer and Portland cement concretes with equivalent flowability. Cement and Concrete Research, 143, 106392.

Madhkhan, M., Azizkhani, R., & Harchegani, M. T. (2012). Effects of pozzolans together with steel and polypropylene fibers on mechanical properties of RCC pavements. Construction and Building materials, 26(1), 102-112.

Maji, A., & Shah, S. P. (1988). Process zone and acoustic-emission measurements in concrete. Experimental mechanics, 28(1), 27-33.

Malaysian Palm Oil Board (2012). Oil Palm & The Environment. Available at: www.mpob.gov.my/ Malaysian Palm Oil Board. (2017). Number and capacities of palm oil sectors 2017.

Malkawi, A. B., Habib, M., Alzubi, Y., & Aladwan, J. (2020). Engineering properties of lightweight geopolymer concrete using palm oil clinker aggregate. International Journal, 18(65), 132-139.

Mandell, J. F., McGarry, F. J., & Li, C. G. (1985). Fatigue crack growth and lifetime trends in injection molded reinforced thermoplastics. In High modulus fiber composites in ground transportation and high volume applications. ASTM International.

Mannan, M. A., & Ganapathy, C. (2004). Concrete from an agricultural waste-oil palm shell (OPS). Building and environment, 39(4), 441-448.

Maranan, G. B., Manalo, A. C., Karunasena, W., & Benmokrane, B. (2015). Pullout behaviour of GFRP bars with anchor head in geopolymer concrete. Composite Structures, 132, 1113-1121.

McCarthy, J. F. (2010). Processes of inclusion and adverse incorporation: oil palm and agrarian change in Sumatra, Indonesia. The Journal of peasant studies, 37(4), 821-850.

McCarthy, J., & Zen, Z. (2010). Regulating the oil palm boom: assessing the effectiveness of environmental governance approaches to agro-industrial pollution in Indonesia. Law & Policy, 32(1), 153-179.

Mehta, P. K. (2002). Greening of the concrete industry for sustainable development. Concrete international, 24(7), 23-28.

Mehta, P. K. A. M., & Monteiro, P. (2014). Concrete: microstructure, properties, and materials. McGraw-Hill Education.

Metelli, G., & Plizzari, G. A. (2014). Influence of the relative rib area on bond behaviour. Magazine of concrete research, 66(6), 277-294.

Mo, K. H., Alengaram, U. J., Visintin, P., Goh, S. H., & Jumaat, M. Z. (2015). Influence of lightweight aggregate on the bond properties of concrete with various strength grades. Construction and Building Materials, 84, 377-386.

Mo, K. H., Ling, T. C., Alengaram, U. J., Yap, S. P., & Yuen, C. W. (2017). Overview of supplementary cementitious materials usage in lightweight aggregate concrete. Construction and Building Materials, 139, 403-418.

Mo, K. H., Yap, K. K. Q., Alengaram, U. J., & Jumaat, M. Z. (2014b). The effect of steel fibres on the enhancement of flexural and compressive toughness and fracture characteristics of oil palm shell concrete. Construction and Building Materials, 55, 20-28.

Mo, K. H., Yap, S. P., Alengaram, U. J., Jumaat, M. Z., & Bu, C. H. (2014a). Impact resistance of hybrid fibre-reinforced oil palm shell concrete. Construction and Building Materials, 50, 499-507.

Mo, K. H., Yeap, K. W., Alengaram, U. J., Jumaat, M. Z., & Bashar, I. I. (2018). Bond strength evaluation of palm oil fuel ash-based geopolymer normal weight and lightweight concretes with steel reinforcement. Journal of adhesion science and Technology, 32(1), 19-35.

Mo, K. H., Yeoh, K. H., Bashar, I. I., Alengaram, U. J., & Jumaat, M. Z. (2017). Shear behaviour and mechanical properties of steel fibre-reinforced cement-based and geopolymer oil palm shell lightweight aggregate concrete. Construction and Building Materials, 148, 369-375.

Mohammad, N., Alam, M. Z., Kabbashi, N. A., & Ahsan, A. (2012). Effective composting of oil palm industrial waste by filamentous fungi: A review. Resources, Conservation and Recycling, 58, 69-78.

Mohammed, B. S., Al-Ganad, M. A., & Abdullahi, M. (2011). Analytical and experimental studies on composite slabs utilising palm oil clinker concrete. Construction and Building Materials, 25(8), 3550-3560.

Mohammed, B. S., Foo, W. L., & Abdullahi, M. (2014). Flexural strength of palm oil clinker concrete beams. Materials & Design, 53, 325-331.

Mohammed, B. S., Foo, W. L., Hossain, K. M. A., & Abdullahi, M. (2013). Shear strength of palm oil clinker concrete beams. Materials & Design, 46, 270-276.

Mohammed, B. S., Hossain, K. M. A., Foo, W. L., & Abdullahi, M. (2011). Rapid chloride permeability test on lightweight concrete made with oil palm clinker. vol, 1, 1863-1870.

Moni, M. N. Z., & Sulaiman, S. A. (2012). Downdraft gasification of oil palm frond: effects of temperature and operation time. Journal of Applied Sciences, 12(24), 2574-2579.

Morris, M., & Waldheim, L. (1998). Energy recovery from solid waste fuels using advanced gasification technology. Waste management, 18(6-8), 557-564.

Mukherjee, A. B., Zevenhoven, R., Bhattacharya, P., Sajwan, K. S., & Kikuchi, R. (2008). Mercury flow via coal and coal utilization by-products: a global perspective. Resources, Conservation and Recycling, 52(4), 571-591.

Muthusamy, K., Jamaludin, N. F. A., Kamaruzzaman, M. N., Ahmad, M. Z., Zamri, N. A., & Budiea, A. M. A. (2021). Compressive strength of palm oil clinker lightweight aggregate concrete containing coal bottom ash as sand replacement. Materials Today: Proceedings, 46, 1724-1728.

Muthusamy, K., Jamaludin, N. F. A., Kamaruzzaman, M. N., Ahmad, M. Z., Zamri, N. A., & Budiea, A. M. A. (2021). Compressive strength of palm oil clinker lightweight aggregate concrete containing coal bottom ash as sand replacement. Materials Today: Proceedings, 46, 1724-1728.

Muthusamy, K., Mirza, J., Zamri, N. A., Hussin, M. W., Majeed, A. P. A., Kusbiantoro, A., & Budiea, A. M. A. (2019). Properties of high strength palm oil clinker lightweight concrete containing palm oil fuel ash in tropical climate. Construction and Building Materials, 199, 163-177.

Muthusamy, K., Mirza, J., Zamri, N. A., Hussin, M. W., Majeed, A. P. A., Kusbiantoro, A., & Budiea, A. M. A. (2019). Properties of high strength palm oil clinker lightweight concrete containing palm oil fuel ash in tropical climate. Construction and Building Materials, 199, 163-177.

Mutsaers, H. J. W. (2019). The challenge of the oil palm: using degraded land for its cultivation. Outlook on Agriculture, 48(3), 190-197.

Nagiah, C., & Azmi, R. (2013). A review of smallholder oil palm production: challenges and opportunities for enhancing sustainability-a Malaysian perspective. Journal of Oil Palm, Environment and Health (JOPEH), 3.

Nasution, M. A., Herawan, T., & Rivani, M. (2014). Analysis of palm biomass as electricity from palm oil mills in North Sumatera. Energy Procedia, 47, 166-172.

Nejati, M., Bin, A. S., & Amran, A. B. (2010). Sustainable development: a competitive advantage or a threat?. Business strategy series.

Neves, R. D., & Fernandes de Almeida, J. C. O. (2005). Compressive behaviour of steel fibre reinforced concrete. Structural concrete, 6(1), 1-8.

Neville, A. (1997). Aggregate bond and modulus of elasticity of concrete. Materials Journal, 94(1), 71-74.

Neville, A. M. (1995). Properties of concrete (Vol. 4). London: Longman.

Neville, A. M., & Brooks, J. J. (2010). Concrete technology (pp. 242-246). England: Longman Scientific & Technical.

Nipattummakul, N., Ahmed, I. I., Gupta, A. K., & Kerdsuwan, S. (2011). Hydrogen and syngas yield from residual branches of oil palm tree using steam gasification. International journal of hydrogen energy, 36(6), 3835-3843.

Nipattummakul, N., Ahmed, I. I., Kerdsuwan, S., & Gupta, A. K. (2012). Steam gasification of oil palm trunk waste for clean syngas production. Applied energy, 92, 778-782.

Ochsendorf, J. A. (2005). Sustainable engineering: The future of structural design. In Structures Congress 2005: Metropolis and Beyond (pp. 1-9).

Oehlers, D. J., Mohamed Ali, M. S., Haskett, M., Lucas, W., Muhamad, R., & Visintin, P. (2011). FRP-reinforced concrete beams: unified approach based on IC theory. Journal of Composites for Construction, 15(3), 293-303.

Oehlers, D. J., Visintin, P., Haskett, M., & Sebastian, W. M. (2013). Flexural ductility fundamental mechanisms governing all RC members in particular FRP RC. Construction and Building Materials, 49, 985-997.

Oehlers, D., Visintin, P., & Haskett, M. (2012a). The ideal bond characteristics for reinforced concrete members. International Symposium on Bond in Concrete. Brescia, Italy.

Oehlers, D., Visintin, P., Haskett, M., & Chen, J. (2012b). Consequences and solutions to our abysmal neglect of the bond-slip behaviour in reinforced concrete. International Symposium on Bond in Concrete. Brescia, Italy.

Okpala, D. C. (1990). Palm kernel shell as a lightweight aggregate in concrete. Building and environment, 25(4), 291-296.

Omar, W., & Mohamed, R. N. (2002). The performance of pretensioned prestressed concrete beams made with lightweight concrete. Malaysian Journal of Civil Engineering, 14(1), 60-70.

Orangun, C. O., Jirsa, J. O., & Breen, J. E. (1977, March). A reevaulation of test data on development length and splices. In Journal Proceedings (Vol. 74, No. 3, pp. 114-122).

Oseghale, S. D., Mohamed, A. F., & Chikere, A. O. (2017). Status evaluation of palm oil waste management sustainability in Malaysia. OIDA International Journal of Sustainable Development, 10(12), 41-48.

Paiva, H., Silva, A. S., Velosa, A., Cachim, P., & Ferreira, V. M. (2017). Microstructure and hardened state properties on pozzolan-containing concrete. Construction and Building Materials, 140, 374-384.

Pan, Z., Sanjayan, J. G., & Rangan, B. V. (2011). Fracture properties of geopolymer paste and concrete. Magazine of concrete research, 63(10), 763-771.

Pleanjai, S., & Gheewala, S. H. (2009). Full chain energy analysis of biodiesel production from palm oil in Thailand. Applied energy, 86, S209-S214.

Posi, P., Teerachanwit, C., Tanutong, C., Limkamoltip, S., Lertnimoolchai, S., Sata, V., & Chindaprasirt, P. (2013). Lightweight geopolymer concrete containing aggregate from recycle lightweight block. Materials & Design (1980-2015), 52, 580-586.

Quiroga, P. N., & Fowler, D. W. (2004). The effects of aggregates characteristics on the performance of Portland cement concrete. 1 University Station C1755. Austin, TX, 78712-0277.

Ragipani, R., Escobar, E., Prentice, D., Bustillos, S., Simonetti, D., Sant, G., & Wang, B. (2021). Selective sulfur removal from semi-dry flue gas desulfurization coal fly ash for concrete and carbon dioxide capture applications. Waste Management, 121, 117-126.

Rajerajeswari, A., Dhinakaran, G., & Ershad, M. (2013). Compressive strength of silica fume based geopolymer concrete. Asian Journal of Applied Science.

Raman, S. N., Ngo, T., Mendis, P., & Mahmud, H. B. (2011). High-strength rice husk ash concrete incorporating quarry dust as a partial substitute for sand. Construction and Building Materials, 25(7), 3123-3130.

Ranjbar, N., Mehrali, M., Alengaram, U. J., Metselaar, H. S. C., & Jumaat, M. Z. (2014). Compressive strength and microstructural analysis of fly ash/palm oil fuel ash based geopolymer mortar under elevated temperatures. Construction and building materials, 65, 114-121.

Rashiddadash, P., Ramezanianpour, A. A., & Mahdikhani, M. (2014). Experimental investigation on flexural toughness of hybrid fiber reinforced concrete (HFRC) containing metakaolin and pumice. Construction and Building Materials, 51, 313-320.

RILEM TC, R. T. R. (1983). Bond test for reinforcement steel, 2. Pull-Out test. (RILEM 7-II-128. RC 6). Materials and Structures.

Ronanki, V. S., Aaleti, S., & Valentim, D. B. (2018). Experimental investigation of bond behavior of mild steel reinforcement in UHPC. Engineering Structures, 176, 707-718.

Rukzon, S., & Chindaprasirt, P. (2009). Use of disposed waste ash from landfills to replace Portland cement. Waste Management & Research, 27(6), 588-594.

Rukzon, S., & Chindaprasirt, P. (2009). Use of disposed waste ash from landfills to replace Portland cement. Waste Management & Research, 27(6), 588-594.

Safiuddin, M., Abdus Salam, M., & Jumaat, M. Z. (2011). Utilization of palm oil fuel ash in concrete: a review. Journal of Civil Engineering and Management, 17(2), 234-247.

Saliba, J., & Mezhoud, D. (2019). Monitoring of steel-concrete bond with the acoustic emission technique. Theoretical and Applied Fracture Mechanics, 100, 416-425.

Sandanayake, M., Bouras, Y., Haigh, R., & Vrcelj, Z. (2020). Current sustainable trends of using waste materials in concrete - a decade review. Sustainability, 12(22), 9622.

Sandanayake, M., Bouras, Y., Haigh, R., & Vrcelj, Z. (2020). Current sustainable trends of using waste materials in concrete—a decade review. Sustainability, 12(22), 9622.

Sarker, P. (2010). Bond strengths of geopolymer and cement concretes. In Advances in Science and Technology (Vol. 69, pp. 143-151). Trans Tech Publications Ltd.

Sata, V., Jaturapitakkul, C., & Kiattikomol, K. (2007). Influence of pozzolan from various by-product materials on mechanical properties of high-strength concrete. Construction and Building Materials, 21(7), 1589-1598.

Sayer, J., Ghazoul, J., Nelson, P., & Boedhihartono, A. K. (2012). Oil palm expansion transforms tropical landscapes and livelihoods. Global Food Security, 1(2), 114-119.

Scheetz, B. E., & Earle, R. (1998). Utilization of fly ash. Current Opinion in Solid State and Materials Science, 3(5), 510-520.

Sfikas, I. P., & Trezos, K. G. (2013). Effect of composition variations on bond properties of self-compacting concrete specimens. Construction and building materials, 41, 252-262.

Shah, S. P., & Sankar, R. (1987). Internal cracking and strain softening response of concrete under uniaxial compression. Materials Journal, 84(3), 200-212.

Shahid, K. A., Syed-Mohsin, S. M., & Ghazali, N. (2016). The potential of cooling effect using palm oil clinker as drainage layer in green roof system. ARPN Journal of Engineering and Applied Sciences, 11(11).

Shannag, M. J. (2011). Characteristics of lightweight concrete containing mineral admixtures. Construction and Building Materials, 25(2), 658-662.

Sharmin, A., Alengaram, U. J., Jumaat, M. Z., Kabir, S. M. A. & Bashar, I. I. (2015). Engineering properties of lightweight geopolymer concrete with oil palm shell and palm oil clinker. Rev. Téc. Ing. Univ. Zulia, 38(1), 34-48.

Sharmin, A., Alengaram, U. J., Jumaat, M. Z., Yusuf, M. O., Kabir, S. A., & Bashar, I. I. (2017). Influence of source materials and the role of oxide composition on the performance of ternary blended sustainable geopolymer mortar. Construction and Building Materials, 144, 608-623.

Shirai, Y., Wakisaka, M., Yacob, S., Hassan, M. A., & Suzuki, S. I. (2003). Reduction of methane released from palm oil mill lagoon in Malaysia and its countermeasures. Mitigation and Adaptation Strategies for Global Change, 8(3), 237-252.

Shuit, S. H., Tan, K. T., Lee, K. T., & Kamaruddin, A. H. (2009). Oil palm biomass as a sustainable energy source: A Malaysian case study. Energy, 34(9), 1225-1235.

Siddiquee, S., Shafawati, S. N., & Naher, L. (2017). Effective composting of empty fruit bunches using potential Trichoderma strains. Biotechnology reports, 13, 1-7.

Sinoh, S. S., Ibrahim, Z., & Othman, F. (2021). Life cycle assessment of palm oil clinker as a binder and aggregate replacement in concrete. Journal of Oil Palm Research, 33(1), 151-170.

Sinoh, S. S., Ibrahim, Z., & Othman, F. (2021). Life cycle assessment of palm oil clinker as a binder and aggregate replacement in concrete. Journal of Oil Palm Research, 33(1), 151-170.

Soleymani, F. (2012). Split tensile strength of palm oil clinker aggregates-based cementitious composites in the optimum state. The Journal of American Science, 8(5), 61-66.

Somna, K., Jaturapitakkul, C., Kajitvichyanukul, P., & Chindaprasirt, P. (2011). NaOH-activated ground fly ash geopolymer cured at ambient temperature. Fuel, 90(6), 2118-2124.

Steinberger, J. K., Krausmann, F., & Eisenmenger, N. (2010). Global patterns of materials use: A socioeconomic and geophysical analysis. Ecological Economics, 69(5), 1148-1158.

Stichnothe, H., & Schuchardt, F. (2011). Life cycle assessment of two palm oil production systems. Biomass and bioenergy, 35(9), 3976-3984.

Stock, A. F., Hannantt, D. J., & Williams, R. I. T. (1979). The effect of aggregate concentration upon the strength and modulus of elasticity of concrete. Magazine of concrete research, 31(109), 225-234.

Suhendro, B. (2014). Toward green concrete for better sustainable environment. Procedia Engineering, 95, 305-320.

Sulaiman, F., Abdullah, N., Gerhauser, H., & Shariff, A. (2011). An outlook of Malaysian energy, oil palm industry and its utilization of wastes as useful resources. Biomass and bioenergy, 35(9), 3775-3786.

Swamynadh, V., & Muthumani, K. (2018). Properties of structural lightweight concrete containing treated oil palm shell as coarse aggregate. Asian Journal of Civil Engineering, 19(6), 673-678.

Tabi, A. N. M., Zakil, F. A., Fauzai, W. N. F. M., Ali, N., & Hassan, O. (2008). The usage of empty fruit bunch (EFB) and palm pressed fibre (PPF) as substrates for the cultivation of Pleurotus ostreatus. Jurnal Teknologi, 49(F), 189-196.

Tasdemir, M. A., Maji, A. K., & Shah, S. P. (1990). Crack propagation in concrete under compression. Journal of engineering mechanics, 116(5), 1058-1076.

Tay, J. H. (1990). Ash from oil-palm waste as a concrete material. Journal of Materials in Civil Engineering, 2(2), 94-105.

Tayeh, B. A., Alyousef, R., Alabduljabbar, H., & Alaskar, A. (2021a). Recycling of rice husk waste for a sustainable concrete: A critical review. Journal of Cleaner Production, 127734.

Tayeh, B. A., Zeyad, A. M., Agwa, I. S., & Amin, M. (2021b). Effect of elevated temperatures on mechanical properties of lightweight geopolymer concrete. Case Studies in Construction Materials, 15, e00673.

Taylor, H. F. (1997). Cement chemistry (Vol. 2, p. 459). London: Thomas Telford.

Torre-Casanova, A., Jason, L., Davenne, L., & Pinelli, X. (2013). Confinement effects on the steel–concrete bond strength and pull-out failure. Engineering Fracture Mechanics, 97, 92-104.

Turk, K., Karatas, M., & Ulucan, Z. C. (2010). Effect of the use of different types and dosages of mineral additions on the bond strength of lap-spliced bars in self-compacting concrete. Materials and structures, 43(4), 557-570.

U. S. Geological Survey (2021). Mineral commodity summaries 2021. Reston, Virginia: U. S. Geological Survey. https://doi.org/10.3133/mcs2021.

United Nations (2019). The least developed countries report 2019. United Nations Conference on Trade and Development (UNCTAD).

United Nations General Assembly (2015). Transforming our world: The 2030 agenda for sustainable development.

Valcuende, M., & Parra, C. (2009). Bond behaviour of reinforcement in self-compacting concretes. Construction and Building Materials, 23(1), 162-170.

Vallance, S., Perkins, H. C., & Dixon, J. E. (2011). What is social sustainability? A clarification of concepts. Geoforum, 42(3), 342-348.

Van Jaarsveld, J. G. S., Van Deventer, J. S. J., & Lorenzen, L. (1997). The potential use of geopolymeric materials to immobilise toxic metals: Part I. Theory and applications. Minerals engineering, 10(7), 659-669.

Vijay, V., Pimm, S. L., Jenkins, C. N., & Smith, S. J. (2016). The impacts of oil palm on recent deforestation and biodiversity loss. PloS one, 11(7), e0159668.

Villela, A. A., D'Alembert, B. J., Rosa, L. P., & Freitas, M. V. (2014). Status and prospects of oil palm in the Brazilian Amazon. Biomass and Bioenergy, 67, 270-278.

Visintin, P., Oehlers, D. J., & Haskett, M. (2013b). Partial-interaction time dependent behaviour of reinforced concrete beams. Engineering Structures, 49, 408-420.

Visintin, P., Oehlers, D. J., Haskett, M., & Wu, C. (2013a). Mechanics-based hinge analysis for reinforced concrete columns. Journal of Structural Engineering, 139(11), 1973-1980.

Visintin, P., Oehlers, D. J., Wu, C., & Griffith, M. C. (2012b). The reinforcement contribution to the cyclic behaviour of reinforced concrete beam hinges. Earthquake engineering & structural dynamics, 41(12), 1591-1608.

Visintin, P., Oehlers, D. J., Wu, C., & Haskett, M. (2012a). A mechanics solution for hinges in RC beams with multiple cracks. Engineering Structures, 36, 61-69.

Wan Hasamudin, W. H., Loh, S. K., Nasrin, A. B., Mohammad, A. S., Nurul, A. B., Muzzammil, N., ... & Lim, W. S. (2016). Biogas Capture and Utilisation in Malaysia. In The 3rd Asia Renewable Energy Workshop (3rd AREW), Hanoi, Vietnam.

Wang, H. T., & Wang, L. C. (2007). Experimental study on mechanical properties of steel fiber reinforced lightweight aggregate concrete. Jianzhu Cailiao Xuebao(Journal of Building Materials), 10(2), 188-194.

Wang, H. T., & Wang, L. C. (2013). Experimental study on static and dynamic mechanical properties of steel fiber reinforced lightweight aggregate concrete. Construction and Building Materials, 38, 1146-1151.

Wanrosli, W. D., Zainuddin, Z., Law, K. N., & Asro, R. (2007). Pulp from oil palm fronds by chemical processes. Industrial crops and products, 25(1), 89-94.

Wardhani, R., & Rahadian, Y. (2021). Sustainability strategy of Indonesian and Malaysian palm oil industry: a qualitative analysis. Sustainability Accounting, Management and Policy Journal.

Westerholm, M., Lagerblad, B., Silfwerbrand, J., & Forssberg, E. (2008). Influence of fine aggregate characteristics on the rheological properties of mortars. Cement and Concrete Composites, 30(4), 274-282.

Xu, H., & Van Deventer, J. S. J. (1999, June). The geopolymerisation of natural alumino-silicates. In Proc. 2nd Internat. Conf. Geopolymere (Vol. 99, pp. 43-63).

Yaap, B., Struebig, M. J., Paoli, G., Koh, L. P., & Koh, L. P. (2010). Mitigating the biodiversity impacts of oil palm development. CAB Reviews, 5(19), 1-11.

Yacob, S., Hassan, M. A., Shirai, Y., Wakisaka, M., & Subash, S. (2006). Baseline study of methane emission from anaerobic ponds of palm oil mill effluent treatment. Science of the total environment, 366(1), 187-196.

Yap, S. P., Alengaram, U. J., & Jumaat, M. Z. (2013). Enhancement of mechanical properties in polypropylene–and nylon–fibre reinforced oil palm shell concrete. Materials & Design, 49, 1034-1041.

Yap, S. P., Bu, C. H., Alengaram, U. J., Mo, K. H., & Jumaat, M. Z. (2014). Flexural toughness characteristics of steel–polypropylene hybrid fibre-reinforced oil palm shell concrete. Materials & Design, 57, 652-659.

Yoshizaki, T., Shirai, Y., Hassan, M. A., Baharuddin, A. S., Abdullah, N. M. R., Sulaiman, A., & Busu, Z. (2013). Improved economic viability of integrated biogas energy and compost production for sustainable palm oil mill management. Journal of Cleaner Production, 44, 1-7.

Yusoff, S. (2006). Renewable energy from palm oil–innovation on effective utilization of waste. Journal of cleaner production, 14(1), 87-93.

Zakaria, M. L. (1986). Strength properties of oil palm clinker concrete. Jurnal Teknologi, 28-37.

Zarina, Y., Mohd Mustafa Al Bakri, A., Kamarudin, H., Nizar, K., & Rafiza, A. R. (2013). Review on the various ash from palm oil waste as geopolymer material.

Zhang, H., Li, L., Sarker, P. K., Long, T., Shi, X., Wang, Q., & Cai, G. (2019). Investigating various factors affecting the long-term compressive strength of heat-cured fly ash geopolymer concrete and the use of orthogonal experimental design method. International Journal of Concrete Structures and Materials, 13(1), 1-18.

Zhang, T., Visintin, P., Oehlers, D. J., & Griffith, M. C. (2014a). Presliding shear failure in prestressed RC beams. II: Behavior. Journal of Structural Engineering, 140(10), 04014070.

Zhang, T., Visintin, P., Oehlers, D. J., & Griffith, M. C. (2014b). Presliding shear failure in prestressed RC beams. I: Partial-Interaction mechanism. Journal of Structural Engineering, 140(10), 04014069.

Zhu, W., Sonebi, M., & Bartos, P. J. M. (2004). Bond and interfacial properties of reinforcement in self-compacting concrete. Materials and structures, 37(7), 442-448.

Zsutty, T. (1985). Empirical study of bar development behavior. Journal of Structural Engineering, 111(1), 205-219.

Zuo, J. & Darwin, D. (2000). Splice Strength of Conventional and High Relative Rib Area Bars in Normal and High-Strength Concrete. Structural Journal, 97(65), 630-641.